

**Synthesis and Reactivity of Transition  
Metal Methylidene Complexes**

**Thesis by**

**William C. Finch**

**In Partial Fulfillment of the Requirements  
for the Degree of  
Doctor of Philosophy**

**California Institute of Technology  
Pasadena, California**

**1986**

**(submitted May 14, 1986)**

ii

to my family

### Acknowledgments

I would like to thank Bob Grubbs for the privilege of working in his group. His patient guidance has been invaluable to my development as a scientist. John Bercaw has shown me that being both a good scientist and a good teacher is possible. The financial support through predoctoral fellowships from the NSF and Union Carbide is gratefully acknowledged.

All members of the Grubbs group, both past and present, deserve credit for putting up with me all these years. Special thanks go to Doug Meinhardt and Eric Anslyn for helpful discussions of NMR, science, and life in general. Mark Brusich has been a great roommate and friend. I thank Bernard Santarsiero for showing me the complexities of crystallography. It has been a pleasure knowing people from the Bercaw, Collins, Gray, Ireland, Dougherty, Goddard and Dervan groups. Softball with the Weenies and the Spuds made summers enjoyable.

Finally, I must thank my family. Their support has kept me going.

**ABSTRACT**

The reaction of metal oxo complexes with methylenation agents, " $\text{Cp}_2\text{TiCH}_2$ " and  $\text{CH}_2\text{PPh}_3$ , was investigated as a means to generate new transition metal methyldene complexes. With " $\text{Cp}_2\text{TiCH}_2$ ", only when the oxo complex has ancillary ligands of the proper electronic and steric characteristics, as in  $\text{WO}(\text{CH}_2\text{XMe}_3)_4$  ( $\text{X} = \text{C}, \text{Si}$ ), is clean reaction observed producing  $\mu\text{-O-}\mu\text{-CH}_2$  complexes. Otherwise the many reaction pathways available to the  $\text{Cp}_2\text{TiCH}_2$  fragment lead to complex reaction mixtures. The oxo ligand is inert to attack by  $\text{CH}_2\text{PPh}_3$  which instead acts as a powerful alkylating agent in the transition metal systems investigated.

The effect of cyclopentadienyl ring substitution on the reactivity of titanocene metallacyclobutanes was also investigated. The observed decrease in reactivity of these compounds with increasing methyl substitution of their cyclopentadienyl rings is related to the increasing destabilization of the transition state between metallacycle and methyldene-olefin complex upon substitution. This destabilization arises from the "reductive" nature of the formation of methyldene-olefin complex from metallacycle.

## Table of Contents

	<u>Page</u>
Chapter I.      A Short Introduction to Transition Metal Methylidene Chemistry	1
Chapter II      Reaction of Metal Oxo Complexes with Methylenation Agents	10
II.1      Introduction.	11
II.2      Reactivity of "Cp <sub>2</sub> TiCH <sub>2</sub> " with Metal Oxo Complexes	
II.2.1   Results	14
II.2.2   Discussion	24
II.3      Reactivity of CH <sub>2</sub> PPh <sub>3</sub> with Metal Oxo Complexes	
II.3.1   Results	31
II.3.2   Discussion	40
II.4      Conclusions	41
II.5      Experimental Section	43
II.6      References	60
Chapter III.    Effects of Cyclopentadienyl Ring Substituents on the Reactivity of Bis(cyclopentadienyl)- titanacyclobutanes)	66
III.1      Introduction	67
III.2      Results	73
III.3      Discussion	93
III.4      Conclusions.	107
III.5      Experimental Section	109
III.6      References	132

**LIST OF ABBREVIATIONS**

acac	acetylacetonate
bipy	2,2'-bipyridine
Cp	$\eta^5$ -cyclopentadienyl
Cp'	$\eta^5$ -(methyl)cyclopentadienyl
<Cp>	$\eta^5$ -(1,2,4-trimethyl)cyclopentadienyl
Cp*	$\eta^5$ -(pentamethyl)cyclopentadienyl
Cp <sup>Cl</sup>	$\eta^5$ -(chloro)cyclopentadienyl
$\overline{\text{Cp}}$	any substituted $\eta^5$ -cyclopentadienyl
d	doublet
dtc	diethyldithiocarbamate
m	multiplet
s	singlet
t	triplet
q	quartet
qn	quintet

## **Chapter 1**

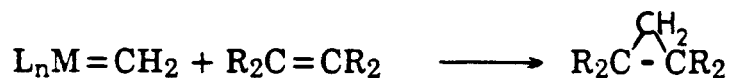
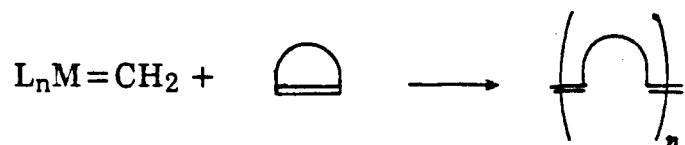
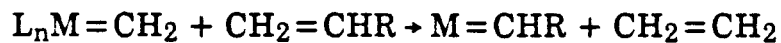
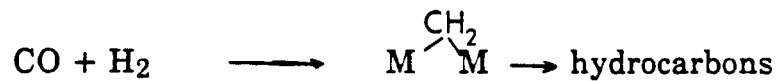
### **A Short Introduction to Transition-Metal Methylidene Chemistry**

In recent years both theoretical and experimental chemists have been interested in the study of transition metal complexes containing terminal or bridging methyldene ligands. Application of various theoretical methods to systems in which a terminal methyldene ligand, the simplest ligand capable of carbon-metal double bonding, is bonded to a transition metal center has led to a better understanding of the nature of carbon-metal multiple bonding.<sup>1</sup>

Complexes containing bridging or terminal methyldene ligands (or the related alkylidene ligands) are important reagents, catalysts, or intermediates for a number of stoichiometric and catalytic transformations. Such transformations include (Table 1.1) Witting-type methylenation of carbonyl compounds,<sup>2</sup> cyclopropanation of olefins,<sup>3</sup> ring-opening polymerization of cyclic olefins,<sup>4</sup> alkyne polymerization,<sup>5</sup> and olefin metathesis.<sup>6</sup> Pettit has found that surface methyldene ligands are probably involved in the formation of hydrocarbons in the reduction of carbon monoxide with hydrogen in the Fischer-Tropsch process.<sup>7</sup> Green and Rooney<sup>8</sup> have proposed that alkylidene species are intermediates in the polymerization of olefins. Bridging methyldene species may also be formed when metal-alkyl complexes interact with oxide supports.<sup>9</sup> The wide variety of reactivity of methyldene complexes makes them attractive synthetic targets.

Species containing terminal methyldene ligands have been observed spectroscopically and have been trapped to give derivatives;<sup>10</sup> however, isolation of stable terminal methylene complexes has proved to be difficult presumably because of the high reactivity of the terminal methyldene ligand. Until recently the only isolated terminal methyldene species were  $\text{Cp}_2\text{Ta}(\text{CH}_2)\text{Me}$ <sup>11</sup> and  $[\text{W}(\text{CH}_2)(\text{PMe}_3)_4\text{Cl}]^+[\text{CF}_3\text{SO}_3]^-$ .<sup>12</sup> A few other stable terminal methyldene complexes now have been isolated including



**Table 1.1 Reactivity of Methylidene Complexes****Methylenation of Carbonyls****Cyclopropanation of Olefins****Ring-opening Polymerization****Olefin Metathesis****Fischer-Tropsch Reaction**

$\text{Cp}^*_2\text{Ta}(\text{CH}_2)\text{H}$ ,<sup>13</sup> and  $\text{Os}(\text{CH}_2)\text{Cl}(\text{NO})(\text{PPh}_3)_2$ .<sup>14</sup> The known synthetic routes to terminal methylidene complexes include diazomethane reactions,<sup>14</sup> protonation of methylidyne species,<sup>12</sup> methyl deprotonation,<sup>11</sup> hydrogen atom abstraction,<sup>15</sup>  $\alpha$ -hydride elimination,<sup>13</sup> hydride abstraction,<sup>10c</sup> chloride abstraction from chloromethyl complexes,<sup>10d</sup> and alkoxide abstraction from alkoxymethyl complexes<sup>10c,d</sup> (Table 1.2).

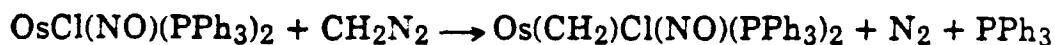
Methylidene ligands bridging two metal centers seem much less reactive than terminal methylidenes. A large number of stable bridging methylidene complexes have been isolated. The most common route to bridging methylidene complexes is the reaction of dihalomethanes with metal complexes.<sup>16</sup> Other routes include treatment of metal dimers with diazomethane<sup>17</sup> or phosphorous ylides,<sup>18</sup> insertion of terminal methylidene complexes into metal ligand bonds,<sup>19</sup> and reaction of trimethyl aluminum with metal halides.<sup>6a,20</sup> (Table 1.3).

In Chapter II of this thesis we present the results of our efforts toward synthesis of new methylidene complexes *via* Wittig-type reactivity of metal oxo complexes with methylenation reagents.

In Chapter III of this thesis we present the results of studies on changes in reactivity of titanocene metallacyclobutanes caused by methyl substitution on their cyclopentadienyl ligands. The observed changes in reactivity are related to changes in the relative energies of metallacyclobutanes and methylidene olefin complexes.

**Table 1.2 Examples of Synthetic Routes to Terminal  
Methyldene Complexes**

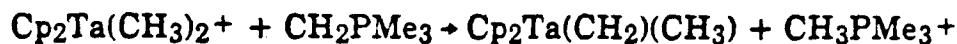
**Diazomethane Reaction**



**Methyldyne Protonation**



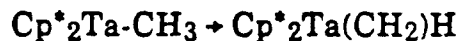
**Methyl Deprotonation**



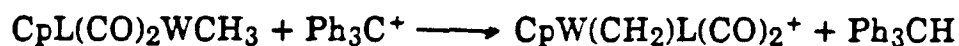
**Hydrogen Atom Abstraction<sup>a</sup>**



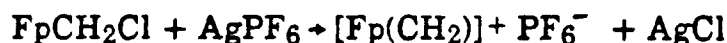
**$\alpha$ -Hydride Elimination**



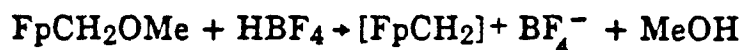
**Hydride Abstraction<sup>a,b</sup>**



**Chloride Abstraction<sup>a,c</sup>**



**Alkoxide Abstraction<sup>a,c</sup>**



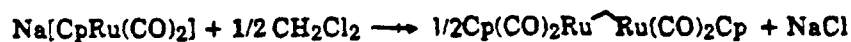
a) Methyldene complex was not isolated

b) L = PEt<sub>3</sub>, PPh<sub>3</sub>

c) Fp = CpFe(CO)<sub>2</sub>

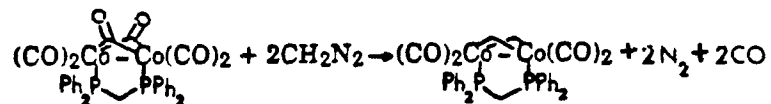
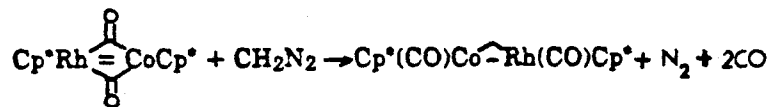
**Table 1.3 Examples of Synthetic Routes to Bridging Methylidene Complexes**

**Reaction of Dihalomethanes**

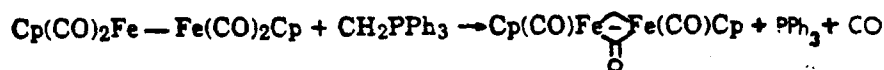


etc

**Reaction of Diazomethane**



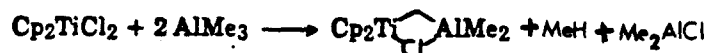
**Reaction of Phosphorous Ylides**



**Insertion of Terminal Methylidenes into Metal-Ligand Bonds<sup>a</sup>**



**Reaction of Trimethyl aluminum with Metal Halides**



a)  $\text{ML}_n = \text{Cp}^*\text{TiCl}_2, \text{Cp}^*\text{ZrCl}_2, \text{PtMe}(\text{PMe}_3)_2, \text{Rh}(\text{COD})$  ( $\text{COD} = \eta^4\text{-1,5-cyclooctadiene}$ ).

## References

1. a). Kostic, N.M.; Fenske, R.F., *J. Am. Chem. Soc.*, **1982**, *104*, 3879. b) Kostic, N.M.; Fenske, R.F. *Organometallics* **1982**, *1*, 974. c) Taylor, T.E.; Hall, M.B. *J. Am. Chem. Soc.*, **1984**, *106*, 1576. d) Francl, M.M.; Pietro, W.J.; Hout, R.F., Jr.; Hehre, W.J. *Organometallics* **1983**, *2*, 815.
2. a) Pine, S.H.; Zahler, R.; Evans, D.A.; Grubbs, R.H. *J. Am. Chem. Soc.* **1980**, *102*, 3270. b) Clawson, L.E.; Buchwald, S.L.; *Tetrahedron Lett.* **1984**, *25*, 5733. c) Brown-Wensley, K.A. Ph.D. Thesis, California Institute of Technology, 1981. d) Cannizzo, L.F.; Grubbs, R.H. *J. Org. Chem.* **1985**, *50*, 2316.
3. Brookhart, M.; Tucker, J.R.; Husk, G.R. *J. Am. Chem. Soc.* **1983**, *105*, 258. Brandt, S.; Helquist, P. *J. Am. Chem. Soc.* **1979**, *101*, 6473.
4. Gilliom, L.R. *J. Am. Chem. Soc.* **1986**, *108*, 733
5. a) Katz, T.J.; Lee, S.J. *J. Am. Chem. Soc.* **1980**, *102*, 422. b) Dyke, A.F.; Knox, S.A.R.; Naigh, P.J.; Taylor, G.E. *J. Chem. Soc. Chem. Commun.* **1980**, 803.
6. a) Tebbe, F.N.; Parshall, G.W.; Overall, D.W. *J. Am. Chem. Soc.* **1979**, *101*, 5074. b) Howard, T.R.; Lee, J.B.; Grubbs, R.H. *J. Am. Chem. Soc.* **1980**, *102*, 6877.
7. a) Brady, R.C.; Pettit, R. *J. Am. Chem. Soc.* **1980**, *102*, 6181. b) Brady, R.C.; Pettit, R. *J. Am. Chem. Soc.* **1981**, *103*, 1287.
8. Ivin, K.J.; Rooney, J.J.; Stewart, C.D.; Green, M.L.H.; Mehtab, R. *J. Chem. Soc., Chem. Commun.* **1978**, 604.

9. a) He, M.-Y.; Burwell, R.L., Jr.; Marks, T.J. *Organometallics* **1983**, *2*, 566. b) Toscano, P.J.; Marks, T.J. *J. Am. Chem. Soc.*, **1985**, *107*, 653.
- 10 a) Churchill, M.R.; Wasserman, H.J.; *Inorg. Chem.* **1982**, *21*, 3913. b) Jernakoff, P.; Cooper, N.J. *J. Am. Chem. Soc.* **1984**, *106*, 3026. c) Kegley, S.E.; Brookhart, M.; Husk, G.R. *Organometallics* **1982**, *1*, 760. d) Bodnar, T.W.; Cutler, A.R. *J. Am. Chem. Soc.* **1983**, *105*, 5926.
11. Schrock R.R.; Sharp, P.R. *J. Am. Chem. Soc.* **1978**, *100*, 2389.
12. Holmes, S.J.; Schrock, R.R. *J. Am. Chem. Soc.* **1981**, *103*, 4599.
13. Bercaw, J.E.; Burger, B.J.; Gibson, V.C.; Parkin, G.; Trimmer, M.S.; van Asselt, A. Poster Session Oxidation Chemistry Conference, California Institute of Technology February 25, 1986.
14. Hill, A.F.; Roper, W.R.; Waters, J.M.; Wright, A.H. *J. Am. Chem. Soc.* **1983**, *105*, 5939.
15. Hayes, J.C.; Pearson, G.D.N.; Cooper, N.J. *J. Am. Chem. Soc.* **1981**, *103*, 4648.
16. a) Jandik, P.; Schubert, U., Schmidbaur, H. *Ang. Chem. Int. Ed. Engl.* **1982**, *21*, 73. b) Sumner, C.E., Jr.; Collier, J.A.; Pettit, R. *Organometallics* **1982**, *1*, 1350. c) Motyl K.M.; Norton, J.R.; Schauer, C.K.; Anderson, O.P. *J. Am. Chem. Soc.* **1982**, *104*, 7375. d) Lin, Y.C.; Calabrese, J.C.; Wreford, S.S. *J. Am. Chem. Soc.* **1983**, *105*, 1679. e) Amane, M.E.; Maisonnat, A.; Dahan, F.; Prince, R.; Poilblanc, R. *Organometallics* **1985**, *4*, 773. f) Theopold, K.H.; Bergman, R.G. *J. Am. Chem. Soc.* **1983**, *105*, 464.
17. a) Green, M.; Hanks, D.R.; Howard, J.A.K.; Louca, P.; Stone, F.G.A. *J. Chem. Soc. Chem. Commun.* **1983**, 757. b) Laws, W.J.; Puddapatt, R.J. *J. Chem. Soc. Chem. Commun.* **1983**, 1020.

18. Korswagen, R.; Ah, R.; Speth, D.; Ziegler, M.L. *Angew. Chem. Int. Ed. Engl.* **1981**, *20*, 1049.
19. Mackenzie, P.B.; Ott, K.C.; Grubbs, R.H. *Pure and Applied Chemistry* **1984**, *56*, 59. Mackenzie, P.B.; Grubbs, R.H. submitted for publication.
20. de Miquel, A.V.; Bailey, P.M.; Meanwell, N.J.; Maitlis, P.M. *Organometallics* **1982**, *1*, 1604.

## **Chapter 2**

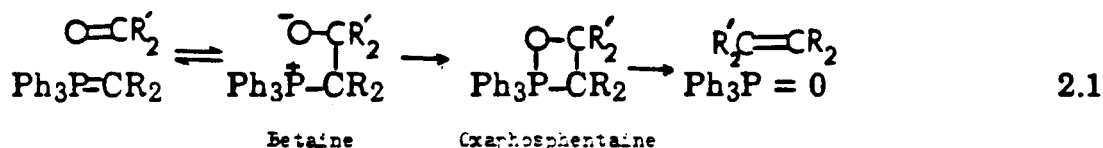
### **Reaction of Metal Oxo Complexes with Methylenation Agents**



## II.1 Introduction

The idea that transition metal oxo complexes may possess reactivity similar to organic carbonyl compounds is not new.<sup>1</sup> Our question was, will metal oxo complexes react with methylenation reagents to produce methyldene complexes, a reaction analogous to the Wittig reaction in which organic carbonyls are converted to terminal olefins with these reagents.

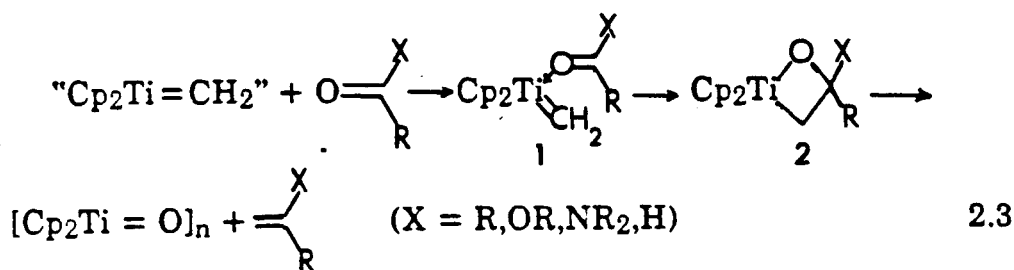
In organic chemistry phosphorous ylides are the classical methylenation reagents. The generally accepted mechanism for the Wittig reaction using phosphorous ylides is shown in equation 2.1.<sup>2</sup> Phosphorous ylides are quite nucleophilic and attack the carbonyl



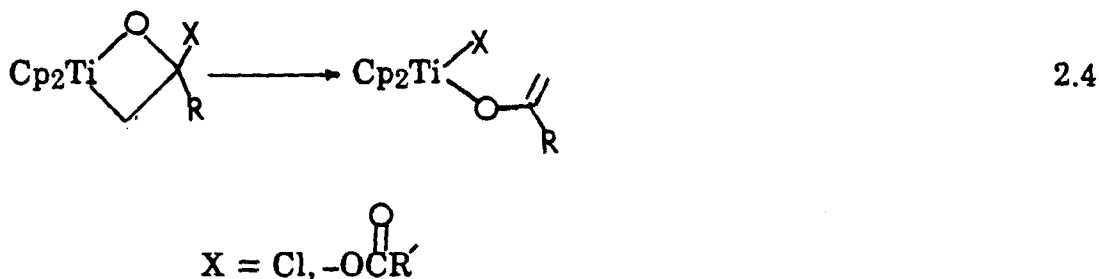
at carbon forming the betaine intermediate, which has been observed in some reactions.<sup>3</sup> The betaine then collapses to the oxaphosphentaine intermediate and then goes on to products. If the carbonyl bears a good leaving group, as in esters, phosphorous ylides cannot be used to produce olefins as elimination of this leaving group resulting in the formation of a phosphonium salt and finally an acylated ylide species is competitive with olefination (equation 2.2)<sup>4</sup>.



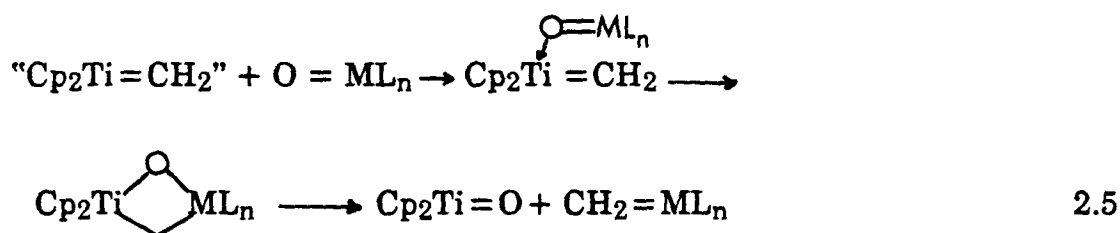
In recent years, the Grubbs group has investigated the reaction chemistry of the unobserved reactive fragment,  $\text{Cp}_2\text{TiCH}_2$ , which may be generated from the Tebbe reagent,<sup>5</sup>  $\text{Cp}_2\text{TiCH}_2\text{Al}(\text{Me})_2\text{Cl}$  or from titanacyclobutanes.<sup>6</sup> This fragment exhibits Wittig-type reactivity, reacting with organic carbonyl compounds, including ketones,<sup>7</sup> aldehydes,<sup>8</sup> esters<sup>9</sup> and amides<sup>10</sup> to produce terminal olefins. The proposed mechanism for this organic reaction is shown in equation 2.3.<sup>8</sup> The carbonyl reacts with



a source of  $\text{Cp}_2\text{TiCH}_2$  possibly producing an intermediate complex, 1, which collapses to an oxatitanacyclobutane, 2, and then goes on to products. No stable species like intermediate 1 has been observed, but stable oxatitanacyclobutanes have been prepared.<sup>11</sup> Only if the carbonyl bears a very good leaving group, e.g.,  $\text{Cl}^-$  or  $\text{RC}(\text{O})\text{O}^-$ , does elimination of the leaving group occur, presumably from the oxatitanacyclobutane to produce titanocene enolate complexes<sup>12</sup> (equation 2.,4).



Since the  $\text{Cp}_2\text{TiCH}_2$  fragment had been shown to be a versatile methylenating agent with organic carbonyls we wished to see if we could extend the chemistry to inorganic systems, i.e., attempt to use the  $\text{Cp}_2\text{TiCH}_2$  fragment to methylenate metal oxo complexes to form terminal methylenes, or possibly  $\mu\text{-O-}\mu\text{-CH}_2$  complexes, **3**, via a mechanism similar to that proposed for the organic systems (equation 2.5).



We will now present our results from the investigation of the reactivity of the  $\text{Cp}_2\text{TiCH}_2$  fragment with metal oxo complexes. Later in this chapter we will present some results on the reactivity of the more classical Wittig methylenating agent, triphenyl phosphorane, with metal oxo complexes.

## II.2 Reactivity of "Cp<sub>2</sub>TiCH<sub>2</sub>" with Metal Oxo Complexes

### II.2.1 Results

The  $\beta,\beta$ -disubstituted titanacyclobutane Cp<sub>2</sub> $\overline{\text{TiCH}_2\text{CMe}_2\text{CH}_2}$ , **4**, is a convenient source of the Cp<sub>2</sub>TiCH<sub>2</sub> fragment producing one equivalent of isobutylene as a by-product. Thus, **4** was used as the source of the Cp<sub>2</sub>TiCH<sub>2</sub> fragment for reaction with various metal oxo complexes. Table 2.1 is a tabulation of the metal oxo complexes used in this study. We have concentrated on oxo complexes of metals of Groups 5-7 for two reasons. The first is that stable methyldiene, or related alkyldiene, complexes have been isolated for group 5 and 6 metals. The second is that group 6 and 7 metals are used industrially as olefin metathesis catalysts<sup>13</sup> indicating that metal methyldienes may be viable for these metals.<sup>14</sup>

For all oxo complexes used in this study, the reaction of **4** as a source of the Cp<sub>2</sub>TiCH<sub>2</sub> fragment with the metal oxo complex was initially conducted on an NMR tube scale, the reaction being monitored by <sup>1</sup>H NMR spectroscopy. Many of the reactions were repeated on a larger preparative scale in an attempt to isolate identifiable products.

The reaction of **4** with WO(OCH<sub>2</sub>CMe<sub>3</sub>)<sub>4</sub>, **5**, in pentane at 0°C yields a new cherry-red colored complex, **21**, in 30% yield. The room temperature NMR data for this complex are shown in Table 2.2. The low field resonances at  $\delta$  6.73 in the <sup>1</sup>H spectrum and  $\delta$  181.9 (J<sub>CH</sub> = 129 Hz) in the <sup>13</sup>C spectrum are indicative of a methyldiene ligand bridging two transition metal centers.<sup>15</sup> The infrared spectrum of **21** shows no bands in the region 820-1020 cm<sup>-1</sup> indicating that **21** has no terminal oxo ligand.<sup>16</sup> Based on this NMR and infrared evidence we formulate **21** as a  $\mu$ -O- $\mu$ -CH<sub>2</sub> bimetallic complex arising

**Table 2.1 Results of Reaction of  $\text{Cp}_2\text{TiCH}_2$  with Metal Oxo Complexes**

	Metal oxo	Result
5	$\text{W}(\text{O})(\text{OCH}_2\text{CMe}_3)_4$	Forms $[\mu\text{-O-}\mu\text{CH}_2][\text{CpTi}][\text{W}(\text{OCH}_2\text{CMe}_3)_4]$
6	$\text{W}(\text{O})(\text{OCH}_2\text{SiMe}_3)_4$	Forms $[\mu\text{-O-}\mu\text{-CH}_2][\text{CpTi}][\text{W}(\text{OCH}_2\text{SiMe}_3)_4]$
7	$\text{W}(\text{O})(\text{OMe})_4$	mixtures of alkoide species
8	$\text{W}(\text{O})(\text{OCMe}_3)_4$	"
9	$\text{W}(\text{O})(\text{OCH}_2\text{Ph})_4$	"
10	$\text{W}(\text{O})(\text{CH}_2\text{CMe}_3)_3\text{Cl}$	observe free $\text{CMe}_4$
11	$\text{Mo}(\text{O})_2(\text{Me})_2\text{bipy}$	$\text{Cp}_2\text{Ti}(\text{CH}_3)\text{Cl}$ formed in possible radical reaction
12	$\text{Mo}(\text{O})_2(\text{dtc})_2$	paramagnetic species
13	$\text{Mo}(\text{O})_2(\text{acac})_2$	"
14	$\text{Re}(\text{O})\text{I}(\text{CH}_3\text{C}\equiv\text{CCH}_3)_2$	"
15	$\text{Re}(\text{O})\text{Cl}_2(\text{OEt})(\text{Pph}_3)_2$	transient terminal methylidene
16	<i>cis</i> - $\text{Re}(\text{O})\text{Cl}_3(\text{PEt}_3)_2$	complex reaction mixture
17	<i>trans</i> - $\text{Re}(\text{O})\text{Cl}_3(\text{PEt}_3)_2$	"
18	$\text{Cp}_2\text{Nb}(\text{O})\text{Cl}$	no stable product
19	$\text{Cp}_2\text{Nb}(\text{O})(\text{nBu})$	"
20	$\text{V}(\text{O})(\text{CH}_2\text{SiMe}_3)_3$	observe free $\text{SiMe}_4$

Table 2.2. NMR Spectral Data for  $\mu$ -O- $\mu$ -CH<sub>2</sub> Complexes

			Assignment
	$\delta$ (ppm)		
$\text{Cp}_2\text{Ti} \begin{array}{c} \diagup \text{O} \\ \diagdown \text{CH}_2 \end{array} \text{W}(\text{OCH}_2\text{CMe}_3)_4$ (21) $^1\text{H}(\text{C}_6\text{D}_6, 25^\circ\text{C})$ :	6.73	(s, 2H)	$\begin{array}{c} (\mu\text{-CH}_2) \\ (\text{C}_5\text{H}_5) \\ (-\text{OCH}_2\text{CMe}_3) \\ (\text{OCH}_2\text{CMe}_3) \end{array}$
	5.95	(s, 10H)	
	4.36	(s, 8H)	
	1.10	(s, 36H)	
$^1\text{H}(\text{tol-d}_8, -61^\circ\text{C})$ :	6.73	(s, 2H)	$\begin{array}{c} (\mu\text{-CH}_2) \\ \text{C}_5\text{H}_5 \end{array}$
	5.95	(s, 10H)	
	4.49	(s, 2H)	$(\text{OCH}_2\text{CMe}_3)$
	4.61	(d, $J = 11.7 \text{ Hz}$ , 2H)	
	4.28	(d, $J = 11.7 \text{ Hz}$ , 2H)	$(\text{OCH}_2\text{CMe}_3)$
	4.40	(s, 2H)	
	1.16	(s, 27H)	
	1.09	(s, 9H)	
$^{13}\text{C}\{^1\text{H}\} (\text{tol-d}_8, 25^\circ\text{C})$ :	181.9b		$\begin{array}{c} (\mu\text{-CH}_2) \\ (\text{C}_5\text{H}_5) \\ (\text{OCH}_2\text{CMe}_3) \\ (\text{OCH}_2\text{CMe}_3) \\ (\text{OCH}_2\text{CMe}_3) \end{array}$
	113.3		
	83.2		
	35.1		
$\text{Cp}_2\text{Ti} \begin{array}{c} \diagup \text{O} \\ \diagdown \text{CH}_2 \end{array} \text{W}(\text{OCH}_2\text{SiMe}_3)_4$ $(23)^1\text{H} (\text{C}_6\text{D}_6, 25^\circ\text{C})$ :	6.84	(s, 2H)	$\begin{array}{c} (\mu\text{-CH}_2) \\ (\text{C}_5\text{H}_5) \\ (\text{OCH}_2\text{SiMe}_3) \\ (\text{OCH}_2\text{SiMe}_3) \end{array}$
	5.97	(s, 10H)	
	4.52	(s, 8H)	
	0.21	(s, 36H)	
	181.7		$\begin{array}{c} (\mu\text{-CH}_2) \\ (\text{C}_5\text{H}_5) \\ (\text{OCH}_2\text{SiMe}_3) \\ (\text{OCH}_2\text{SiMe}_3) \end{array}$
$^{13}\text{C}\{^1\text{H}\} (\text{C}_6\text{D}_6, 25^\circ\text{C})$ :	112.2		
	66.9		
	-2.3		

a.  $^1\text{H}$  Shifts relative to  $\text{C}_6\text{D}_5\text{H}$  at  $\delta$  7.15 or  $\text{C}_6\text{D}_5\text{CHD}_2$  at  $\delta$  2.10,  $^{13}\text{C}$  shifts relative to  $\text{C}_6\text{D}_6$  at  $\delta$  128.0 or  $\text{PhCD}_3$  at  $\delta$  21.0.

b.  $J_{\text{CH}}$  = 129 Hz as measured from the proton coupled  $^{13}\text{C}$  INEPT spectrum.

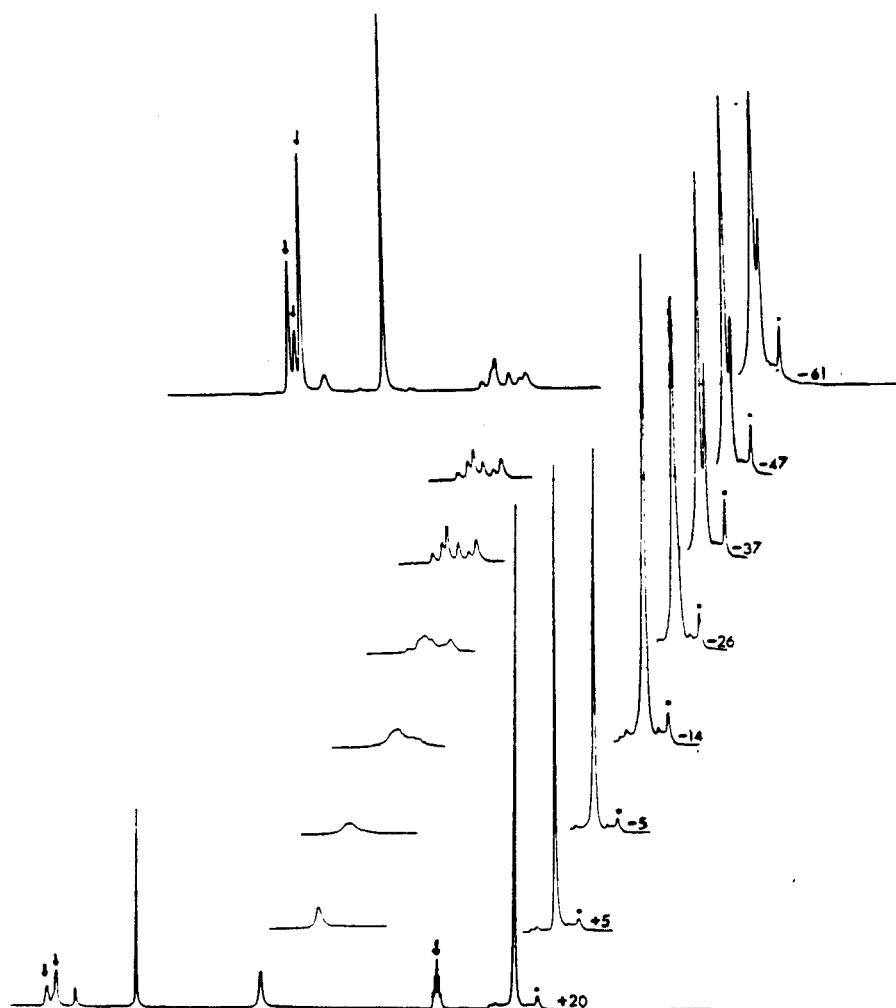
from the formal dimerization of the  $\text{Cp}_2\text{TiCH}_2$  fragment with  $\text{WO}(\text{OCH}_2\text{CMe}_3)_4$ .

Variable temperature  $^1\text{H}$  NMR spectroscopy revealed that **21** is a fluxional molecule (Figure 2.1). As the temperature is lowered the singlet at 4.35 arising from the methylene units of the alkoxide ligand splits into an AB four-line pattern and two singlets, relative integrals 2:1:1. The singlet at 1.10 arising from the *t*-Butyl groups of the alkoxide ligands splits into two resonances in the ratio 3:1. The resonances arising from the  $\mu\text{-CH}_2$  and the cyclopentadienyl groups show no temperature dependence. The low temperature limit is reached at  $-61^\circ\text{C}$ . Except for a general broadening of all resonances no further change in the spectrum occurs upon further cooling to  $-78^\circ\text{C}$ .

Since the cyclopentadienyl and  $\mu\text{-CH}_2$   $^1\text{H}$  NMR resonances of **21** remain singlets at all temperatures, the static structure of **21** must possess a plane of symmetry. The pattern of resonances arising from the alkoxide methylene units at the low temperature limit indicates that in **21** there are three distinct types of alkoxide ligands in the ratio 2:1:1. A static  $\mu\text{-O-}\mu\text{-CH}_2$  structure consistent with the low temperature  $^1\text{H}$  NMR data is shown in Figure 2.2.

Two of the alkoxide ligands lie in the symmetry plane containing the  $\mu\text{-O}$  and  $\mu\text{-CH}_2$  ligands and the tungsten and titanium atoms. These ligands give rise to the two singlets; in certain conformations the methylene protons of these ligands are related by the symmetry plane of the molecule. Hence, no geminal coupling is observed from these protons; they are rotationally equivalent. The methylene protons of the other two alkoxide ligands are diastereotopic in all conformations and so give rise to the AB pattern with a

Figure 2.1 Variable Temperature  $^1\text{H}$  NMR Spectroscopy of 21.



\* an impurity

↓ residual protons of solvent



typical geminal coupling of 11.7 Hz.<sup>18</sup> At low temperature two resonances in the ratio 3:1 arising from the t-Butyl methyl groups appear because in **21** three of the alkoxide ligands are *trans* to oxygen atoms and the fourth is *trans* to a carbon atom.

As the temperature is raised from -61°C a process begins which makes all the alkoxide ligands equivalent on the NMR timescale. Since a six-coordinate tungsten center would be expected to be stereochemically rigid, we believe that the fluxional behavior of **21** results from the breakage of at least one of the bridges forming a five-coordinate tungsten center. The alkoxide ligands then become equivalent through a pseudo-rotational process at the five-coordinate center.<sup>19</sup> Possible intermediates involved in the fluxional behavior of **21** are shown in Figure 2.3. We have no evidence to indicate which, if any, of these possibilities is correct; however, formation of transient terminal ligands from bridging ligands have been proposed to explain fluxional behavior in several other systems. (cf. *cis-trans* isomerization of  $\mu\text{-CH}_2(\text{Cp}'\text{Co}(\text{CO}))_2$ <sup>20</sup> and  $(\mu\text{-CO})(\mu\text{-CMe}_2)[\text{CpRu}(\text{CO})]_2$ <sup>21</sup> which have activation free energies,  $\Delta G^\ddagger$ , of +17 kcal/mol<sup>-1</sup> at -10°C and +20 kcal/mol<sup>-1</sup> at 108°C respectively.) From the coalescence of the t-Butyl resonances of **21** at -30° C we can estimate that  $\Delta G^\ddagger$  for the process causing ligand scrambling in **21** is ca. +13 kcal/mol<sup>-1</sup> at -30°C.<sup>22</sup>

Complex **21** is extremely soluble in aromatic solvents and is soluble in ethereal solvents and pentane. In solution **21** is not stable. In aromatic solvents it decomposes at room temperature ( $\tau_{1/2} \sim 12$  hrs). Decomposition seems to be faster in ethereal solvents. It is quite moisture and air sensitive in solution. In the solid state **21** is more stable toward oxygen, lasting ca 2 hrs in dry air at room temperature, but it is still quite moisture sensitive. Acidolysis

Figure 2.2 Proposed Structure of **21**.

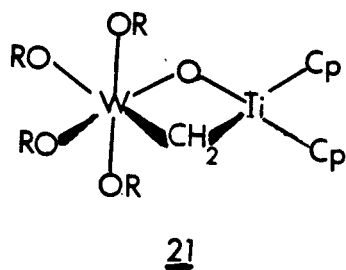
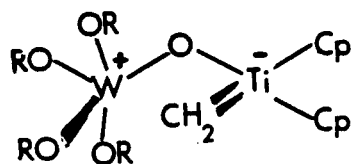
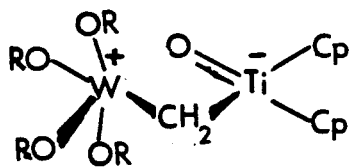
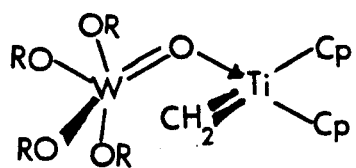
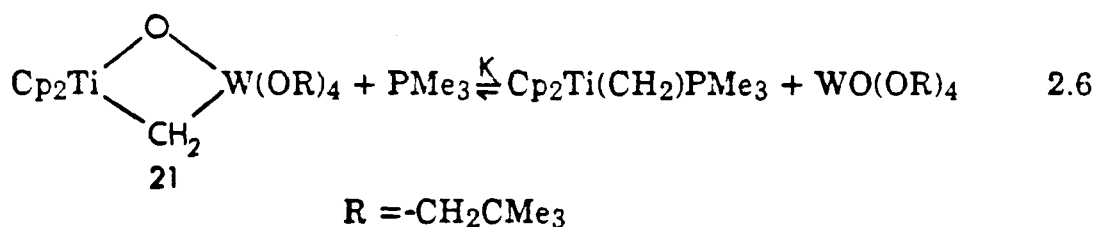


Figure 2.3 Possible Intermediates, Five-coordinate at Tungsten, Responsible for the Fluxional Behavior of **21**.



of **21** with excess HCl(g) yields  $\text{Cp}_2\text{TiCl}_2$ ,  $\text{HOCH}_2\text{CMe}_3$ ,  $\text{CH}_4$ , and an unidentified tungsten species; infrared evidence indicates that this species is not  $\text{WOCl}_4$ .

The reactivity of **21** was investigated. Unlike the Tebbe reagent,  $\text{Cp}_2\text{Ti}(\overline{\text{CH}_2\text{Al}(\text{Me})_2\text{Cl}})$ , **21** does not exhibit Wittig type reactivity; no terminal olefin is formed when **21** is treated with benzaldehyde or acetone. Addition of Lewis acids,  $\text{AlCl}_3$  and  $\text{AlMe}_2\text{Cl}$ , rapidly decomposed **21**; no new methyldiene species was observed. There is no reaction between **21** and  $\text{PPh}_3$ , but when **21** is treated with approximately ten equivalents of the smaller more basic phosphine,  $\text{PMe}_3$ , its dimer structure is disrupted yielding a mixture of  $\text{Cp}_2\text{Ti}(\text{CH}_2)\text{PMe}_3$ ,  $\text{WO}(\text{OCH}_2\text{CMe}_3)_4$ , **21**, and free phosphine (equation 2.6). The equilibrium constant,  $K$ , was determined to be  $6.2 \times 10^{-3}$  at room temperature,  $25^\circ\text{C}$ . Unlike



$$K = [\text{Cp}_2\text{Ti}(\text{CH}_2)\text{PMe}_3][\text{WO(OR)}_4] / [\text{21}][\text{PMe}_3]$$

some other  $\mu\text{-CH}_2$  containing complexes,<sup>35</sup> **21** does not readily react with CO; the reaction with CO was attempted with 300 torr and 50 psi of CO pressure. There is also no reaction between **21** and excess diphenylacetylene, a good trap for the  $\text{Cp}_2\text{TiCH}_2$  fragment.<sup>23</sup>

To date only one analog of **21** has been prepared by the reaction of **4** with a tungsten (VI) oxo complexes. The reaction of **4** with  $\text{WO}(\text{OCH}_2\text{SiMe}_3)_4$

produces a new complex, **22**, with physical properties similar to those of **21**. Unfortunately, although crystals of both **21** and **22** could be formed, they were unsuitable for structural analysis by x-ray diffraction methods. Attempts to prepare other analogs of **21** *via* the reaction of **4** with  $\text{WO}(\text{OMe})_4$ ,  $\text{WO}(\text{OCMe}_3)_4$ ,  $\text{WO}(\text{OCH}_2\text{Ph})_4$  were not successful; only complex mixtures of alkoxide containing species were observed in these reactions. The same reaction with  $\text{W}(\text{O})(\text{CH}_2\text{CMe}_3)_3\text{Cl}$  produced free alkane,  $\text{CMe}_4$  ( $^1\text{H}$  NMR), but no identifiable organometallic product was observed.

As can be seen from Table 2.1, all the metal oxo complexes reacted with " $\text{Cp}_2\text{TiCH}_2$ ", but led to no identifiable stable product. A number of reactions produced paramagnetic species *c.f.* reaction of  $\text{Mo}(\text{O})_2(\text{acac})_2$ ,  $\text{Mo}(\text{O})_2(\text{dtc})_2$  and  $\text{Re}(\text{O})\text{I}(\text{CH}_3\text{C}\equiv\text{CCH}_3)_2$ .

The only identifiable product in the reaction of  $\text{Mo}(\text{O})_2(\text{Me})_2(\text{bipy})$ , **6**, was  $\text{Cp}_2\text{Ti}(\text{CH}_3)\text{Cl}$ , no  $\text{Cp}_2\text{Ti}(\text{CH}_3)\text{Cl}$  was observed when the reaction was carried out in  $\text{CD}_2\text{Cl}_2$ . No Mo- $\text{CH}_2$  species was observed. The formation of  $\text{Cp}_2\text{Ti}(\text{CH}_3)\text{Cl}$  may indicate a radical reaction in which electron transfer occurs from  $\text{Cp}_2\text{TiCH}_2$ <sup>24</sup> to **6** followed by hydrogen abstraction from **6** to form  $\text{Cp}_2\text{Ti}(\text{CH}_3)$  which might then react with chlorinated solvent to form  $\text{Cp}_2\text{Ti}(\text{CH}_3)\text{Cl}$ . No identifiable product was observed when the reaction of **6** was repeated in either benzene- $\text{d}_6$  (NMR tube scale) or in toluene (preparative scale).

The  $^1\text{H}$  NMR spectrum of the reaction mixture of **4** with  $\text{Re}(\text{O})\text{Cl}_2(\text{OEt})(\text{PPh}_3)_2$ , **8**, exhibited multiplets in the spectral region  $\delta$  12-13, a region appropriate for terminal methyldiene complexes.<sup>15</sup> The reaction mixture was quite complex, and all attempts to cleanly isolate the species responsible for the downfield  $^1\text{H}$  NMR signals were not successful.

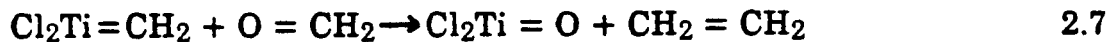
The reaction of 4 with rhenium oxo complexes similar to 8, *cis* and *trans*  $\text{Re}(\text{O})\text{Cl}_3(\text{PEt}_3)_2$  were also attempted. These reactions also led to complex reaction mixtures from which no identifiable compounds could be isolated.

The reaction of 4 with three Group 5 metal oxo complexes,  $\text{Cp}_2\text{Nb}(\text{O})\text{Cl}$ ,  $\text{Cp}_2\text{Nb}(\text{O})\text{nBu}$ , and  $\text{V}(\text{O})(\text{CH}_2\text{SiMe}_3)_3$ , was attempted. The niobium complexes reacted with 4 but no identifiable products could be isolated. The reaction of  $\text{V}(\text{O})(\text{CH}_2\text{SiMe}_3)_3$  with 4 produced free  $\text{SiMe}_4$  ( $^1\text{H}$  NMR). No identifiable organometallic product was observed.

## II.2.2 Discussion

The thermochemical data relating to transition metal methyldiene and oxo compounds is limited. Metal-oxygen bond energies of neutral and cationic metal monoxides have been measured.<sup>26</sup> Metal-carbon bond energies of cationic metal-methyldienes have been measured.<sup>27</sup> Metal-oxo and metal-methyldiene bond energies have not been determined experimentally in systems in which the metal center is surrounded by a realistic, in a synthetic sense, array of ligands. Theoretical calculations provide a means for estimation of thermochemical values in these systems.

Rappé and Goddard<sup>28</sup> have calculated bond energies for a number of systems (Table 2.3) including  $\text{Cl}_2\text{TiCH}_2$ , a model for the reactive  $\text{Cp}_2\text{TiCH}_2$  fragment. The oxophilic nature of titanium can be seen from the data in Table 2.3. The difference in titanium-oxo and titanium methyldiene bond strengths is quite large, larger than in the other systems shown in Table 2.3. This large bond energy difference is the driving force for the Wittig reactivity of titanium methyldiene. Using bond energies<sup>29</sup> for formaldehyde,  $D(\text{C}=\text{O}) = 175 \text{ kcal/mol}^{-1}$ , and ethylene,  $D(\text{C}=\text{C}) = 163 \text{ kcal/mol}^{-1}$ , and the values from Table 2.3, leads to a calculated exothermicity of  $50 \text{ kcal/mol}^{-1}$  for the reaction shown in equation 2.7 despite the large C-O double bond strength.



$$\Delta H \sim -50 \text{ kcal/mol}^{-1}$$

Table 2.3 Theoretical Values for Metal Oxo and Metal Methylidene Bond Energies

$L_nM$	$D(M=X)$ kcal/mol <sup>-1</sup>	
	$X = O$	$X = CH_2$
$Cl_2Ti$	140	78
$Cl_2(O)Cr$	51	48
$Cl_2(O)Mo$	79	71
$Cl_4Cr$	82	--
$Cl_4Mo$	102	--

It should be noted that the oxo ligand in  $Cl_2TiO$  is triply bonded to the metal. In the experimentally studied titanocene system, the orbital required to make the third Ti-O bond is destabilized due to strong interaction with the cyclopentadienyl rings so that the actual bond strength should be somewhat lower than predicted by the model system. Data from Table 2.3 seem to indicate that the third metal oxo bond is probably worth a maximum of 20-30 kcal/mol<sup>-1</sup> (compare  $Cr(O)_2Cl_2$  with  $CrOCl_4$  and  $Mo(O)_2Cl_2$  with  $MoOCl_4$ ).<sup>30</sup> Even subtracting this amount from the Ti-O bond strength in  $Cl_2TiO$  leaves the difference between titanium oxo and titanium methylidene bond strengths larger than the corresponding differences in other metal systems. Thus, we expected that methylene transfer between  $Cp_2TiCH_2$  and metal oxo complexes to form a new terminal methylidene complex would be exothermic; however, in the cleanest reactions studied, the formation of **21** and **22**, the methylene transfer stops half-way forming the dibridged  $\mu$ -O-

$\mu\text{CH}_2$  complexes. The dibridged species is thermodynamically more stable than a mixture of two species, having terminal ligands.

The greater stability of species with bridging ligands relative to similar species with the same ligands in terminal positions has been investigated theoretically. Lichtenberger<sup>31</sup> has done comparative Fenske-Hall calculations on the unknown monomeric species,  $\text{CpMn}(\text{CO})_2(\text{CH}_2)$ , and the known dimer  $(\mu\text{-CH}_2)[\text{CpMn}(\text{CO})_2]_2$ . He finds the species with the bridging methyldene ligand is greatly stabilized relative to the terminal methyldene species due to the strong interactions between the frontier orbitals of  $\text{CH}_2$  and the frontier orbitals of the metal dimer fragment (Figure 2.4). Hoffmann<sup>32</sup> using extended-Hückel calculations has studied  $\text{M}_2\text{L}_8\text{E}_2$  systems and found that similar interactions (Figure 2.5) make the dibridged species  $(\mu\text{-E})_2(\text{ML}_4)_2$ , more stable than the species with E in a terminal position for formally  $d^0$  metal centers.

The  $\text{Cp}_2\text{Ti}$  fragment<sup>33</sup> and the  $\text{W}(\text{OCH}_2\text{XMe}_3)_4$  ( $\text{X} = \text{C}, \text{Si}$ ) fragment have frontier orbitals of the proper symmetry to interact with the frontier orbitals of the methyldene and oxo ligands (Figure 2.6). Both metal centers are formally  $d^0$ , and thus, the theoretical results (vide supra) would indicate that the dibridged structures of 21 and 22 should be the most stable as observed. To disrupt the dibridged structure requires conversion of four  $\sigma$  bonds to two  $\sigma$  bonds and two  $\pi$  bonds. The MO arguments (vide supra) simply boil down to the fact that in these high valent metal systems  $\sigma$  bonding is more important than  $\pi$  bonding.

The dibridged structure of 21 can be disrupted by the addition of a very good ligand,  $\text{PMe}_3$ . The equilibrium constant measured for this reaction,  $K = 6.2 \times 10^{-3}$ , shows that  $\Delta G_{298}$  for reaction shown in equation 2.6 is 3.0



Figure 2.4. Orbital Interaction Diagram at the Frontier Orbitals of  $\text{CH}_2$  and the Frontier Orbitals of a Metal Dimer Fragment.<sup>31</sup>

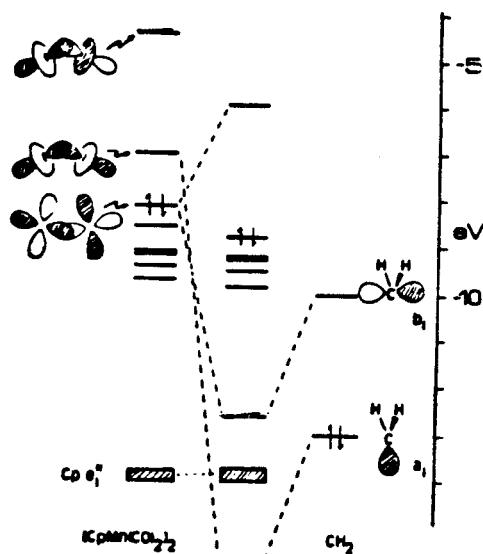


Figure 2.5. Orbital Interactions for a Dibridged Complex  $(\mu\text{-E})_2(\text{ML}_4)_2$ .<sup>32</sup>

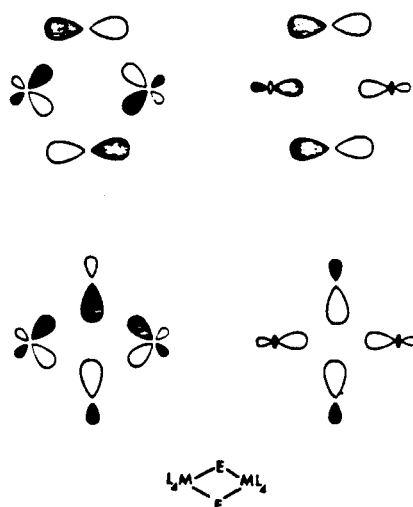
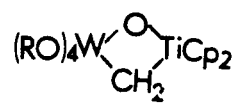
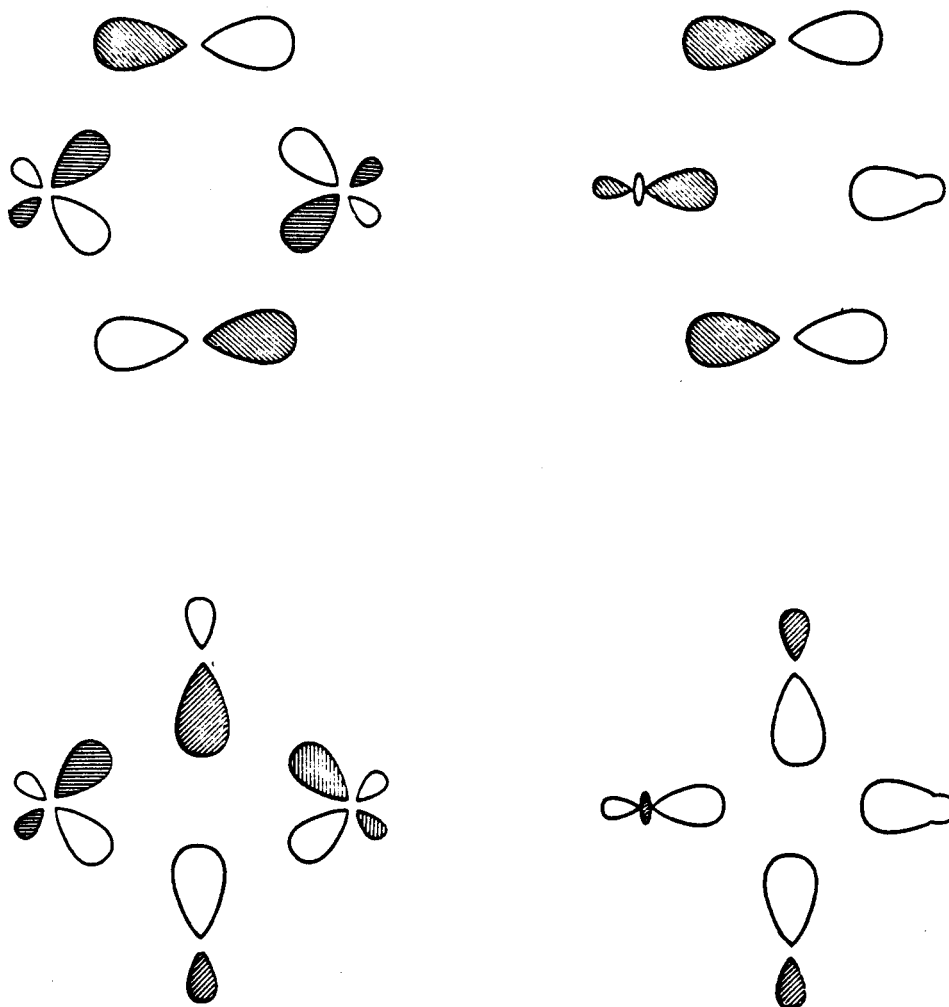
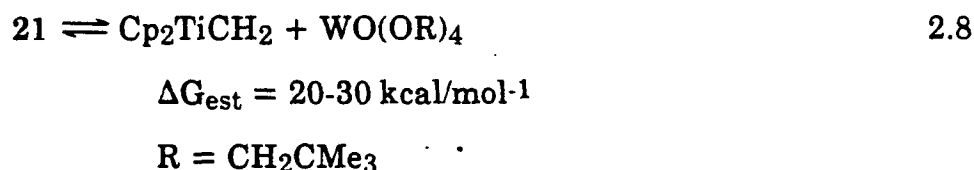


Figure 2.6. Orbital Interaction for  $(\mu\text{-O})(\mu\text{-CH}_2)[\text{Cp}_2\text{Ti}][\text{W}(\text{OR})_4]$



kcal/mol<sup>-1</sup>. Making several assumptions,<sup>34</sup> we can crudely estimate that the free energy change required to break up **21** is on the order of 20-30 kcal/mol<sup>-1</sup> (equation 2.8). This is approximately twice the energy required to break one bridge, as estimated from the 13 kcal/mol<sup>-1</sup> barrier for alkoxide scrambling (vide supra).



Thus, it is not surprising that **21** is not easily disrupted by added reagents. No Wittig chemistry is observed with organic carbonyl compounds. No reaction occurs with diphenyl acetylene, CO, or PPh<sub>3</sub>. Possibly, these reagents are not nucleophilic enough to disrupt the structure of **21**. The low reactivity of **21** is reminiscent of the low reactivity of the dibridged species, (μ-CH<sub>2</sub>)<sub>2</sub>[TiCp<sub>2</sub>]<sub>2</sub> formed by the formal dimerization of two Cp<sub>2</sub>TiCH<sub>2</sub> fragments.<sup>37</sup>

Compounds **21** and **22** are the only examples of isolated μ-O-μ-CH<sub>2</sub> species. Marks<sup>38</sup> has found evidence that such species can form when actinide alkyls interact with alumina supports. Compounds **21** and **22** may be models for species formed in reactions involving catalysts supported on metal oxides. Thus, this structure of these complexes would be interesting. Unfortunately, although crystals of both **21** and **22** could be formed, they did not diffract well enough for structural analysis by x-ray diffraction methods.

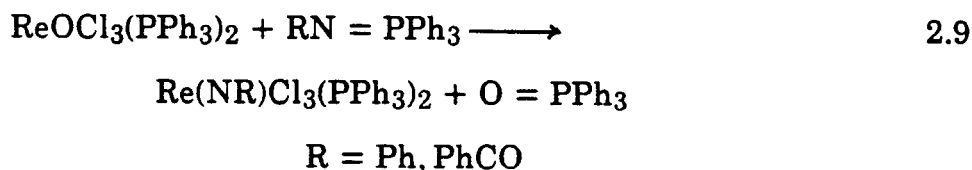
Our failure to make analogs of **21** and **22** and the results of the reaction of **4** with other metal oxo complexes (Table 2.1) indicate that, in

general, metal oxo complexes probably have too many reactive pathways to allow clean production of new methyldene complexes by reaction with  $\text{Cp}_2\text{TiCH}_2$ . Metal oxo complexes are good oxidizing agents,<sup>17</sup> and  $\text{Cp}_2\text{TiCH}_2$  has been shown to act as a reducing agent.<sup>25</sup> Thus, electron transfer processes to form odd-electron species is not surprising. Most of the oxo complexes studied have electronegative ligands like halides or alkoxides. Recent work in our laboratory<sup>39</sup> has shown that  $\text{Cp}_2\text{TiCH}_2$  can insert into the bonds between transition metals and such ligands. The reaction of **4** with some metal oxo complexes having alkyl ligands instead of electronegative ligands were tried, but without success. Free alkane derived from the alkyl ligands was the only identifiable product from the reaction of **4** with  $\text{VO}(\text{CH}_2\text{SiMe}_3)_3$ , **20**, and  $\text{WO}(\text{CH}_2\text{CMe}_3)_3\text{Cl}$ , **10**. Osborn<sup>40</sup> has found that the interaction of Lewis acids with metal oxo complexes bearing alkyl ligands can induce  $\alpha$ -hydrogen abstraction producing free alkane and an alkylidene complex. The  $14e$  fragment  $\text{Cp}_2\text{TiCH}_2$  has never been observed free in solution and is expected to be quite Lewis acidic. Hence, production of alkane from the reaction of **4** with **10** and **20** may be due to the induction of  $\alpha$ -hydrogen abstraction reactions. Clean reaction of  $\text{Cp}_2\text{TiCH}_2$  with metal oxo complexes in a Wittig manner is atypical. The clean production of **21** and **22** may be due to the fact that the alkoxide ligands in those systems stabilized the high oxidation state of tungsten, preventing redox side reactions, and were of the right steric bulk to prevent ready insertion of  $\text{Cp}_2\text{TiCH}_2$  into the metal alkoxide bonds while still allowing reaction at the oxo ligand. Clearly, the reaction of  $\text{Cp}_2\text{TiCH}_2$  with metal oxo complexes does not provide a general route to metal methyldene complexes.

## II.3 Reactivity of $\text{CH}_2\text{PPh}_3$ with Metal Oxo Complexes

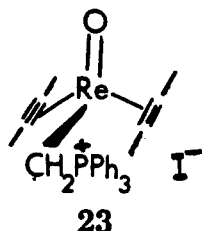
### II.3.1 Results

Chatt and Dilworth<sup>41</sup> have reported that the reactions of phosphinimenes with  $\text{ReOCl}_3(\text{PPh}_3)_2$  cleanly give rhenium imido complexes (equation 2.9). We thought that the analogous reaction of  $\text{ReOCl}_3(\text{PPh}_3)_2$  with



$\text{CH}_2\text{PPh}_3$  possibly might lead to the formation of a terminal methyldiene complex. Upon attempting this reaction we found that  $\text{ReOCl}_3(\text{PPh}_3)_2$  rapidly reacts with more than one equivalent of  $\text{CH}_2\text{PPh}_3$  leaving unreacted starting rhenium oxo and producing an intractable solid;  $^{31}\text{P}$  NMR of the reaction mixture shows no  $\text{OPPh}_3$  is formed.

Reaction of  $\text{Re}(\text{O})\text{I}(\text{CH}_3\text{C}\equiv\text{CCH}_3)_2$  with  $\text{CH}_2\text{PPh}_3$  in benzene yields a new compound insoluble in benzene but readily soluble in chlorinated solvents. This solubility indicates that the new compound is a salt. Infrared data indicate that the terminal oxo ligand remains. We formulate the new product as a cationic ylide complex, **23**, in which the  $\text{CH}_2\text{PPh}_3$  moiety has displaced the iodide



from the starting oxo complex. The NMR data (Table 2.4) are consistent with this formulation. Such a displacement of halide by  $\text{CH}_2\text{PPh}_3$  has been observed in the reaction of  $\text{Cp}_2\text{MCl}_2$  ( $\text{M} = \text{Ti}, \text{Zr}$ ) with  $\text{CH}_2\text{PMe}_3$ .<sup>42</sup>

The reaction of  $\text{WO}(\text{OCH}_2\text{CMe}_3)_4$  with one equivalent of  $\text{CH}_2\text{PPh}_3$  produces a mixture of compounds from which the salt  $[\text{CH}_3\text{PPh}_3]^+ [\text{WO}(\text{OCH}_2\text{CMe}_3)_5]^-$ , **24**, can be isolated. The crude reaction mixture contains 50% of **24**. The other species present have not been identified as no other species can be cleanly isolated. The reaction mixture slowly deposits colorless insoluble material possibly indicating that the other species present are not stable.

Acidolysis of the reaction mixture with excess trifluoroacetic acid produces neopentyl alcohol as the only volatile organic product ( $^1\text{H}$  NMR and GC). Acidolysis with  $\text{CF}_3\text{COOD}$  shows no deuterium incorporation into the neopentyl alcohol produced (except of course in the hydroxyl position  $^1\text{H}$  and  $^2\text{H}$  NMR). Thus, it is unlikely that the proton needed to form  $\text{CH}_3\text{PPh}_3^+$  came from the neopentoxy ligands of  $\text{WO}(\text{OCH}_2\text{CMe}_3)_4$ .

A possible mechanism for the formation of a mixture of 50% **24** and 50% of other alkoxide containing species is shown in Scheme 1. The displacement of anionic ligands by  $\text{CH}_2\text{PPh}_3$  has been observed (vide supra) so that the formation of **25** has precedence. Since the methylene group is bonded



Table 2.4 (continued)

	Infrared				
			$\delta^a$ (ppm)		Assignment
		$^{31}\text{P}\{\text{H}\}(\text{CDCl}_3)$	+ 34.7		
	(KBr) 955 $\text{cm}^{-1}$ (Re = O)				
$\text{WO}(\text{OCH}_2\text{CMe}_3)_4$		$^1\text{H}(\text{C}_6\text{D}_6)$	4.53 1.01	(s, 8H) (s, 36H)	$\text{OCH}_2\text{CMe}_3$ $\text{OCH}_2\text{CMe}_3$
	( $\text{C}_6\text{D}_6$ ) 960 $\text{cm}^{-1}$ (W = O)				
	(KBr) 890 $\text{cm}^{-1}$				



Table 2.4 (continued)

	Infrared				Assignment
		<sup>1</sup> H (C <sub>6</sub> D <sub>6</sub> )	δ a (ppm)		
[ClH <sub>3</sub> PPh <sub>3</sub> ] <sup>+</sup> [WO(OC(H) <sub>2</sub> CMe <sub>3</sub> ) <sub>5</sub> ] <sup>-</sup>		<sup>1</sup> H (THF-d <sub>8</sub> )	6.9-7.9 4.62 4.52 3.11 1.39 1.23	(m, 15H) (s, 8H) (s, 2H) (d, J <sub>PH</sub> = 13 Hz, 3H) (s, 9H) (s, 36H)	ClH <sub>3</sub> PPh <sub>3</sub> eq OC(H) <sub>2</sub> CMe <sub>3</sub> ax OC(H) <sub>2</sub> CMe <sub>3</sub> ClH <sub>3</sub> PPh <sub>3</sub> ax OC(H) <sub>2</sub> CMe <sub>3</sub> eq OC(H) <sub>2</sub> CMe <sub>3</sub>
			7.5-8.1 4.16 3.90 3.33 0.89 0.85	(m, 15H) (s, 8H) (s, 2H) (d, J <sub>PH</sub> = 14 Hz, 3H) (s, 9H) (s, 36H)	

Table 2.4 (continued)

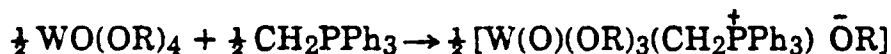
	Infrared				Assignment
		$^{13}\text{C}\{^1\text{H}\}$ (THF- $d_8$ )	$\delta^a$ (ppm)		
			135.2 135.7 130.7 118.0  84.1 78.5 35.1 34.5 28.2 27.8 9.3	(d, $J_{\text{CP}} = 11$ Hz) (d, $J_{\text{CP}} = 39$ Hz) (d, $J_{\text{CP}} = 82$ Hz)       (d, $J_{\text{PC}} = 56.1$ )	$\text{CH}_3\text{PPh}_3$  eq $\text{OCH}_2\text{CMe}_3$ ax $\text{OCH}_2\text{CMe}_3$ eq $\text{OCH}_2\text{CMe}_3$ ax $\text{OCH}_2\text{CMe}_3$ eq $\text{OCH}_2\text{CMe}_3$ ax $\text{OCH}_2\text{CMe}_3$ eq $\text{OCH}_2\text{CMe}_3$ $\text{CH}_3\text{PPh}$
		$^{31}\text{P}\{^1\text{H}\}$ ( $\text{C}_6\text{D}_6$ )	21.6		
	$(\text{C}_6\text{D}_6)$ 875 $\text{cm}^{-1}$ $\nu$ ( $W = 0$ )				

a. All spectra were recorded at room temperature.  $^1\text{H}$  and  $^{13}\text{C}$  shifts are relative to signals due to solvent.  $^1\text{H}$  NMR:  $\text{C}_6\text{D}_6$ ,  $\delta$  7.15;  $\text{CD}_2\text{Cl}_2$ ,  $\delta$  5.32; THF- $d_8$   $\delta$  1.73.  $^{13}\text{C}$  NMR:  $\text{C}_6\text{D}_6$ ,  $\delta$  128;  $\text{CD}_2\text{Cl}_2$ ,  $\delta$  53.8; THF- $d_8$   $\delta$  25.3.  $^{31}\text{P}$  shifts are relative to external 85%  $\text{H}_3\text{PO}_4$ .

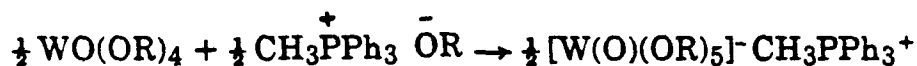
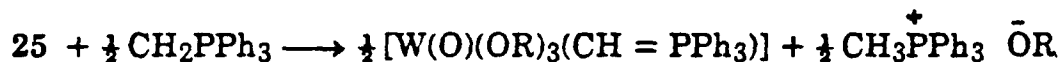
b.  $J_{\text{CH}}$  measured from  $^{13}\text{C}$  satellites in  $^1\text{H}$  spectrum is 132.9 Hz.

between a positively charged phosphorous center and a high valent metal center, its hydrogen atoms should be acidic. Rapid deprotonation of **25** would produce **26** and  $\text{CH}_3\text{PPh}_3^+ \text{OR}^-$  ( $\text{R}=\text{CH}_2\text{CMe}_3$ ) which may react with  $\text{WO}(\text{OR})_4$  to form **24**. Such displacements of anionic ligands followed by rapid deprotonation to form species analogous to **26** have been observed in the formation of  $\text{Cp}_2\text{M}(\text{CHPPh}_3)\text{Cl}$  ( $\text{M} = \text{Zr}, \text{Hf}$ ) from the reaction of  $\text{Cp}_2\text{MCl}_2$  with  $\text{CH}_2\text{PPh}_3$ .<sup>43</sup> It is also analogous to the formation of an acylated phosphorane in the reaction of  $\text{CH}_2\text{PPh}_3$  with organic esters (vide supra).

#### Scheme 1



**25**



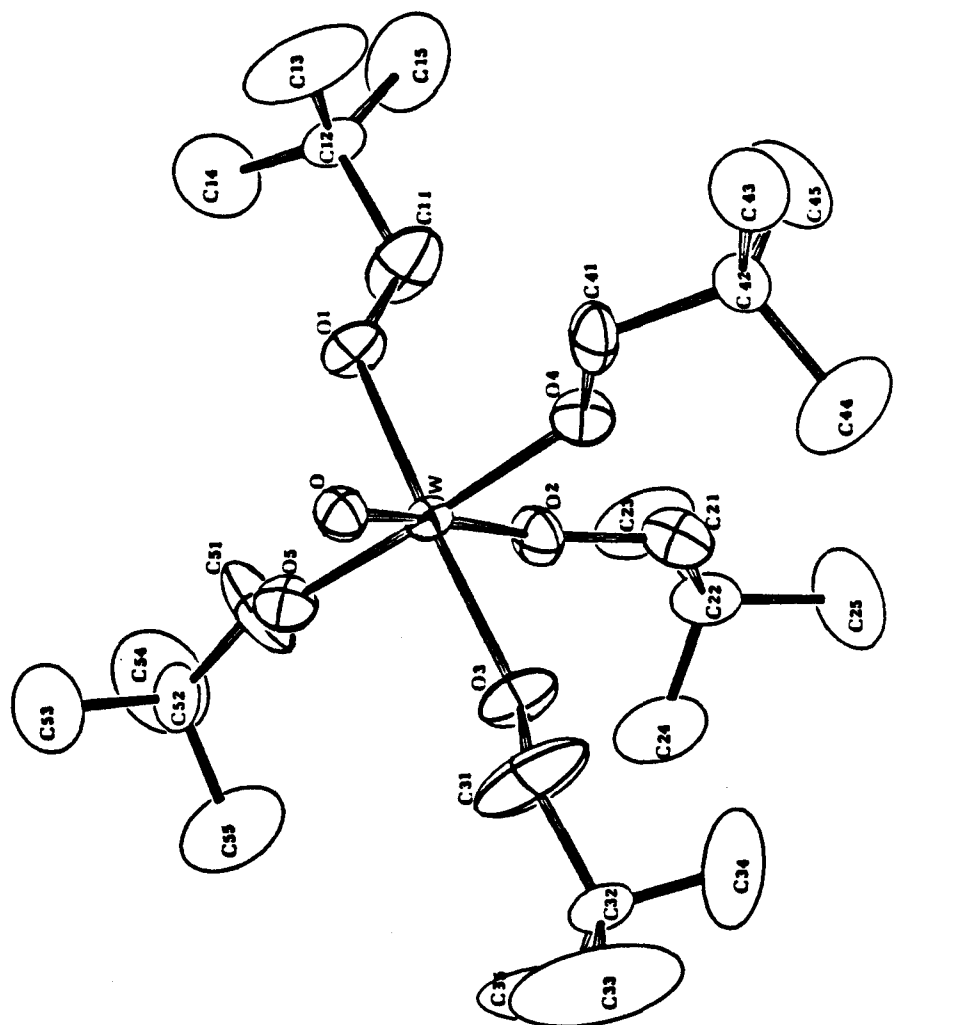
**24**



If one equivalent of neopentyl alcohol is added to the reaction mixture of **5** and  $\text{CH}_2\text{PPh}_3$ , **24**, is the only product produced ( $^1\text{H}$  NMR). In preparative scale reactions, **24**, can be isolated in good yield as colorless crystalline material.

A crystal of **24** was found suitable for a structure determination by x-ray diffraction methods. The structure of the cation,  $\text{CH}_3\text{PPh}_3^+$ , is unexceptional. The structure of the  $\text{WO}(\text{OCH}_2\text{CMe}_3)_5^-$  anion is shown in Figure 2.7. The geometry about tungsten is a distorted-octahedral one. The short W-O (oxo) bond distance, 1.693(5) Å, shows a high degree of multiple bonding between the oxygen and tungsten.<sup>44</sup> Repulsion between the  $\pi$  electrons of the tungsten-oxo bond<sup>45</sup> and the alkoxide ligands *cis* to the oxo ligand, bends these ligands down slightly away from the oxo ligand, and the average O-W-O(*cis*-alkoxide) angle is 93.8(2). The W-O(alkoxy) distance in **24**, 1.934(5) (average), is short enough to be suggestive of some alkoxy-to-tungsten  $\pi$  bonding.<sup>44</sup> The large W-OX-CX1 (X = 1-5) angles, 132.0(6) (average), may be an indication of alkoxy  $\pi$  bonding;<sup>46</sup> however, steric interactions between the ligands probably play the major role in determining these angles. Although the oxo ligand has a large *trans* influence,<sup>47</sup> the W-O(alkoxy) distance is no greater for the alkoxide *trans* to the oxo ligand than it is for the alkoxides *cis* to that ligand.

The presence of a good  $\pi$ -donating ligand *trans* to the oxo ligand would be expected to weaken the W-O(oxo) bond. Such a weakening may be indicated by changes in the W-O(oxo) stretching frequency. In  $\text{WO}(\text{OCH}_2\text{CMe}_3)_4$  this frequency is 960  $\text{cm}^{-1}$  (in  $\text{C}_6\text{D}_6$ ) while in **24**, with a good  $\pi$ -donating alkoxide *trans* to the oxo, it is lower, 875  $\text{cm}^{-1}$ . Interestingly, the infrared spectrum of  $\text{WO}(\text{OCH}_2\text{CMe}_3)_4$  in a KBr pellet shows the oxo stretch at 890  $\text{cm}^{-1}$ . Possibly a solid state reaction occurs to produce  $\text{K}^+[\text{WO}(\text{OCH}_2\text{CMe}_3)_4\text{Br}]^-$  in the KBr pellet.

Figure 2.7 – Ortep Drawing of  $[\text{WO}(\text{OCH}_2\text{CMe}_3)_5]^-$ 

ATOM	ATOM	DISTANCE
W	O	1.6931
W	O1	1.9634
W	O2	1.9784
W	O3	1.9703
W	O4	1.8859
W	O5	1.8840
O1	C11	1.2866
O2	C21	1.4316
O3	C31	1.1894
O4	C41	1.3626
O5	C51	1.3409

ATOM	ATOM	ANGLE
O1	W	96.64
O2	W	174.21
O3	W	91.22
O4	W	93.99
O5	W	93.34
O2	W	88.82
O3	W	172.08
O4	W	88.37
O5	W	86.26
O3	W	83.35
O4	W	84.30
O5	W	88.93
O4	W	92.09
O5	W	92.33
O6	W	171.43
C11	O1	131.76
C21	O2	131.62
C31	O3	138.30
C41	O4	127.06
C51	O5	131.37

Reaction of  $\text{CH}_2\text{PPh}_3$  with *trans*- $\text{ReOCl}_3(\text{PEt}_3)_2$  and  $\text{Cp}_2\text{Nb}(\text{O})\text{Cl}$  led to intractable materials. No  $\text{OPPh}_3$  was formed in these reactions ( $^{31}\text{P}$  NMR) so methylene transfer did not occur.

### II.3.2 Discussion

Phosphorous ylides exhibit a wide variety of reactions with transition metal complexes.<sup>48</sup> Since the reaction of phosphinimines with metal oxo complexes can cleanly produce metal imido complexes, we felt that the reaction of phosphorous ylides with oxo complexes might produce methyldiene complexes in a reaction analogous to the Wittig reaction in organic chemistry. In the systems we have studied we have found that this reaction does not lead to methyldiene complexes, but instead,  $\text{CH}_2\text{PPh}_3$  acts as a powerful alkylating agent and apparently does not interact with the oxo ligand at all. Such reactivity is analogous to the reactivity of  $\text{CH}_2\text{PPh}_3$  with organic carbonyls bearing good leaving groups (vide supra).

Since  $\text{ReOCl}_3(\text{PPh}_3)_2$  bears three chloride ligands, multiple alkylation is possible, leading to the uptake of more than one equivalent of  $\text{CH}_2\text{PPh}_3$  and the formation of intractable material.  $\text{Re}(\text{O})\text{I}(\text{CH}_3\text{C}\equiv\text{CCH}_3)_2$  bears only one good anionic leaving group, the iodide, and its reaction with  $\text{CH}_2\text{PPh}_3$  leads cleanly to **23**. In **23** there appears to be no interaction between the oxo ligand and the phosphorous atom, the  $^{31}\text{P}$  chemical shift is more consistent with a phosphonium cation than five-coordinate phosphorous,<sup>49</sup> and the Re-O stretching frequency is not too different from its value in  $\text{ReOI}(\text{CH}_3\text{C}\equiv\text{CCH}_3)_2$ .

When  $\text{CH}_2\text{PPh}_3$  is bonded to a low valent metal center as in **23**, formally a  $\text{Re(III)}$  complex, the methylene protons are not lost readily. In the reaction of the high valent complex,  $\text{WO}(\text{OCH}_2\text{CMe}_3)_4$ , with  $\text{CH}_2\text{PPh}_3$  deprotonation of the intermediate phosphonium species, **25**, apparently can occur readily.

The metal oxo complexes used in this study all had other alkoxide or halide ligands. Apparently in the reaction with  $\text{CH}_2\text{PPh}_3$  these ligands can act as good leaving groups in these inorganic systems just like they do in organic systems in the reaction of  $\text{CH}_2\text{PPh}_3$  with esters or acid halides. The reaction of  $\text{CH}_2\text{PPh}_3$  with oxo complexes having only alkyl ligands was not investigated. Possibly such reactions could lead to methylene transfer; however, the lack of interaction between the oxo ligand and a cationic phosphorous center in **23** may indicate the oxo ligand would be generally inert toward attack by phosphorous ylides. This inertness could easily arise from the high multiple bond character of metal oxo bonds. Thus, reaction of metal oxo complexes with  $\text{CH}_2\text{PPh}_3$  in a Wittig manner does not appear to be a viable means to produce metal methyldene complexes.

## II.4 Conclusions

The reaction of metal oxo complexes with the methylenation reagents  $\text{Cp}_2\text{TiCH}_2$  or  $\text{CH}_2\text{PPh}_3$  is not a viable method to synthesize new metal methyldene complexes. The oxo ligand appears to be the least reactive ligand in the metal oxo complexes. In certain instances when the auxiliary ligands have the proper electronic and steric characteristics, clean reactions of metal

oxo complexes with these reagents can occur, but most often the reactions lead to complex reaction mixtures.



## II.5 Experimental Section

All manipulations of air and/or moisture sensitive compounds were carried out either with the use of standard Schlenk or vacuum line techniques or in a N<sub>2</sub>-filled Vacuum Atmospheres Dri-Lab equipped with an Mo-40-1 purification train and a DK-3E Dri-Kool. The argon used in Schlenk work was purified by passage through columns of BASF-RS-11 (Chemalog) and Linde 4Å molecular sieves.

The solvents used were treated as follows. Pentane was freed of olefinic impurities by stirring over conc. H<sub>2</sub>SO<sub>4</sub>. It was washed with water, pre-dried over anhydrous MgSO<sub>4</sub> and dried with CaH<sub>2</sub>. It was degassed and stirred over sodium benzophenone ketyl solubilized by the addition of a small amount of tetraglyme. Toluene, diethyl ether, tetrahydrofuran, benzene, benzene-d<sub>6</sub>, and toluene-d<sub>8</sub> were degassed and stirred over sodium benzophenone ketyl. Methylene chloride-d<sub>2</sub> and chloroform-d<sub>1</sub> were stirred over CaH<sub>2</sub> and degassed by several freeze-pump-thaw cycles. All solvents were vacuum transferred into dry storage flasks equipped with Teflon closures and stored under Ar.

Metallacycle, 4,<sup>6</sup> WO(OMe)<sub>4</sub>,<sup>50</sup> WO(OCH<sub>2</sub>Ph)<sub>4</sub>,<sup>50</sup> WO(CH<sub>2</sub>CMe<sub>3</sub>)<sub>3</sub>-Cl,<sup>51</sup> Mo(O)<sub>2</sub>(Me)<sub>2</sub>(bipy),<sup>52</sup> Mo(O)<sub>2</sub>(dtc)<sub>2</sub>,<sup>53</sup> Mo(O)<sub>2</sub>(acac)<sub>2</sub>,<sup>54</sup> Re(O)I-(CH<sub>3</sub>C=CCH<sub>3</sub>)<sub>2</sub>,<sup>55</sup> Re(O)Cl<sub>2</sub>(OEt)(PPh<sub>3</sub>)<sub>2</sub>,<sup>56</sup> Re(O)Cl<sub>3</sub>(PPh<sub>3</sub>)<sub>2</sub>,<sup>56</sup> *cis* and *trans* Re(O)Cl<sub>3</sub>(PEt<sub>3</sub>)<sub>2</sub>,<sup>57</sup> Cp<sub>2</sub>Nb(O)Cl,<sup>58</sup> Cp<sub>2</sub>Nb(O)(nBu),<sup>59</sup> VO(CH<sub>2</sub>SiMe<sub>3</sub>)<sub>3</sub>,<sup>60</sup> and salt-free CH<sub>2</sub>PPh<sub>3</sub><sup>61</sup> were prepared by literature methods. WO(OCMe<sub>3</sub>)<sub>4</sub> was prepared by K. C. Ott. WOCl<sub>4</sub> was prepared by reacting WO<sub>3</sub> or Na<sub>2</sub>WO<sub>4</sub>·2H<sub>2</sub>O with refluxing SOCl<sub>2</sub>.<sup>62</sup> The SOCl<sub>2</sub> was removed *in vacuo* and the product isolated by sublimation (120°C 0.001 torr). Acetone was vacuum

transferred from  $\text{MgSO}_4$  and stored under Ar. Benzaldehyde was freshly distilled before use. Trimethylphosphine (Strem) was distilled from Na, degassed, and stored under vacuum in a tube equipped with a Teflon closure. Diphenylacetylene, triphenyl phosphine, carbon monoxide, aluminium trichloride, dimethyl aluminium chloride (Texas Alkyls) were used as received.

NMR spectra were recorded using a Varian EM-390 (CW 90 MHz) or a JEOL FX-90Q (FT 90 MHz) spectrometer. Infrared spectra were recorded on a Shmadzu IR-4354 spectrophotometer. Analyses were performed by Schwarzkopft Microanalytical Laboratory or Mic/Anal Inc.

All reactions of 4 with metal oxo complexes were first investigated on an NMR tube scale with reagents concentrations on the order of 0.1 M. For room temperature reactions the solid reagents were weighed into an NMR tube in the dry box. The tube was fitted with a rubber septum and ca 400  $\mu\text{l}$  of solvent was added *via* syringe. For low temperature reactions the reagents were weighed into an NMR tube which was then fitted to a Teflon needle valve adaptor *via* an O-ring fitting. Through this adapter the tube could be attached to a vacuum line, evacuated, cooled to 77K ( $\text{LN}_2$ ) and solvent vacuum transferred in. The tube was then sealed with a torch and warmed to the desired temperature.

#### Preparation of $\text{WO}(\text{OCH}_2\text{XMe}_2)_4$ ( $\text{X} = \text{C}, \text{Si}$ ) (5) and (6)

Under an argon atmosphere, 3.4g (10 mmol) of  $\text{WOCl}_4$  is dissolved in 50 ml of benzene. Against a counter-flow of argon, 13.7g (155 mmol) of solid neo-pentyl alcohol is added to the red solution. The reaction mixture is heated to reflux for 30 min and changes color from red to greenish-yellow. The mixture is cooled to room temperature and anhydrous ammonia is bubbled

through the solution causing the precipitation of  $\text{NH}_4\text{Cl}$ . The resulting suspension is filtered through Celite to yield a light yellow filtrate. Removal of the volatiles from the filtrate *in vacuo* leaves a light yellow solid. The solid is dissolved in 50 ml of boiling pentane. The pentane solution is cooled to  $-20^\circ\text{C}$  and the product precipitates as a white powder which is isolated by decanting off the mother liquor and drying *in vacuo*. A second crop of material may be obtained by concentration of the mother liquor (Yield 3.1g, 57%). The product is rapidly hydrolyzed in air and must be stored under an inert atmosphere.  $^1\text{H}$  NMR data are shown in Table 2.4. IR  $\text{C}_6\text{D}_6$  solution: 2950 (s), 2895 (m), 2850 (m), 1475 (m), 1460 (m), 1385 (m), 1360 (m), 1210 (w), 1040 (s,br), 1020 (s), 960 (m), 850 (w,br), 800 (w,br), 725 (w), 660 (s,br), 450 (w). IR KBr pellet: 2930 (s,br), 2870 (s,br), 1475 (m), 1460 (m), 1390(m), 1360 (m), 1282 (w), 1258 (w), 1215 (w), 1199 (w), 1041 (s,br), 1015 (s,br), 890 (m,br), 750 (w).

The same method was used to prepare  $\text{WO}(\text{OCH}_2\text{SiMe}_3)_4$  in low yield (3%).  $^1\text{H}$  NMR  $\text{C}_6\text{D}_6$ :  $\delta$  4.67 (s,8H), 0.27 (s,36H).

Preparation of  $(\mu\text{-CH}_2)(\mu\text{-O})[\text{Cp}_2\text{Ti}][\text{W}(\text{OCH}_2\text{XMe}_3)_4]$  ( $\text{X} = \text{C}, \text{Si}$ ) (21) and (22)

In a Schlenk tube, 100 mg (0.4 mmol) of 4 and 220 mg (0.4 mmol) of 5 are dissolved in 30 ml of pentane at  $0^\circ\text{C}$ . The reaction mixture is stirred 1 hr at  $0^\circ\text{C}$  changing color from brownish-red to cherry red. The solution is filtered and concentrated until solids begin to appear. The solution is cooled to  $-50^\circ\text{C}$ . The product comes out of solution as a pink powder which is isolated by decanting off the mother liquor. The powder is redissolved in a minimum of a pentane-toluene, 10:1 (v/v), mixture at room temperature. The resulting solution is slowly cooled to  $-50^\circ\text{C}$  and product, 21, crystallizes out as cherry-red platelets. (Yield 90 mg, 28%). Calculated for  $\text{C}_{31}\text{H}_{56}\text{TiW}$ : C, 50.28; H,

7.62. Found: C, 51.09; H, 7.84. NMR data are shown in Table 2.2. IR  $C_6D_6$  solution: 2940 (s), 2870 (sh), 2750 (w), 1485 (w), 1460 (w,br), 1385 (w), 1340 (w), 1105 (m), 1070 (s), 1045 (s), 1020 (s), 800 (m,br), 750 (w), 725 (w), 690 (m,sh), 650 (m), 630 (m,sh). IR is essentially the same in a KBr pellet.

The same method was used to prepare **22** isolated as cherry red platelets in 10% yield. The NMR data are shown in Table 2.2.

### Variable -Temperature NMR Study of 21

An NMR tube was charged with a solution of 10 mg of **21** in 400  $\mu$ l of toluene- $d_8$ .  $^1H$  NMR spectra were recorded on the FX-90Q (90 MHz) spectrometer over the range  $-78^\circ C$  to  $+20^\circ C$ . The results are shown in Figure 2.1.

### Acidolysis of 21

In the dry box, a solution of 12 mg of **21** in  $C_6D_6$  was loaded into an NMR tube. The tube was capped with a rubber septum and removed from the drybox. An excess of anhydrous  $HCl_{(g)}$  was injected into the tube *via* syringe. Immediate reaction took place; the solution changed color from cherry-red to orange.  $Cp_2TiCl_2$  ( $\delta$  5.93), neo-pentyl alcohol ( $\delta$  3.14, 0.79), and  $CH_4$  ( $\delta$  0.15) were observed by  $^1H$  NMR spectroscopy. An IR of the solution showed that  $WOCl_4$  had not formed<sup>63</sup> in the reaction and the tungsten containing product remains unidentified.

Attempts to treat **21** with exactly one equivalent of trifluoroacetic acid at  $-78^\circ C$  resulted in a complex reaction mixture and no metal containing species could be identified.

### Attempted Reaction of 21 with Acetone and Benzaldehyde

In the drybox an NMR tube was charged with 11 mg (0.015 mmol) of 21 which was dissolved in 400  $\mu$ l of  $C_6D_6$ . The tube was capped with a rubber septum and was removed from the drybox. One equivalent of a carbonyl was added *via* syringe. The reaction mixture was monitored by  $^1H$  NMR spectroscopy using the signal of residual protons of solvent as an internal standard. 21 eventually decomposes but the carbonyl is not consumed.

### Reaction of 21 with Lewis Acids, $Me_2AlCl$ or $AlCl_3$

In the drybox an NMR tube was charged with 10 mg (0.014 mmol) of 21 and 400  $\mu$ l  $C_6D_6$  were added. One equivalent of Lewis acid was added. Immediate reaction takes place; the color of the solution changes from cherry-red to brownish yellow. The tube was capped, removed from the drybox and an NMR spectrum was recorded. The only identifiable product was  $Cp_2TiCl_2$  ( $\delta$  5.93). Unidentified products give rise to broad overlapping signals between  $\delta$  0.5 and 1.7 due to alkoxide methyl groups and signals in the region  $\delta$  3.2-4.0 due to alkoxide methylene groups.

### Reaction of 21 with $PMe_3$

In the drybox 18 mg (0.024 mmol) of 21 in 400  $\mu$ l toluene- $d_8$  were loaded into an NMR tube. The tube was fitted with a Teflon needle valve adapter *via* an O-ring fitting. The tube was removed from the drybox and attached to a vacuum line via the Teflon needle valve adapter. The solution was frozen with  $LN_2$  and the tube evacuated.  $PMe_3$  (10 equivalents) was vacuum transferred into the tube. The tube was then sealed. The sample was warmed to room temperature and the reaction monitored by  $^1H$  NMR spectroscopy. After  $\frac{1}{2}$  hr. equilibrium had been established; 21,  $WO(OCH_2CMe_3)_4$ ,  $Cp_2Ti(CH_2)PMe_3$ ,<sup>64</sup> and free  $PMe_3$  were observed. The

equilibrium constant  $K = [\text{Cp}_2\text{Ti}(\text{CH}_2)\text{PMe}_3][\text{WO}(\text{OCH}_2\text{CMe}_3)_4]/[\text{21}][\text{PMe}_3]$  was determined from the relative integrals of appropriate signals. A correction, determined by the magnitude of the Cp resonance integral of  $\text{Cp}_2\text{Ti}(\text{CH}_2)\text{PMe}_3$ , was applied to the integral of free  $\text{PMe}_3$  to account for intensity due to coordinated  $\text{PMe}_3$ .

#### Attempted Reaction of 21 with CO

a) In the drybox an NMR tube was loaded with 10 mg (0.014 mmol) of 21 and the tube fitted with a Teflon needle valve adapter *via* an O-ring fitting. The tube was removed from the drybox, attached to a vacuum line, and evacuated. Toluene- $d_8$ , *ca* 400  $\mu\text{l}$ , was vacuum transferred into the tube at 77K. The tube was vented to 300 torr CO and then sealed. The tube was warmed to room temperature. No immediate reaction was observed. Eventually (over several days), 21 decomposes thermally yielding a complex reaction mixture.

b) In a pressure bottle 40 mg of 21 was dissolved in 5 ml  $\text{Et}_2\text{O}$  at  $-50^\circ\text{C}$ . The bottle was pressurized with 50 psi of CO. The reaction mixture was allowed to warm slowly to  $0^\circ\text{C}$  (over 1 hr) and stirred at  $0^\circ\text{C}$  for 2 hrs. The CO was vented and the solution transferred to a Schlenk tube *via* cannulus. The volatiles were removed *in vacuo* and the resulting red residue dissolved in  $\text{C}_6\text{D}_6$ .  $^1\text{H}$  NMR spectroscopy revealed that the residue contained only starting material.

#### Attempted Reaction of 21 with Excess Diphenylacetylene

In the drybox 10 mg (0.014 mmol) of 21 and 19 mg (0.11 mmol) of diphenylacetylene were loaded into an NMR tube. The tube was capped with a rubber septum, removed from the drybox, and cooled to  $0^\circ\text{C}$  in an ice bath. Toluene- $d_8$ , 400  $\mu\text{l}$ , was added *via* syringe. The tube was maintained at  $0^\circ\text{C}$ . It

was removed periodically and examined by  $^1\text{H}$  NMR spectroscopy. After 24 hrs at  $0^\circ\text{C}$  there was no reaction evident except slight thermal decomposition of **21**.

Preparation of  $\text{Re}(\text{O})(\text{CH}_3\text{C}\equiv\text{CCH}_3)_2(\text{CH}_2\text{PPh}_3)^+\text{I}^-$  (**23**)

A yellow solution of 127 mg (0.46 mmol) of  $\text{CH}_2\text{PPh}_3$  in 3 ml benzene was added dropwise to a yellow solution of 200 mg (0.46 mmol)  $\text{Re}(\text{O})(\text{CH}_3\text{C}\equiv\text{CCH}_3)_2\text{I}$  in 3 ml benzene. After stirring for 15 min a pale yellow precipitate begins to form. The reaction mixture was stirred for a total of 2 hrs. The supernate was decanted off and the pale yellow solid was washed with three 2 ml aliquots of benzene. The solid was dried *in vacuo* overnight. (Yield 150 mg, 46%) Calculated for  $\text{C}_{27}\text{H}_{29}\text{IOPRe}$ : C, 45.45; H, 4.10. Found: C, 45.76; H, 4.03. NMR data are shown in Table 2.4. IR KBr pellet: 3000 (br,m), 2890 (m), 1780 (w), 1602 (m), 1480 (s), 1432 (vs), 1360 (m), 1320 (m), 1180 (w), 1150 (s), 1100 (vs), 1040 (w), 990 (m), 955 (vs), 902 (w), 780 (s), 742 (vs), 720 (vs), 683 (vs), 625 (m), 580 (m), 500 (s), 482 (sh).

Reaction of  $\text{WO}(\text{OCH}_2\text{CMe}_3)_4$  with  $\text{CH}_2\text{PPh}_3$

a) In the drybox, an NMR tube was loaded with 20 mg (0.04 mmol) of  $\text{WO}(\text{OCH}_2\text{CMe}_3)_4$  and 10 mg (0.04 mmol) of  $\text{CH}_2\text{PPh}_3$ . The solids were dissolved in 400  $\mu\text{l}$  of  $\text{C}_6\text{D}_6$  and the tube capped with a rubber septum. The tube was removed from the drybox and the results for the reaction were observed by  $^1\text{H}$  NMR. Immediate reaction had occurred. Based on the total integrated intensity of alkoxide methylene protons **24** comprises *ca* 50% of the reaction mixture. Other major alkoxide resonances appear at  $\delta$  4.96, 4.46, and 4.22 (alkoxide methylene protons) and 1.28, 1.13 (br), 1.00 (alkoxide *t*Bu protons).

b) In a Schlenk tube 200 mg (0.72 mmole) of  $\text{CH}_2\text{PPh}_3$  and 397 mg (0.72 mmol) of  $\text{WO}(\text{OCH}_2\text{CMe}_3)_4$  were dissolved in 10 ml of benzene. The reaction was stirred for  $1 \frac{1}{2}$  hrs. The volatiles were removed *in vacuo* leaving an oily residue. The residue was triturated with pentane and a white solid formed. The pentane solution was decanted away from the white solid and reduced to dryness leaving an oily residue.  $^1\text{H}$  NMR spectroscopy of this residue in  $\text{C}_6\text{D}_6$  revealed the same mixture of alkoxide species as observed in the NMR tube scale reaction (*vide supra*). The white solid isolated as above could not be completely redissolved in benzene; a white solid was filtered off. Pentane was layered on top of the benzene solution and the mixture was cooled to  $0^\circ\text{C}$ . A total of 60 mg of crystals of **24** and an intractable white solid came out of the solution.

Acidolysis of the Reaction Mixture  $\text{CH}_2\text{PPh}_3 + \text{WO}(\text{OCH}_2\text{CMe}_3)_4$ .

In the drybox, 10 mg (0.04 mmol) of  $\text{CH}_2\text{PPh}_3$  and 20 mg (0.04 mmol) of  $\text{WO}(\text{OCH}_2\text{CMe}_3)_4$  were loaded into an NMR tube. The NMR tube was capped with a rubber septum.  $\text{C}_6\text{D}_6$  (400  $\mu\text{l}$ ) was added *via* syringe and the tube shaken periodically for 10 min. 50  $\mu\text{l}$  of  $\text{CF}_3\text{COOD}$  were added *via* syringe white solid, presumably, a phosphonium salt, precipitates.  $^1\text{H}$  NMR spectroscopy indicated that neo-pentyl alcohol was the only organic product in solution. This was confirmed by GC analysis of the reaction mixture performed on a Shimadzu GC-Mini2 flame ionization instrument modified for capillary use and equipped with a Hewlett-Packard Model 339A integrator (Column: 0.24 mm x 40 m DB1).

The above experiment was repeated with protio toluene as the solvent and 8  $\mu\text{l}$  of  $\text{C}_6\text{D}_6$  as a deuterium internal standard.  $^1\text{H}$  NMR spectroscopy again revealed neo-pentyl alcohol as the only organic product.



$^2\text{H}\{^1\text{H}\}$  NMR showed a broad peak at  $\delta$  1.93 due to exchangeable deuterons, but no deuterium incorporation into alkoxy methylene or t-butyl groups was evident.

Preparation of  $\text{CH}_3\text{PPh}_3^+ \text{WO}(\text{OCH}_2\text{CMe}_3)_5^-$ , (24)

A yellow solution of 100 mg (0.36 mmol) of  $\text{CH}_2\text{PPh}_3$  in 5 ml benzene was added to a colorless solution of 200 mg (0.36 mmol) of  $\text{WO}(\text{OCH}_2\text{CMe}_3)_4$  and 32 mg (0.36 mmole) of neo-pentyl alcohol in 5 ml benzene. The color of the ylide immediately disappears. The reaction mixture is stirred for 15 min. The volatiles were removed *in vacuo* leaving a white powder. The powder was dissolved in 2 ml benzene. The resulting colorless solution was filtered and 5 ml pentane were layered on top of it. The layers were allowed to slowly diffuse into one another at 0°C. Large colorless crystals of the product formed. The mother liquor was decanted off and the crystals were washed with two 3 ml aliquots of pentane. The crystals were then dried *in vacuo*. (Yield 193 mg, 59%). Calculated for  $\text{C}_{44}\text{H}_{73}\text{O}_6\text{PW}$ : C, 57.89; H, 8.06; P, 3.39. Found: C, 57.87; H, 8.09; P, 3.78. NMR data are shown in Table 2.4. IR  $\text{C}_6\text{D}_6$  solution: 2930 (s), 2890 (m), 2840 (m), 1475 (m), 1438 (m), 1382 (m), 1355 (m,br), 1325 (sh,w), 1065 (vs), 1020 (s), 900 (m), 875 (s), 740 (m), 715 (w), 681 (m), 640 (s), 620 (sh).

X-ray Structure Determination of 24

An irregularly shaped colorless crystal (approximate dimensions 0.3 x 0.4 x 0.5 mm) was mounted in a glass capillary under  $\text{N}_2$ . Oscillation photographs revealed that the crystal diffracted well and indicated monoclinic symmetry. A small data set,  $10 < 2\theta < 13^\circ$ ,  $+h +k, \pm\ell$ , was collected on an Enraf-Nonius CAD4 diffractometer with graphite monochromator and  $\text{MoK}\alpha$  radiation. Systematic absences ( $0k0$  absent for  $k$  odd,  $h01$  absent for  $h + \ell$  odd)

showed that the space group was  $P2_1/n$ . A full data set was then collected, ( $5 < 2\theta < 50^\circ$ ,  $\pm h$ ,  $\pm k$ ,  $\pm l$ ). The unit cell parameters (Table 2.5) were obtained by a least-squares refinement of 25 reflections. Three check reflections, measured every 100 reflections, indicated minimal decomposition. Intensities were corrected for Lorentz and polarization effects. No absorption correction was applied. The data was placed on an absolute scale by means of a Wilson plot. The form factors for H were from Stewart et al.<sup>65</sup> and those for the other atoms were from the International Tables for X-ray Crystallography.<sup>66</sup> The values for W and P were corrected for anomalous dispersion. Details of data collection are included in Table 2.5.

The location of the W was derived from a three-dimensional Patterson map. A series of structure factor calculations and Fourier syntheses enabled all non-hydrogen atoms to be located. At this stage several cycles of least-squares refinement, minimizing<sup>67</sup>  $\sum w[F_o^2 - (F_c/k)^2]^2$ , of non-hydrogen atom coordinates and isotropic thermal parameters were then conducted. Alkoxide ligand (3); O3, C3X (X = 1-5) parameters did not converge in these refinement cycles possibly due to disorder. Attempts to model each atom of this ligand with two equally populated sites led to divergence in the least-squares refinement; no further attempts to model the disorder were made. At this time the hydrogens of the methyl group of the methyltriphenyl phosphonium cation could be located on a Fourier map. All other hydrogen atoms were placed in calculated idealized positions. All hydrogen atoms were assigned isotropic thermal parameters  $1\text{\AA}^2$  greater than that of the carbon atom to which they were bonded. The coordinates and thermal parameters of all hydrogen atoms were not refined further.

Full matrix least-squares refinement of the non-hydrogen atoms with anisotropic thermal parameters would not reach convergence due to oscillations in the alkoxide (3) parameters. Ten cycles of damped (damping factor 0.6) least-squares refinement were required to refine the alkoxide (3) parameters. A further six cycles of full matrix undamped least-squares refinement led to  $S$  (Goodness of fit)<sup>67</sup> = 1.77,  $R$  = 0.108 and  $R_{30}$  = 0.057 final shift/errors  $\leq 0.1$  except for alkoxide (3) where shift/error  $\leq 0.5$ . A final difference Fourier map showed small features close to the W atom. All calculations were conducted on a VAX 11/750 computer using the CRYM systems of programs. Tables of bond lengths and angles (Table 2.6), non-H atom coordinates and Gaussian amplitudes (Table 2.7), H-atom coordinates and isotropic thermal parameters (Table 2.8) follow.

**Table 2.5 – Summary of Crystal Data and Intensity Collection Information**

Formula	WC <sub>44</sub> H <sub>73</sub> O <sub>6</sub> P
Formula weight	912.89
Space group	P2 <sub>1</sub> /n
<i>a</i>	11.895(1) Å
<i>b</i>	22.084(4) Å
<i>c</i>	18.553(3) Å
$\beta$	94.013(12)°
<i>V</i>	4861.6(65) Å <sup>3</sup>
<i>Z</i>	4
$\lambda$	0.7107 Å
<i>D<sub>calc</sub></i>	1.248 g/cm <sup>3</sup>
Scans	$\theta$ -2 $\theta$
Reflections	$5 < 2\theta < 50^\circ$ , $\pm h$ , $\pm k$ , $\pm \ell$
Background time/scan time	0.5
Collected	27962 reflections
Averaged	8496 reflections
Final no. of parameters	469
Final cycle:	
<i>R</i>	0.108(7070*)
<i>R</i> <sub>3<math>\sigma</math></sub>	0.057(3743)
<i>S</i>	1.77(8496)

\* The number of reflections contributing to sums in parentheses.

Table 2.6 – Bond Lengths and Angles for  $\text{CH}_3\text{PPh}_3^+[\text{WO}(\text{OCH}_2\text{CMe}_3)_6]^-$ 

## Bond Lengths (Å)

ATOM	ATOM	DISTANCE	SIGMA
W	O	1.6931	0.005
W	O1	1.9534	0.005
W	O2	1.9784	0.008
W	O3	1.9703	0.008
W	O4	1.8859	0.005
W	O5	1.8840	0.005
O1	C11	1.2850	0.013
C11	C12	1.4619	0.015
C12	C13	1.5243	0.021
C12	C14	1.3841	0.019
C12	C15	1.4084	0.018
O2	C21	1.4315	0.012
C21	C22	1.5026	0.014
C22	C23	1.4431	0.016
C22	C24	1.4420	0.017
C22	C25	1.4938	0.019
O3	C31	1.1894	0.015
C31	C32	1.3881	0.018
C32	C33	1.3834	0.021
C32	C34	1.2875	0.026
C32	C35	1.2958	0.025
O4	C41	1.3525	0.010
C41	C42	1.4972	0.013
C42	C43	1.5009	0.014
C42	C44	1.4614	0.018
C42	C45	1.5130	0.015
O5	C51	1.3409	0.014
ATOM	ATOM	DISTANCE	SIGMA
C51	C52	1.3901	0.016
C52	C53	1.4359	0.016
C52	C54	1.4128	0.018
C52	C55	1.4652	0.023
P	C	1.7647	0.008
P	C61	1.8107	0.008
P	C71	1.7651	0.008
P	C81	1.8017	0.008
C61	C62	1.3650	0.012
C61	C66	1.3987	0.011
C62	C63	1.3760	0.013
C63	C64	1.3594	0.014
C64	C65	1.3456	0.014
C65	C66	1.3769	0.013
C71	C72	1.3779	0.011
C71	C76	1.4018	0.011
C72	C73	1.3480	0.012
C73	C74	1.3883	0.014
C74	C75	1.3652	0.013
C75	C76	1.3661	0.012
C81	C82	1.3718	0.013
C81	C86	1.3467	0.013
C82	C83	1.3667	0.015
C83	C84	1.3276	0.017
C84	C85	1.3220	0.017
C85	C86	1.4106	0.016

Table 2.6(cont.)

## Bond Angles(deg)

ATOM	ATOM	ATOM	ANGLE	SIGMA	ATOM	ATOM	ATOM	ANGLE	SIGMA
01	W	0	96.64	0.226	C44	C42	C43	110.48	0.916
02	W	0	174.21	0.231	C45	C42	C43	105.28	0.814
03	W	0	91.22	0.245	C45	C42	C44	109.08	0.936
04	W	0	93.90	0.229	C51	05	W	131.37	0.655
05	W	0	93.34	0.234	C52	C51	05	124.10	1.080
06	W	0	88.82	0.221	C53	C52	C51	113.37	0.985
07	W	01	172.08	0.237	C54	C52	C51	116.43	1.071
08	W	01	88.37	0.220	C55	C52	C51	109.04	1.161
09	W	01	86.25	0.224	C56	C52	C53	108.76	1.023
10	W	02	83.35	0.241	C55	C52	C54	102.67	1.121
11	W	02	84.30	0.225	C55	C52	C54	105.38	1.195
12	W	02	88.93	0.229	C61	P	C	110.05	0.369
13	W	03	92.09	0.240	C71	P	C	109.30	0.370
14	W	03	92.33	0.244	C81	P	C	108.53	0.378
15	W	04	171.43	0.229	C81	P	C	113.09	0.366
16	W	04	131.76	0.622	C81	P	C	106.84	0.373
17	W	04	121.56	0.953	C81	P	C	108.81	0.374
18	W	04	104.90	1.028	C82	C61	P	120.45	0.623
19	W	04	109.27	1.028	C86	C61	P	119.63	0.599
20	W	04	113.39	1.009	C86	C61	P	119.91	0.761
21	W	04	110.65	1.167	C83	C62	C61	120.85	0.835
22	W	04	108.42	1.126	C84	C63	C62	118.30	0.916
23	W	04	110.09	1.123	C85	C64	C63	122.28	0.962
24	W	04	131.62	0.539	C86	C65	C64	120.37	0.907
25	W	04	111.88	0.801	C86	C66	C61	118.26	0.788
26	W	04	107.88	0.908	C72	C71	P	122.86	0.603
27	W	04	110.66	0.923	C76	C71	P	118.91	0.591
28	W	04	107.76	0.967	C76	C71	P	118.19	0.720
29	W	04	110.47	0.980	C73	C72	C71	120.18	0.787
30	W	04	110.64	1.029	C74	C73	C72	121.73	0.867
31	W	04	109.37	1.032	C75	C74	C73	118.83	0.887
32	W	04	138.30	0.819	C76	C75	C74	120.06	0.855
33	W	04	129.24	0.819	C75	C76	C71	120.84	0.778
34	W	04	115.32	1.188	C82	C81	P	118.99	0.667
35	W	04	101.10	1.393	C86	C81	P	122.41	0.675
36	W	04	116.41	1.376	C86	C81	P	118.58	0.830
37	W	04	102.15	1.468	C83	C82	C81	119.75	0.938
38	W	04	107.68	1.431	C84	C83	C82	122.21	1.095
39	W	04	113.24	1.644	C85	C84	C83	118.85	1.137
40	W	04	127.06	0.511	C86	C85	C84	121.24	1.069
41	W	04	117.69	0.744	C86	C86	C85	119.31	0.909
42	W	04	114.07	0.783					
43	W	04	109.53	0.891					
44	W	04	108.21	0.796					

## Labeling Scheme

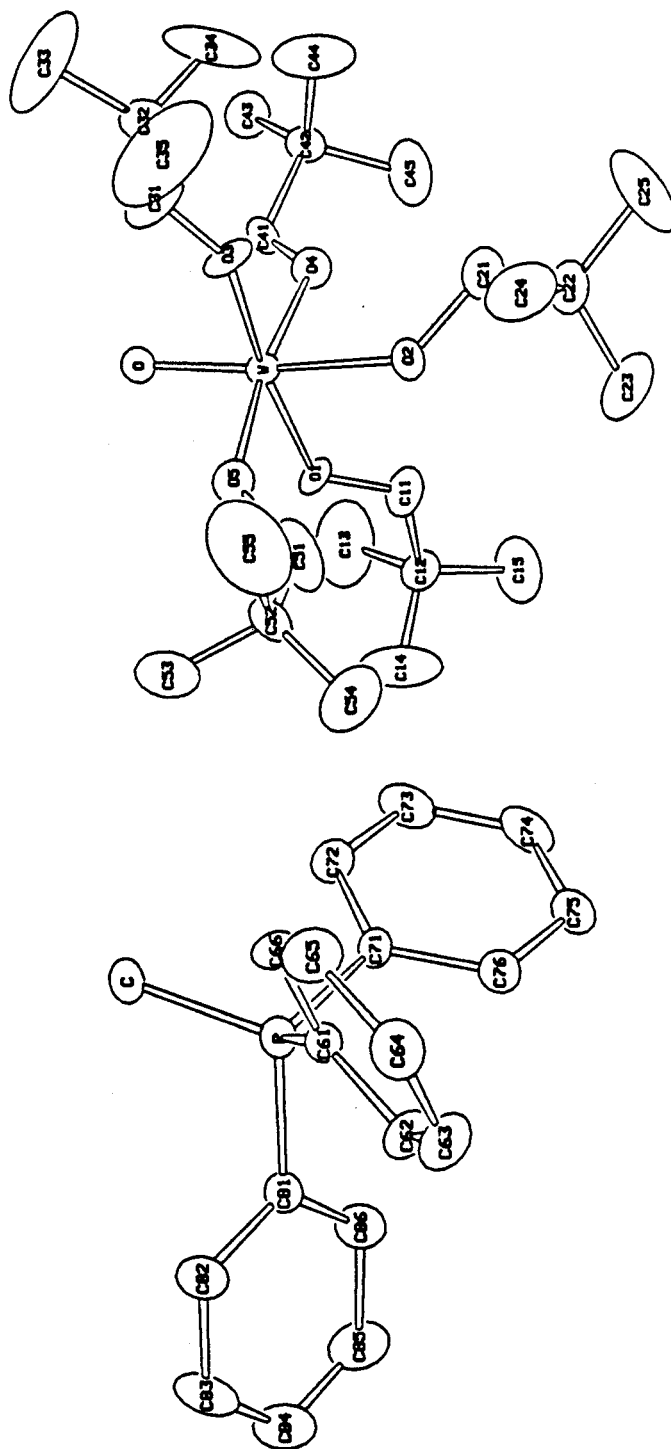


Table 2.7 - Final Non-Hydrogen Atom Coordinates ( $\times 10^5$ ) and Gaussian Amplitudes ( $\text{\AA}^2, \times 10^4$ ) for 24

	X	Y	Z	U11	U22	U33	U12	U13	U23	UEq
W	36248 (3)	23412 (2)	4581 (2)	529 (2)	683 (3)	756 (3)	-73 (3)	36 (2)	-23 (3)	644 (1)
O	41934 (45)	16499 (22)	5333 (26)	866 (47)	812 (41)	817 (48)	-25 (30)	31 (37)	87 (32)	828 (17)
O1	56427 (45)	27823 (22)	4427 (36)	827 (46)	494 (41)	1436 (52)	-225 (37)	32 (40)	-5 (36)	918 (22)
C11	52968 (98)	32769 (46)	1337 (66)	1238 (114)	912 (96)	2813 (169)	-323 (98)	-261 (111)	453 (91)	1673 (56)
C12	64608 (82)	34944 (44)	1562 (55)	684 (83)	998 (91)	1499 (106)	-418 (72)	113 (81)	218 (75)	1859 (41)
C13	71382 (132)	29719 (82)	-1734 (121)	1398 (152)	2866 (214)	6192 (367)	-145 (169)	1167 (192)	1361 (217)	3426 (112)
C14	68664 (138)	35976 (81)	8626 (72)	2488 (263)	4336 (262)	1537 (138)	-1637 (186)	-271 (134)	-498 (146)	2864 (88)
C15	66668 (126)	40181 (64)	-2733 (91)	2246 (188)	2166 (152)	4377 (254)	-1639 (137)	-763 (173)	1931 (166)	2666 (86)
O2	28195 (52)	31156 (23)	3357 (20)	1164 (58)	832 (46)	968 (48)	74 (42)	-14 (42)	236 (36)	979 (21)
C21	26593 (98)	33417 (43)	-2297 (53)	1521 (117)	1866 (91)	1268 (98)	44 (64)	395 (86)	83 (72)	1284 (41)
C22	13366 (87)	38523 (44)	177 (53)	1691 (106)	959 (91)	1535 (110)	313 (76)	577 (86)	13 (78)	1142 (41)
C23	26836 (112)	43449 (49)	2512 (92)	1492 (134)	1848 (163)	3934 (214)	-184 (94)	667 (148)	-366 (118)	2136 (78)
C24	6779 (108)	36672 (59)	6863 (75)	1493 (138)	2321 (154)	2481 (156)	-277 (115)	788 (118)	-841 (121)	2662 (83)
C25	5495 (145)	46405 (79)	-6564 (77)	2347 (223)	4118 (263)	2647 (183)	2145 (199)	133 (158)	1013 (153)	3663 (89)
O3	26948 (52)	26677 (27)	4882 (35)	952 (57)	979 (54)	1946 (68)	-893 (45)	37 (51)	-216 (48)	1293 (26)
C31	16495 (169)	15267 (77)	4788 (57)	1877 (124)	1328 (126)	4545 (248)	-82 (84)	231 (145)	-191 (134)	2315 (83)
C32	6697 (87)	13822 (49)	4682 (91)	1977 (124)	1595 (118)	1438 (113)	-445 (87)	223 (87)	377 (89)	1211 (47)
C33	2626 (146)	7675 (62)	4467 (127)	2442 (268)	1152 (126)	7732 (432)	-486 (136)	2292 (244)	-551 (192)	3685 (125)
C34	175 (192)	16166 (114)	-954 (126)	4236 (326)	6788 (392)	4298 (318)	-4196 (313)	-3449 (276)	3682 (361)	5275 (149)
C35	676 (187)	15847 (97)	16685 (131)	3685 (317)	3795 (291)	5879 (371)	-1831 (256)	3693 (281)	-1216 (261)	4363 (131)
O4	35448 (46)	23344 (24)	-5588 (27)	936 (48)	952 (44)	921 (43)	284 (43)	274 (37)	-263 (38)	927 (18)
C41	46781 (81)	19474 (38)	-9966 (49)	1133 (93)	928 (76)	1664 (86)	56 (76)	123 (67)	369 (83)	1641 (36)
C42	37231 (81)	19569 (43)	-17667 (45)	972 (89)	1878 (85)	714 (69)	78 (76)	117 (62)	-117 (62)	918 (33)
C43	43361 (166)	14992 (45)	-22148 (53)	1741 (129)	1282 (97)	1376 (99)	181 (92)	135 (92)	-228 (74)	1463 (44)
C44	46248 (123)	18651 (74)	-18679 (78)	1376 (130)	3855 (221)	2652 (172)	-376 (156)	-8 (129)	-1436 (155)	2633 (89)
C45	37392 (48)	18651 (74)	-18679 (78)	1376 (130)	3855 (221)	2652 (172)	-376 (156)	-8 (129)	-1436 (155)	2633 (89)
O5	37392 (48)	18651 (74)	-18679 (78)	1376 (130)	3855 (221)	2652 (172)	-376 (156)	-8 (129)	-1436 (155)	2633 (89)
C51	35457 (89)	36114 (45)	25064 (52)	18654 (59)	3512 (222)	1293 (99)	942 (85)	652 (197)	186 (92)	1925 (56)
C52	42222 (116)	25068 (58)	30262 (56)	2323 (162)	2331 (164)	2226 (161)	236 (127)	172 (176)	-173 (88)	1019 (21)
C53	36484 (162)	35066 (62)	29127 (73)	4654 (366)	1558 (143)	1558 (143)	1558 (143)	652 (197)	186 (92)	1925 (56)
C54	23736 (144)	28897 (102)	26646 (123)	1419 (143)	5617 (343)	4966 (353)	1617 (199)	768 (184)	-173 (88)	1019 (21)
P	14698 (21)	48861 (16)	66784 (12)	736 (28)	658 (18)	866 (19)	88 (16)	36 (16)	36 (16)	734 (6)
C	14619 (76)	32877 (33)	66853 (42)	785 (72)	689 (63)	1077 (71)	133 (55)	-91 (59)	151 (51)	861 (29)
C61	1949 (72)	43472 (35)	71167 (38)	828 (73)	615 (65)	666 (66)	46 (59)	71 (56)	-47 (47)	682 (27)
C62	2286 (81)	48838 (39)	78924 (48)	1816 (87)	743 (73)	1122 (87)	-125 (68)	227 (72)	-163 (59)	961 (34)
C63	-6888 (98)	56868 (46)	78248 (52)	1262 (166)	934 (84)	1332 (96)	126 (80)	425 (88)	-388 (88)	1168 (39)
C64	-16389 (89)	47434 (48)	74624 (52)	1839 (97)	1288 (166)	1145 (93)	344 (84)	463 (86)	-67 (74)	1142 (48)
C65	-7927 (83)	42116 (48)	74522 (51)	932 (87)	861 (75)	1221 (89)	-48 (80)	466 (73)	-216 (75)	1135 (46)
C71	14252 (66)	43453 (35)	51978 (46)	971 (81)	892 (73)	886 (65)	166 (58)	38 (14)	808 (31)	868 (26)
C72	15826 (72)	39433 (36)	45361 (47)	716 (84)	1745 (169)	976 (85)	102 (86)	287 (66)	-181 (57)	844 (31)
C73	16899 (74)	41918 (49)	45325 (48)	599 (77)	1745 (169)	976 (85)	102 (86)	287 (66)	-181 (57)	844 (31)
C74	15898 (74)	48986 (55)	43925 (48)	916 (87)	1116 (87)	967 (75)	-129 (76)	287 (66)	-181 (57)	844 (31)
C75	13961 (77)	51961 (41)	49487 (51)	916 (87)	1116 (87)	967 (75)	-129 (76)	287 (66)	-181 (57)	844 (31)
C76	13195 (72)	49486 (38)	56292 (45)	761 (72)	856 (71)	886 (70)	162 (63)	113 (62)	-293 (64)	978 (34)
C81	26378 (73)	43736 (35)	71866 (54)	729 (75)	728 (76)	762 (64)	19 (58)	185 (79)	266 (74)	1226 (49)
C82	26896 (98)	41705 (43)	78723 (54)	1247 (104)	1387 (96)	1695 (88)	-454 (83)	-185 (79)	266 (74)	1226 (49)
C83	37934 (166)	43877 (59)	82163 (54)	1240 (127)	2293 (155)	1173 (121)	-397 (99)	-587 (98)	-265 (99)	1568 (53)
C84	44869 (99)	47856 (64)	80134 (86)	1161 (117)	1857 (137)	1523 (121)	-294 (99)	-212 (98)	-265 (99)	1568 (53)
C85	43807 (98)	46994 (49)	73468 (89)	1696 (167)	1845 (114)	1783 (126)	-724 (93)	-114 (98)	-114 (98)	1484 (49)
C86	33526 (92)	47719 (44)	69634 (47)	1666 (97)	1271 (97)	1643 (87)	-267 (86)	-11 (74)	-19 (69)	1169 (39)



Table 2.8 – Hydrogen Atom Coordinates ( $\times 10^4$ ) and B's ( $\text{\AA}^2$ ) for 24

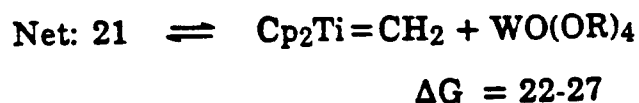
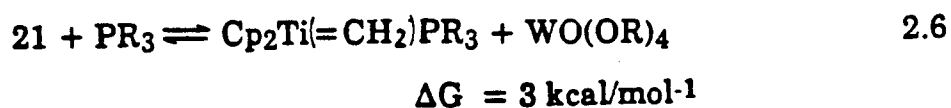
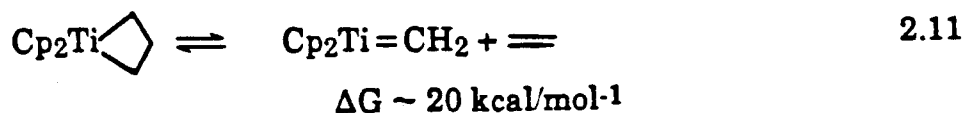
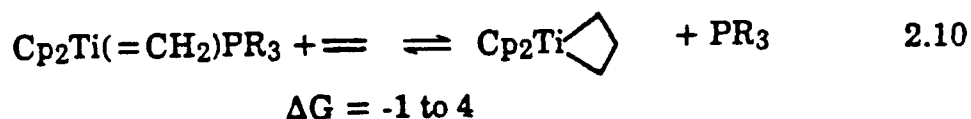
	X	Y	Z	B		X	Y	Z	B
H111	4767	3639	175	12.00	H433	3630	1250	-2490	10.00
H112	5133	3240	-457	12.00	H441	2350	1400	-1600	17.00
H131	6421	2810	-439	16.00	H442	2130	2270	-1750	17.00
H132	7485	2795	94	16.00	H443	2320	1650	-2080	17.00
H133	7428	3237	-557	16.00	H451	4580	2440	-2710	12.00
H141	6398	3493	1231	19.00	H452	4060	2820	-1750	12.00
H142	7224	3976	967	19.00	H453	3120	2770	-2200	12.00
H143	7565	3297	987	19.00	H511	3467	3364	1602	12.00
H151	5942	4047	-614	16.00	H512	4677	3184	1864	12.00
H152	7211	3893	-637	16.00	H531	4723	2341	2797	11.00
H153	6827	4373	-96	16.00	H532	3686	2285	3252	11.00
H211	1454	2990	-382	11.00	H533	4612	2736	3481	16.00
H212	2345	3416	-684	11.00	H541	3787	3925	2623	16.00
H231	2873	4243	227	14.00	H542	4080	3625	3368	16.00
H232	2020	4432	782	14.00	H543	2830	3716	3093	16.00
H233	1943	4715	15	14.00	H551	2190	2695	2128	20.00
H241	809	3213	707	13.00	H552	1967	3074	2807	20.00
H242	-96	3708	537	13.00	H553	2477	2429	2893	20.00
H243	931	3842	1077	13.00	H1	1580	3120	7210	7.00
H251	552	3781	-988	16.00	H2	790	3100	6570	7.00
H252	638	4450	-736	16.00	H3	2190	3120	6440	7.00
H253	-248	4023	-429	16.00	H621	913	5149	7494	8.00
H311	1952	1305	1046	21.00	H631	-692	5484	8110	10.00
H312	2086	1175	235	21.00	H641	-2317	4921	7986	9.00
H331	912	505	559	23.00	H651	-2401	3963	7441	9.00
H332	-141	562	20	23.00	H661	-820	3600	6804	8.00
H333	-266	613	845	23.00	H721	1590	3505	5271	7.00
H341	213	2003	-184	28.00	H731	1773	3915	4093	9.00
H342	-769	1897	310	28.00	H741	1667	4970	3916	9.00
H343	-616	1468	-338	28.00	H751	1329	5628	4848	8.00
H351	926	1673	1409	25.00	H761	1192	5254	6055	8.00
H352	-170	1293	1417	25.00	H821	2384	3842	8090	10.00
H353	-220	1963	1131	25.00	H831	3950	4294	8807	13.00
H411	3996	1514	-825	8.00	H841	5174	4944	8276	11.00
H412	4892	2004	-957	8.00	H851	4756	5307	7137	11.00
H431	5190	1690	-2310	10.00	H861	3228	4900	6378	9.00
H432	4690	1080	-1740	10.00					

## II.6 References

1. Giacomelli, A.; Floriani, C.; Duarte, A.O.D.S.; Chiesi-Villa, A.; Guastini, C, *Inorg. Chem.* **1982**, *21*, 3310.
2. March, J. "Advanced Organic Chemistry" 2nd ed., McGraw Hill:1977, p. 867.
3. Wittig, G.; Schollkopf, U. *Chem. Ber.* **1954**, *87*, 1318.
4. Berstmann, H.J. *Angew Chem. Int. Ed. Engl.* **1965**, *4*, 645.
5. Tebbe, F.N.; Parshall, G.W.; Reddy, G.S. *J. Am. Chem. Soc.* **1978**, *100*, 3611.
6. Straus, D.A.; Grubbs, R.H. *Organometallics* **1982**, *1*, 1658.
7. Clawson, L.E.; Buchwald, S.L.; Grubbs, R.H. *Tet. Lett.* **1984**, *25*, 5733.
8. Brown-Wensley, K.A., Ph.D. Thesis, California Institute of Technology, 1981.
9. Pine, S.H.; Zahler, R.; Evans, D.A.; Grubbs, R.H. *J. Am. Chem. Soc.* **1980**, *102*, 3270.
10. Pine, S.H., private communication.
11. Ho, S.C.H., Ph.D. Thesis, California Institute of Technology, 1986.
12. a) Stille, J.R.; Grubbs, R.H. Grubbs, *J. Am. Chem. Soc.* **1983**, *105*, 1664. b) Cannizzo, L.F.; Grubbs, R.H. *J. Org. Chem.* **1985**, *50*, 2316.
13. a) Grubbs, R.H. *Prog. Inorg. Chem.* **1978**, *24*, 1. b) Grubbs, R.H. in "Comprehensive Organometallic Chemistry", Vol. 8, Wilkinson, G. Ed., Pergamon Press:1982, p. 499.
14. The mechanism of olefin metathesis involves alkylidene intermediates (see Ref. 13). Thus, formation of methyldiene complexes of Group 6 and 7 metals is at least possible.

15. Herrmann, W.A. *Adv. Organometallic Chem.* **1982**, *20*, 159.
16. Terminal metal oxo stretches normally occur in the spectral region 900-1050  $\text{cm}^{-1}$ .<sup>17</sup> The tungsten-oxo stretching frequency in  $\text{WO}(\text{OCH}_2\text{CMe}_3)_4$  occurs at 960  $\text{cm}^{-1}$ . This band disappears upon the formation of **21**.
17. Griffith, W.P. *Coord. Chem. Rev.* **1970**, *5*, 449.
18. Silverstein, R.M.; Bassler, G.C.; Morrill, T.C. "Spectrometric Identification of Organic Compounds" 3rd ed. Wiley: 1974, p. 190.
19. Five-coordination at a metal center often gives rise to fluxional behavior. See. Cotton, F.A.; Wilkinson, G. "Advanced Inorganic Chemistry" 4th ed. Wiley:1980, p. 1219.
20. Theopald, K.H.; Bergman; R.G. *J. Am. Chem. Soc.* **1983**, *105*, 464.
21. Dyke, A.F.; Knox, S.A.R.; Mead, K.A.; Woodward, P. *J. Chem. Soc. Chem. Commun.* **1981**, 861.
22. The graphical method of Shanoan-Atidi was used to estimate this value of  $\Delta G^\ddagger$ . This value is the average of forward and reverse values which are the same within experimental error. See Shanoan-Atitdi, H.; Bar-Eli, K.H. *J. Phys. Chem.* **1970** *74*, 961.
23. McKinney, R.J.; Tulip, T.H.; Thorn, D.L.; Coolbaugh, T.S.; Tebbe, F.N. *J. Am. Chem. Soc.* **1981**, *103*, 5584.
24. Such electron transfer reactions of ' $\text{Cp}_2\text{TiCH}_2$ ' have been observed in the reaction of **4** with benzyl and allyl halides.<sup>25</sup>
25. Buchwald, S.L.; Anslyn, E.V.; Grubbs, R.H. *J. Am. Chem. Soc.* **1985**, *107*, 1766.
26. Murad, E. *J. Geophys. Res.* **1978**, *83*, 5525.

27. Armentrout, P.B.; Halle, L.F.; Beauchamp, J.L. *J. Am. Chem. Soc.* 1981, 103, 6501.
28. Rappé, A.K.; Goddard, W.A. III *J. Am. Chem. Soc.* 1982, 104, 448.
29. Gordon, A.J.; Ford, R.A. "The Chemist's Companion" Wiley 1972, p. 113.
30. See ref. 28 for a discussion of why  $X_4M=O$  species have triply bonded oxo ligands and  $X_2(O)M=O$  species have doubly bonded oxo ligands.
31. Calabro, D.C.; Lichtenberger, D.L.; Herrmann, W.A. *J. Am. Chem. Soc.* 1981, 103, 6852.
32. Shaik, S.; Hoffmann, R.; Fisel, C.R.; Summerville, R.H. *J. Am. Chem. Soc.* 1980, 102, 4555.
33. Lauher, J.W.; Hoffmann, R. *J. Am. Chem. Soc.* 1976, 98, 1729.
34. Reaction of metallacyclobutanes with phosphines<sup>35</sup> show that  $\Delta G$  for the reaction in equation 2.10 should be on the order of -1 to 4 kcal/mol<sup>-1</sup>. Calculations on a model system,<sup>36</sup>  $Cl_2Ti=CH_2$  indicate that  $\Delta G$  for the reaction in 2.11 should be ca 20 kcal/mol<sup>-1</sup>. Thus:



35. Ott, K.C., Ph.D. Thesis, California Institute of Technology, 1982.
36. Upton, T.H.; Rappé, A.K. *J. Am. Chem. Soc.* **1985**, *107*, 1206.
37. Ott, K.C.; Grubbs, R.H. *J. Am. Chem. Soc.*, **1981**, *103*, 5922.
38. a) He, M.Y.; Xiong, G.; Toscano, P.J.; Burwell, R.L., Jr.; Marks, T.J. *J. Am. Chem. Soc.* **1985**, *107*, 640. b) He, N.Y.; Burwsall, R.L., Jr.; Marks, T.J. *Organometallics*, **1983**, *2*, 566.
39. a) MacKenzie, P.B.; Ott, K.C.; Grubbs, R.H. *Pure and Applied Chem.* **1984**, *56*, 59. b) MacKenzie, P.B.; Grubbs, R.H., submitted for publication.
40. Kress, J.; Wesoleak, M.; Osborn, J.A.; *J. Chem. Soc. Chem. Commun.* **1982**, 514.
41. Chatt, J.; Dilworth, J.R. *J. Chem. Soc. Chem. Commun.* **1972**, 549.
42. Kaska, W.C. *Coord. Chem. Rev.* **1983**, *48*, 2.
43. Baldwin, J.C.; Keder, N.L.; Strouse, C.E.; Kaska, W.C. *Z. Naturforsch Teil B.* **1980**, *35*, 1289.
44. Based on covalent radii a tungsten oxygen single bond should be 2.06Å long, See Chisholm, M.H. *Polyhedron* **1983**, *2*, 681.
45. Chisholm, M.H. Folting, K.; Huffmann, J.C. Kirkpatrick, J.C. *Inorg. Chem.* **1984**, *23*, 1021.
46. Huffmann, J.C.; Moley, K.G.; Marsella, J.A.; Caulton, K. *J. Am. Chem. Soc.* **1980**, *102*, 3009.
47. Examples of the labilization of ligands trans to an oxo are given in Chatt, J.; Rowe, G.A. *J. Chem. Soc.* **1962**, 4019,
48. For a recent review of the reactivity of phosphorous ylides with transition metal complexes see, Ref. 42.

49. a) Maryanoff, B.E.; Reitz, A.B.; Mutter, M.S.; Innars, R.R.; Almond, H.R., Jr. *J. Am. Chem. Soc.* **1985**, *107*, 1068. b) Mavel, G. *Ann. Rep. NMR Spectroscopy* **1973**, *58*, 1.
50. Funk, H.V.; Weiss, W.; Mohaupt, G. *Z. Anorg. u. Allgen Chem.* **1960**, *304*, 238.
51. Kress, J.R.M.; Russell, M.J.M.; Wesolek, M.G.; Osborn, J.A. *J. Chem. Soc. Chem. Commun.* **1980**, 431.
52. Schrauzer, G.N.; Hughes, L.A.; Strampach, N.; Robinson, P.R.; Schlemper, E.O. *Organometallics*, **1982**, *1*, 44.
53. Moore, F.W.; Larsen, M.L. *Inorg. Chem.* **1967**, *6*, 998.
54. Morgan, G.T.; Castell, R.A. *J. Chem. Soc.* **1929**, 3252.
55. Mayer, J.M.; Tulip, T.H. *J. Am. Chem. Soc.* **1984**, *106*, 3878.
56. Johnson, N.P.; Lock, C.J.L.; Wilkinson, G. *Inorg. Synth.* **1967**, *9*, 147.
57. Chatt, J.; Garforth, J.D.; Johnson, N.P.; Raub, G.A., *J. Chem. Soc.* **1964**, 601.
58. Sala-Pala, J.; Roue, J.; Guorchais, J.E. *J. Mol. Catal.* **1980**, *7*, 141.
59. Lemenovskii, D.A.; Baukova, T.V.; Knizhnikov, V.A.; Perevalovd, E.G.; Nesmeyanov, A.N. *Dokl. Akad. Nauk. SSR* Eng. Ed. **1976**, *222*, 65.
60. Mowat, M.; Shortland, A.; Yagupsky, G.; Hill, N.J.; Yagupsky, M.; Wilkinson, G. *J. Chem. Soc. Dalton*, **1972**, 533.
61. Koster, R.; Simic, D.; Gassberger, M.A. *Justus Liebigs, Ann. Chem.* **1970** *739*, 211.
62. Funk, H.V.; Mohaupt, G. *Z. Anorg. u. Allgen Chem.* **1962**, *315*, 205.

63. In  $C_6D_6$  the infrared spectrum of  $WOCl_4$  consists of two bands: 800 (m), 480 (vs, br). The infrared spectrum of the acidolysis reaction mixture showed unidentified bands at 1040 and 825  $cm^{-1}$ .
64.  $^1H$  NMR:  $\delta$  12.06, d,  $J_{PH} = 7.3$  Hz,  $CH_2$ ; 5.30, D,  $J_{PH} = 2.5$  Hz, Cp. Identical to spectrum of authentic sample prepared by J. D. Meinhart. The resonance due to the coordinated  $PMe_3$  was not observed as it was obscured by the free  $PMe_3$  signal.
65. Stewart, R.F.; Davidson, E.R.; Simpson, W.T. *J. Chem. Phys.* **1965**, 42, 3175.
66. "International Tables for X-ray Crystallography" Kynoch Press: Birmingham, England, 1974; Vol. IV.
67. The weights,  $w = [s + r^2b + (0.02 s)^2]^{-1} (Lp/k^2)^2$ ,  $s$  = scan counts,  $r$  = scan to background time ratio,  $b$  = total background counts,  $k$  = scale factor of  $F$ ;  $R = \Sigma |F_o| - |F_c| / \Sigma |F_o|$  (sums of reflections with  $I > 0$ );  $R_{3\sigma} = R$  (sums of reflections with  $I > 3\sigma$ );  $S = [\Sigma w(F_o^2 - (F_c/k)^2)^2 / (n - v)]^{1/2}$ ,  $n$  = number of reflections,  $v$  = number of parameters.

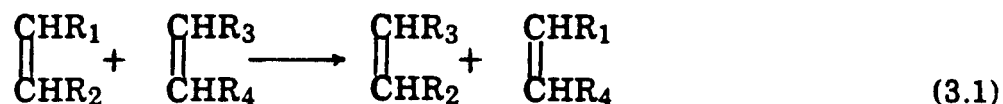
### Chapter III

**Effects of Cyclopentadienyl Ring Substituents on the  
Reactivity of Bis(cyclopentadienyl)titanacyclobutanes**



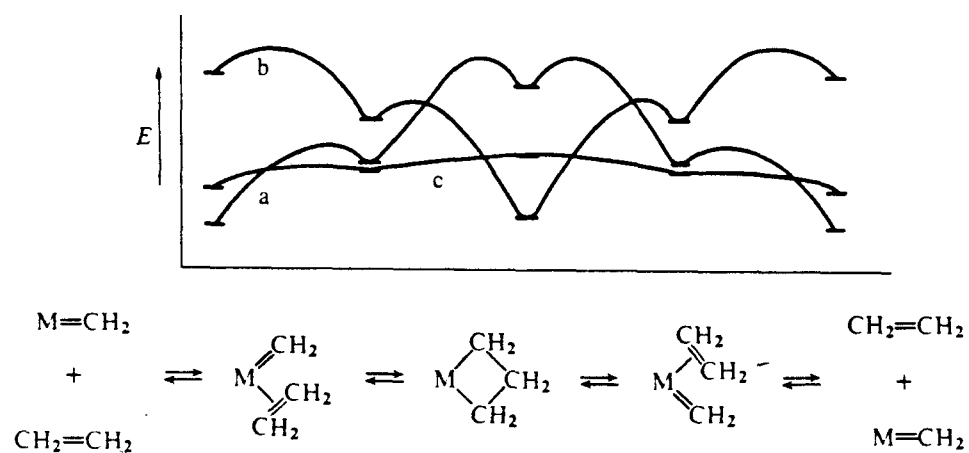
### III.1 Introduction

Olefin metathesis is a process in which the ends of two olefins are exchanged (equation 3.1). Much experimental work has led to the acceptance of a non-pairwise mechanism involving metal alkylidene

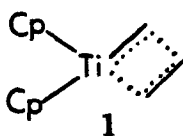


and metallacyclobutane intermediates.<sup>1</sup> The reactive energies of these intermediates depends on the metal system. Osborn has found an active homogenous system in which metal alkylidene complexes are more stable than metallacyclobutanes,<sup>2</sup> path a in the reaction profile shown in Figure 3.1. Schrock<sup>3</sup> has found an active system, starting with  $(\text{RO})_2\text{W}(\text{NR}')(\text{=CHtBu})$  complexes, in which the energy differences are probably smaller (path c, Figure 3.1). The masked titanium methylidene species,  $\text{Cp}_2\text{TiCH}_2\text{Al}(\text{Me})_2\text{Cl}$ , known as the Tebbe reagent, acts as a slow catalyst for the degenerate metathesis of terminal olefins.<sup>4</sup> The reaction of the Tebbe reagent with olefins in the presence of Lewis bases allows the isolation of bis(cyclopentadienyl)titanacyclobutanes.<sup>5</sup> These titanacyclobutanes are catalysts for the degenerate methathesis of terminal olefins, but they are very poor catalysts for the productive metathesis of acyclic internal olefins.<sup>5c</sup> In these titanacyclobutane systems the metallacycle is the lowest energy intermediate in the metathesis reaction (path b, Figure 3.1).

Figure 3.1 Reaction Profiles for Possible Metathesis Reaction Pathways



Theoretical studies on the titanium metathesis system have been conducted. Hoffmann and co-workers<sup>5</sup> using the extended Hückel method, found in their calculations on the titanocene metathesis system that the lowest energy structure was of a "non-classical" one, 1. Contrary to experimental observations they find the carbene olefin structure to be lower in energy, by a *ca* 1 eV, than the metallacyclobutane structure.



Rappé has done calculations on a model system in which the cyclopentadienyl groups of the actual system are replaced with chlorines.<sup>7</sup> In these calculations the titanacyclobutane structure was found to be lowest in energy, in agreement with experimental observations. The methyldiene-olefin complex was found to be 11.5 kcal/mol<sup>-1</sup> higher in energy; however, essentially no potential well was found at this geometry. Free titanocenemethyldiene and olefin were found to be 10.4 kcal/mol<sup>-1</sup> above the methyldiene-olefin complex.

Both calculations indicate the barrier for olefin metathesis should be small as is observed by experiment.

Bis(cyclopentadienyl)titanacyclobutanes have been studied experimentally in several ways. Straus<sup>8</sup> has measured the stability of titanacycles as a function of substitution on the metallacyclobutane ring. A number of kinetic studies on this reaction of the metallacycle,  $\text{Cp}_2\text{Ti}\overline{\text{CH}_2\text{CH}(\text{tBu})\text{CH}_2}$ , with trapping reagents, either organic carbonyls or

acetylenes (forming olefins via Wittig reactivity or metallacyclobutenes, respectively) have been performed.<sup>9</sup> These studies have shown that:

1. The reactions are first order in metallacycle.
2. The reactions with acetylenes show saturation type kinetics, *ie*, the reaction rate increases with increasing trapping reagent concentration until a plateau is reached after which added trap does not increase the rate.
- 3) The concentration of trapping reagent sufficient for saturation depends on the identity of the trapping reagent.
- 4) No intermediates are observed.
- 5) Rate is inhibited by added olefin.

Anslyn<sup>9b</sup> has found in competitive trapping experiments using several different metallacycles and some related species, including  $\text{Cp}_2\text{Ti}(\text{CH}_2)\text{PMe}_3$  and  $\text{Cp}_2\text{TiCH}_2\text{Al}(\text{Me})_2\text{Cl}$  found that the identity of the leaving group, an olefin in the case of metallacycles,  $\text{PMe}_3$  in the case of  $\text{Cp}_2\text{Ti}(\text{CH}_2)\text{PMe}_3$ , and  $\text{Me}_2\text{AlCl}$  in the case of  $\text{Cp}_2\text{TiCH}_2\text{Al}(\text{Me})_2\text{Cl}$ , affects the ratio of trapping by two competing trapping reagents. Thus, the leaving group seems to be still interacting with the metal center as the trapping reagent attacks.

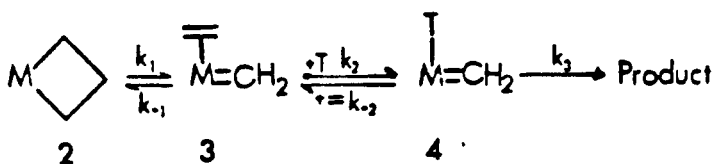
A mechanism consistent with all observations is shown in Scheme 1, in which the formation of methyldiene-olefin complex, 3, is rate determining. The rate law for such a mechanism, assuming the steady-state approximation for intermediates 3 and 4, is:

$$\frac{-d[2]}{dt} = k_{obs} [2],$$

where

$$k_{obs} = \frac{k_1 k_2 k_3 [T]}{(k_3 k_{-1} + k_{-2} k_{-1} [T] + k_2 k_3 [T])}$$

Scheme 1



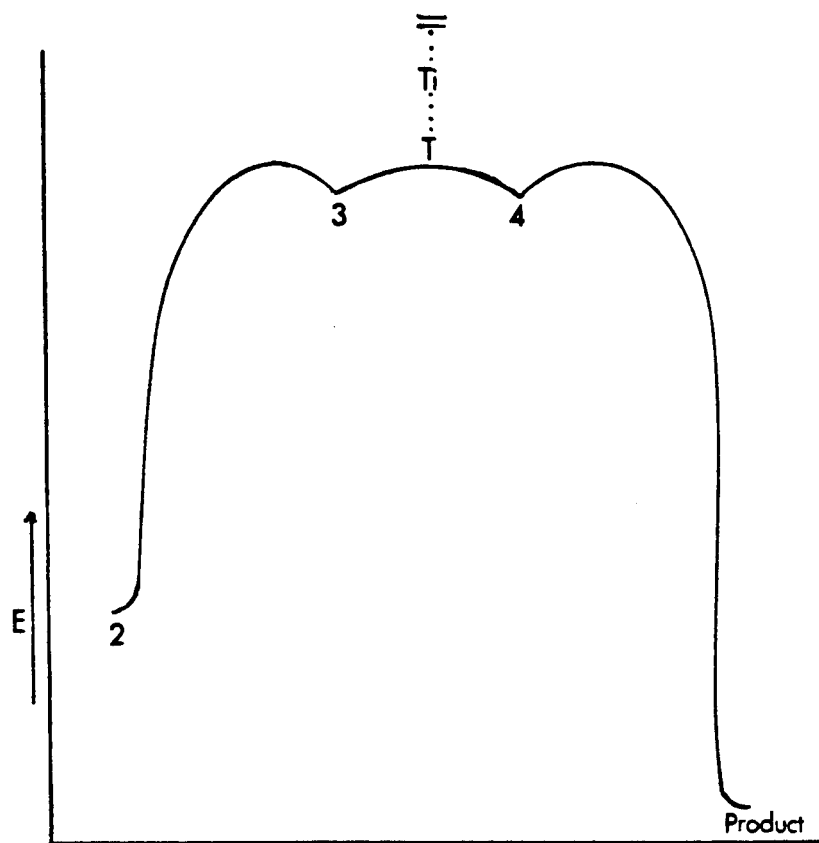
T = Trapping reagent

M = Cp<sub>2</sub>Ti

An energy profile of this mechanism is shown in Figure 3.2. Saturation occurs when  $k_2[T] \gg k_{-1}$ , in which case  $k_{obs} \approx k_1$ ;  $k_2$  should depend on the identity of the trap so that the concentration needed to reach saturation is trap dependent. Inhibition by added olefin is also accounted for. The dependence on leaving group in competitive trapping experiments arises from the S<sub>N</sub>2 like transition state between intermediates 3 and 4.

Another approach to study the titanacyclobutane system is to determine what effect substitution on the cyclopentadienyl rings has on the reactivity of these metallacycles. This approach is the subject of this chapter.

Figure 3.2. Energy Profile for the Proposed Mechanism of the Reaction of Titanacyclobutanes with Trapping Reagents.



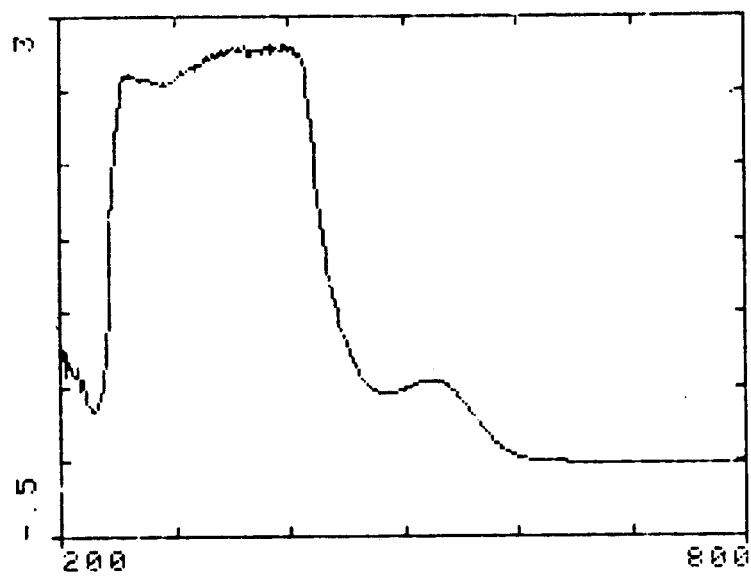
### III.2 Results

A number of ring substituted titanocene dichlorides can be readily prepared.<sup>10</sup> The compounds  $\text{Cp}_2'\text{TiCl}_2$  ( $\text{Cp}' = \text{C}_5\text{H}_4\text{Me}$ ),  $\text{Cp}'\text{CpTiCl}_2$ ,  $\langle\text{Cp}\rangle\text{CpTiCl}_2$  ( $\langle\text{Cp}\rangle = 1,2,4\text{-C}_5\text{H}_2\text{Me}_3$ ),  $\text{Cp}_2^*\text{TiCl}_2$  ( $\text{Cp}^* = \text{C}_5\text{Me}_5$ ) and  $\text{Cp}^*\text{CpTiCl}_2$  were prepared for use in this study.

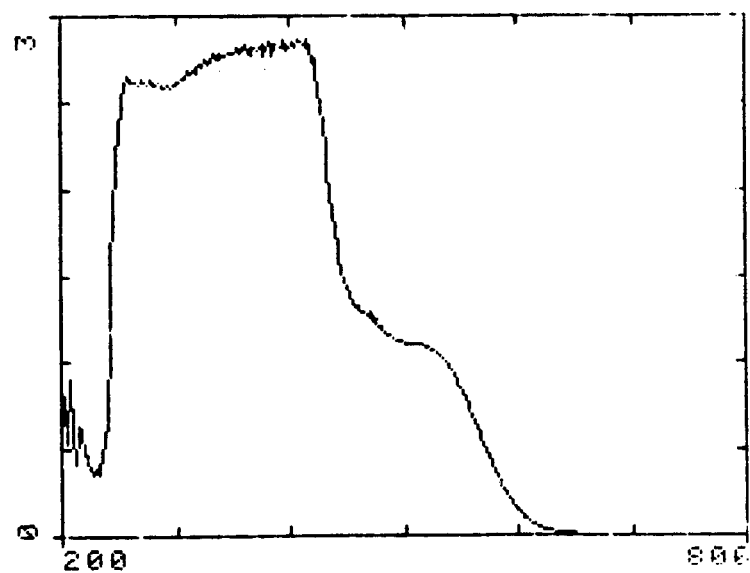
The uv/vis spectra of these ring-substituted titanocene dichlorides were recorded. They all exhibit a weak absorbance between 500 and 560 nm, which in the plain-ring compound has been assigned to a symmetry forbidden  $A_1 \rightarrow A_2$  transition.<sup>11</sup> This band moves to lower energy as electron donating substituents are added to the rings. The absorption spectra of the compounds having single substituents on the rings are qualitatively similar to the plain-ring compound spectrum; in addition to the band between 500 nm and 560 nm they have a broad plateau of absorption between 260 and 410 nm (see Figure 3.3a). The compounds with more highly substituted rings, *i.e.* those with  $\langle\text{Cp}\rangle$  and  $\text{Cp}^*$  ligands, not only exhibit this broad plateau of absorption, but also a band between 470 and 490 nm (See Figure 3.3b). The lowest energy transitions for the titanocene dichlorides examined are shown in Table 3.1.

The  $(49,47)\text{Ti}$  NMR spectra of these ring-substituted titanocene dichlorides were also recorded. Both the  $^{49}\text{Ti}$  and  $^{47}\text{Ti}$  resonances appear in the same spectrum with the  $^{49}\text{Ti}$  resonance 268.1 ppm downfield of the  $^{47}\text{Ti}$  resonance. Due to its higher quadrupole moment the  $^{47}\text{Ti}$  resonance is always broader than the  $^{49}\text{Ti}$  resonance. The results of the  $(49,47)\text{Ti}$  NMR measurements are shown in Table 3.2. Increasing methyl substitution of the rings causes an increasingly downfield shift of the  $(49,47)\text{Ti}$  resonances. Substitution of the electron-donating TMS (trimethylsilyl) group and the electron-withdrawing Cl group onto the rings also causes a downfield shift of the  $(49,47)\text{Ti}$  resonances.

Figure 3.3 uv/vis Spectra of Ring-Substituted Titanocene Dichlorides



a) Spectrum of  $\text{Cp}'\text{CpTiCl}_2$



b) Spectrum of  $\langle\text{Cp}\rangle\text{CpTiCl}_2$



**Table 3.1 Absorption Maxima of Lowest Energy  
Transitions in the uv/vis Spectra of Ring-  
Substituted Titanocene Dichlorides**

Compound <sup>a</sup>	$\lambda_{\max}(\epsilon)^b$
$\text{Cp}_2\text{TiCl}_2$	523 (190)
$\text{Cp}'\text{CpTiCl}_2$	525 (170)
$\text{Cp}'_2\text{TiCl}_2$	528 (200)
$\text{Cp}^{\text{tms}}\text{CpTiCl}_2$	532 (190)
$\langle \text{Cp} \rangle \text{CpTiCl}_2$	510 (shoulder on 472 band)
$\text{Cp}_2^*\text{TiCl}_2$	560 (shoulder on 486 band)

a.  $3.3 \times 10^{-3}$  M solutions in  $\text{CHCl}_3$   
b.  $\lambda$  in nm,  $\epsilon$  in  $\text{M}^{-1} \text{cm}^{-1}$

Table 3.2  $(49,47)\text{Ti}$  NMR<sup>a</sup> of a Number of Titanium Compounds

Compound	$\delta(47,49)\text{Ti}$ (ppm) <sup>b</sup>	$\nu_{\frac{1}{2}}^{49}\text{Ti}$ (Hz)	$\nu_{\frac{1}{2}}^{47}\text{Ti}$ (Hz)	Ref.
$\text{TiCl}_4$	0	3		12
$\text{TiBr}_4$	482.9	3		12
$\text{Cp}_2\text{TiCl}_2$	-771.8	44	84	this work
$\text{Cp}'\text{CpTiCl}_2$	-744.4	66	184	"
$\text{Cp}^{\text{tms}}\text{CpTiCl}_2$	-747.3	85	257	"
$\text{Cp}^{\text{Cl}}\text{CpTiCl}_2$	-740.1	110	----	"
$\text{Cp}'_2\text{TiCl}_2$	-719.3	125	235	"
$\text{Cp}_2^{\text{Cl}}\text{TiCl}_2$	-708.8	136	----	"
$\langle \text{Cp} \rangle \text{CpTiCl}_2$	-666.4	107	195	"
$\text{Cp}_2^*\text{TiCl}_2$	-442.3	70	213	"

a).  $^{49}\text{Ti}$  (5.51%;  $I = 7/2$ ,  $Q = 0.24 \times 10^{-28} \text{ M}^2$ );  $^{47}\text{Ti}$  (7.28%;  $I = 5/2$ ,  $Q = 0.29 \times 10^{-28} \text{ M}^2$ ). See Ref. 12.

b) Reference: external neat  $\text{TiCl}_4$ . Positive  $\delta$  values are downfield.

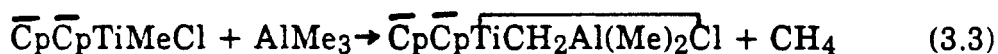
From the ring substituted titanocene dichlorides the corresponding titanocene methyl chlorides can be prepared in good yield (equation 3.2). The C-H coupling constants of the methyl group



$\overline{\text{Cp}}$  = substituted or unsubstituted ring

bonded to titanium are included in Table 3.3. The C-H coupling constant decreases with increasing methyl substitution of the cyclopentadienyl rings.

The ring-substituted titanocene methyl chlorides seem to be the best starting materials for the preparation of ring-substituted analogs of the Tebbe reagent (equation 3.3). The materials are identical to materials produced by the direct reaction of the titanocene dichlorides with two equivalents of  $\text{AlMe}_3$ .<sup>10</sup>



The ring substituted Tebbe analogs could be used to synthesize various titanacyclobutanes *via* modifications of established routes used for the parent system (equation 3.4). The metallacycles

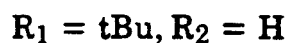
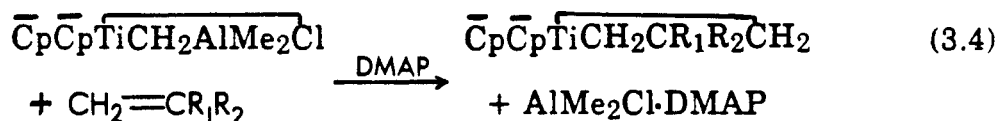
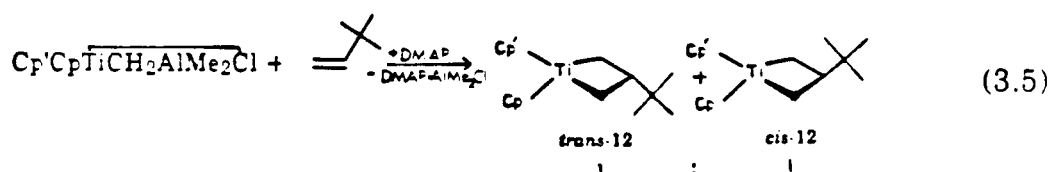


Table 3.3 C-H Coupling Constants of Methyl Groups Attached to a Metal Center

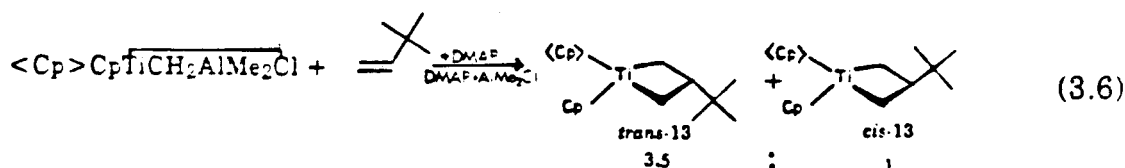
Compound	$J_{CH}$ (Hz)	Ref.
$CpCl_2TiMeCl$	129.9	9b
$CpCl^*TiMeCl$	129.1	9b
$Cp_2TiMeCl$	128.9	13
$Cp^*CpTiMeCl$ (5)	128.4	this work
$Cp_2^*TiMeCl$ (6)	128.2	"
$<Cp>CpTiMeCl$ (7)	127.7	"
$Cp^*CpTiMeCl$ (8)	127.2	"
$Cp_2^*TiMeCl$ (9)	126.5	"
$Cp_2ZrMeCl$	120.7	13
$Cp_2ZrMe(OMe)$	118.8	13
$(Cp_2ZrMe)_2O$	118.6	13
$Cp_2ZrMe_2$	117.4	13
$Cp_2^*ZrMe_2$	116.8	13

$\text{Cp}_2'\overline{\text{TiCH}_2\text{CMe}_2\text{CH}_2}$ , 10,  $\text{Cp}_2'\overline{\text{TiCH}_2\text{CH}(\text{tBu})\text{CH}_2}$ , 11, were synthesized in this manner. The reaction of  $\text{Cp}'\text{Cp}\overline{\text{TiCH}_2\text{AlMe}_2\text{Cl}}$  with neohexene and DMAP (dimethylaminopyridene) produces a 1:1 mixture of *trans*-12 and *cis*-12 (equation 3.5).<sup>14</sup> Apparently this is the



equilibrium ratio as it does not change upon heating, even in the presence of added olefin. Attempts to separate the isomers by crystallization failed; they co-crystallize in the same 1:1 ratio.

Reaction of  $\langle \text{Cp} \rangle \text{Cp}\overline{\text{TiCH}_2\text{AlMe}_2\text{Cl}}$  with neohexene and DMAP produces a 3.4:1 ratio *trans*-13 to *cis*-13 (equation 3.6).<sup>14</sup>



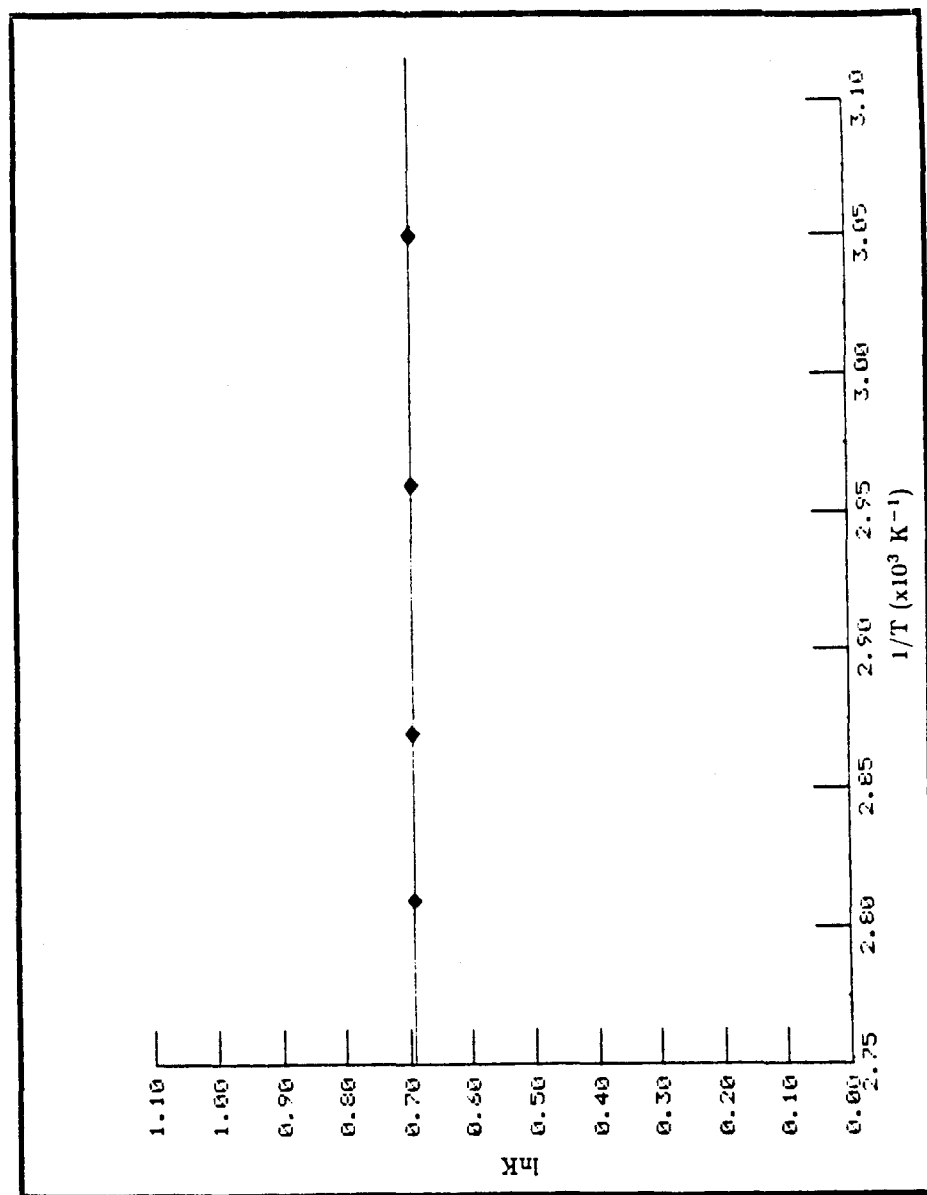
Attempts to separate *trans*-13 and *cis*-13 failed. Recrystallization from toluene led to a 3.5:1 *trans/cis* ratio of the isomers. Recrystallization from diethyl ether led to a 2.2:1 ratio. Conducting the metallacycle synthesis at low temperatures did not significantly increase the fraction of *trans*-13 in the reaction mixture.

The 3.4:1 ratio of *trans*-13/*cis*-13 is a kinetic ratio. Material with this initial ratio was allowed to equilibrate (both with and without added olefin) at various temperatures from 55 to 83°C. The equilibrium constant  $K = [\textit{trans}-$

13]/[*cis*-13] is essentially invariant at 2.0 over this temperature range and the van't Hoff plot (Figure 3.4) shows a flat line. This result indicates that  $\Delta H$  and  $\Delta S$  for the equilibration of *trans*-13 and *cis*-13 are both small, as expected since *trans*-13 and *cis*-13 have the same number and kinds of bonds and should have similar structures.

The rate in which a *ca* 3.5:1 mixture of *trans*-13/*cis*-13 attains equilibrium in the absence of added olefin was monitored at several temperatures. Forward and reverse rate constants for the equilibration *cis*-13  $\rightleftharpoons$  *trans*-13 could be estimated from this data. The results are shown in Table 3.4. These rate constants are smaller than rate constants observed for trapping reactions of these metallacycles with diphenylacetylene (*vide infra*). During the equilibrations *ca* 5% decomposition of metallacycle occurs so that we cannot rule out that freed olefin, though not observed, may catalyze the equilibration of *trans*-13 and *cis*-13. Qualitatively, the addition of two equivalents of olefin did not increase the rate of this equilibration. In the presence of 2 equivalents of added labeled olefin, *cis*-1,2-dideuterio-3,3-dimethylbutene, per equivalent of titanium *ca* 8% of the labeled olefin is incorporated into metallacycle when a mixture of *trans*-13 and *cis*-13 is heated to 68°C for 75 min.

Figure 3.4 van't Hoff Plot for the Equilibrium *cis*-13  $\rightleftharpoons$  *trans*-13.



$$\ln K = \Delta H/RT + \Delta S/R$$

$$\Delta H \sim 0$$

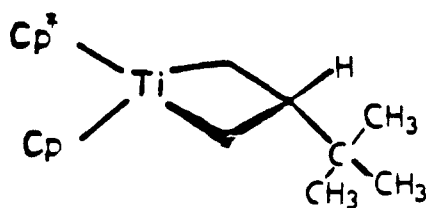
$$\Delta S = 0.3 \text{ eu}$$

Table 3.4 Kinetic Data for the Equilibration  $cis-13 \xrightleftharpoons[k_{-1}]{k_1} trans-13$ 

T(°C)	$k_1(\times 10^5 \text{ s}^{-1})$	$k_{-1}(\times 10^5 \text{ s}^{-1})$
63.5	7.3	3.5
68.5	16.0	7.7
74.0	27.0	13.0
78.5	40.0	19.0

[Ti] = 0.11M For  $k_1$ :  $\Delta H^\ddagger = 26 \pm 2 \text{ kcal/mol}^\cdot$ ;  $\Delta S^\ddagger = -2 \pm 7 \text{ eu}$ ,  $\rho = -0.991$ . For  $k_{-1}$ :  $\Delta H^\ddagger = 25 \pm 3 \text{ kcal/mol}^\cdot$ ;  $\Delta S^\ddagger = -3 \pm 7 \text{ eu}$ ,  $\rho = -0.990$

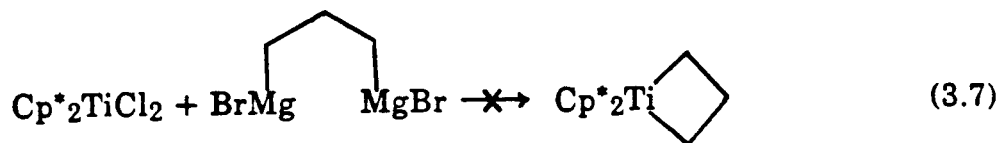
Reaction of  $\text{Cp}^*\text{CpTiCH}_2\text{AlMe}_2\text{Cl}$  with neohexene and DMAP produced only one isomer of a new metallacycle presumably 16; however, it was not cleanly isolated.



16



Attempts to prepare the metallacycle  $\text{Cp}^*_2\text{TiCH}_2\text{CH}_2\text{CH}_2$  using the method developed by Bickelhaupt<sup>15</sup> for the plain ring system (equation 3.7) proved unsuccessful.

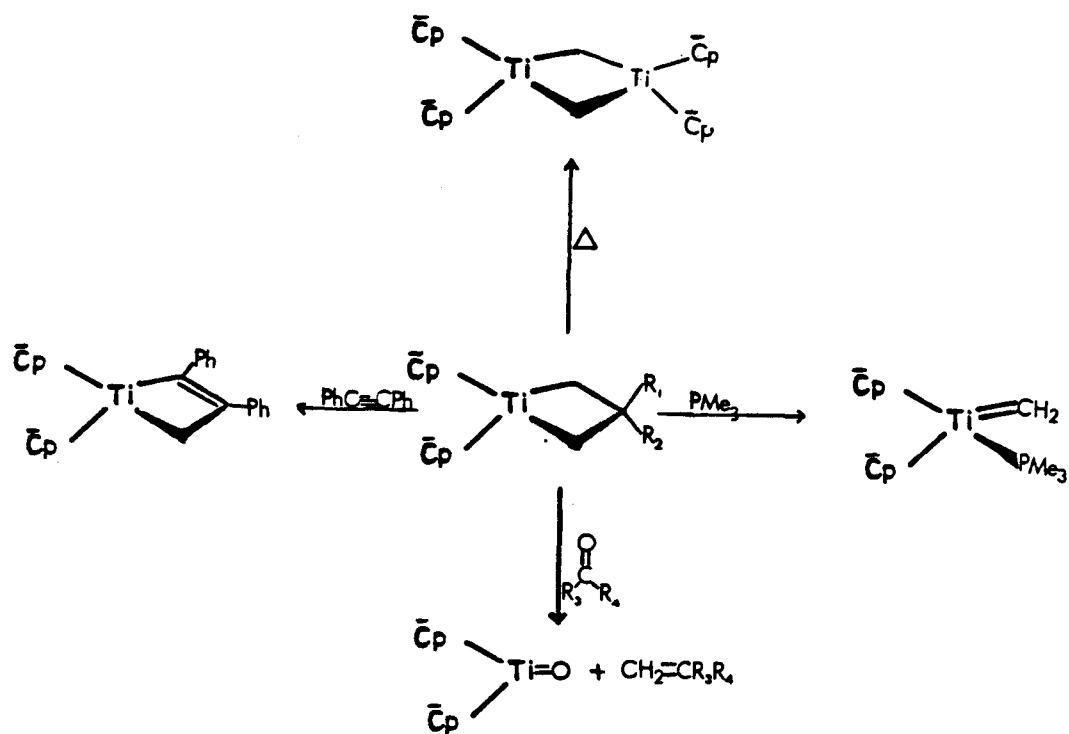


All the titanacyclobutanes synthesized for this study are similar spectroscopically to the parent systems. In the proton NMR spectra the  $\alpha\text{H}$ 's of the metallacycle ring resonate in the region 1.8-2.4 ppm and  $\beta\text{-H}$ 's are in the characteristic high-field region 0.14 to -0.2 ppm. In the t-butyl metallacycles, *trans*-12, *cis*-12, *trans*-13, *cis*-13, and 14 the  $\beta\text{-H}$ 's appear as quintets and the  $\alpha\text{-H}$ 's appear as triplets, indicating the  $\alpha\text{-H}$  geminal coupling constant and the *cis* and *trans*  $\alpha\text{-H}$  to  $\beta\text{-H}$  coupling constants are essentially the same. In <sup>13</sup>C NMR spectra the t-butyl metallacycles show  $\alpha\text{-C}$  resonances between 67.0 and 68.0 ppm and  $\beta\text{-C}$  resonances between 20.0 and 30.0 ppm.

The reactivity of these titanacycles are similar to that of the parent metallacycles (Figure 3.5). Thermally they decompose to form an observable amount of titanocene methyldiene dimers (<sup>1</sup>H NMR); however, attempts to cleanly isolate authentic samples of these dimers were not successful. They react with  $\text{PMe}_3$  to liberate olefin and form titanocene methyldiene-phosphine complexes. They react irreversibly with organic carbonyls to form oxo polymers and terminal olefins; no intermediates are observed in this reaction. They react with diphenylacetylene to produce metallacyclobutenes; again no intermediate can be observed.

The metallacyclobutenes could be independently synthesized from the reaction of the corresponding Tebbe reagent with diphenylacetylene. One of the most characteristic spectroscopic features of these metallacyclobutenes

Figure 3.5. Reactivity of Ring-Substituted Metallocycles.



is the low field resonance of the  $sp^2$  hybridized  $\alpha$ -carbon in their  $^{13}C$  NMR spectra.<sup>16</sup>

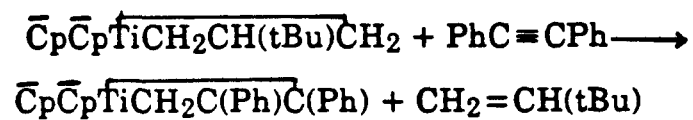
The irreversibility of the reaction of titanacyclobutanes with carbonyls and acetylenes makes these reagents good trapping reagents for kinetic studies. The kinetics of the reaction of the t-butylmetallacycles  $Cp_2\overline{TiCH_2CH(tBu)CH_2}$  (17), 11, *trans*-12, *cis*-12, *trans*-13 and *cis*-13 with diphenylacetylene and acetone were studied. The results are shown in Table 3.5 and Table 3.6, respectively. Activation parameters for the reaction of 11, *trans*-13, *cis*-13 with diphenyl acetylene were derived from kinetics data obtained at 55.0, 63.5, 68.5, and 73.5°C and are listed in Tables 3.7, 3.8 and 3.9. A comparison of activation free energies at 55°C as calculated from the values of  $k_{obs}$  found at this temperature to those calculated from activation parameters is shown in Table 3.10. Essentially the same values are obtained from either method.

The reaction of a mixture of *trans*-13 and *cis*-13 with seven equivalents of diphenylacetylene and ten equivalents of labeled olefin, 1,2-*cis*-dideuterio-3,3-dimethylbutene, was carried out to 60% conversion of metallacyclobutane to metallacyclobutene at 72°C. No deuterium incorporation into the metallacyclobutane starting material or the metallacyclobutene product was observed.

Anslyn<sup>9b</sup> has studied the kinetics of the reaction of  $Cp_2\overline{TiCH_2CMe_2CH_2}$  (18) and 10 with diphenyl acetylene. His results are shown in Table 3.11.

The kinetics of the reaction of 10 and 18 with acetone were also studied. These results are shown in Table 3.12.

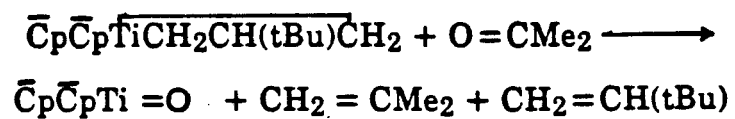
Table 3.5 Kinetics Data for the Reaction:



$\overline{\text{Cp}}$	Metallcycle	$k_{\text{obs}}(\times 10^5 \text{ s}^{-1})$	rel. rates
$\text{Cp}_2$	17	68	16
$\text{Cp}'\text{Cp}$	<i>trans</i> -12	40	9.3
$\text{Cp}'\text{Cp}$	<i>cis</i> -12	40	9.3
$\text{Cp}'_2$	11	10	2.3
$\langle \text{Cp} \rangle \text{Cp}$	<i>trans</i> -13	4.5	1.1
$\langle \text{Cp} \rangle \text{Cp}$	<i>cis</i> -13	4.3	1

$[\text{Ti}]_{\text{TOT}} = 0.11 \text{ M}$   $[\text{PhC}\equiv\text{CPh}]_0 = 0.83 \text{ M}$

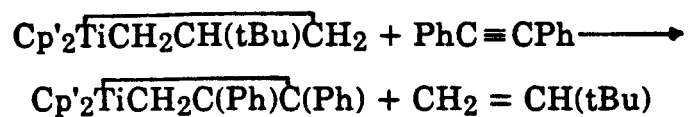
Table 3.6 Kinetics Data for the Reaction:



$\overline{\text{Cp}}$	Metallcycle	$k_{\text{obs}}(\times 10^5 \text{ s}^{-1})$	rel. rates
Cp <sub>2</sub>	17	30	15
Cp'Cp	<i>trans</i> -12	20	10
Cp'Cp	<i>cis</i> -12	20	10
Cp' <sub>2</sub>	11	5	2.5
<Cp>Cp	<i>trans</i> -13	2	1
<Cp>Cp	<i>cis</i> -13	2	1

$$[\text{Ti}]_{\text{TOT}} = 0.16 \text{ M } [\text{O}=\text{CMe}_2]_0 = 0.48 \text{ M}$$

Table 3.7 Activation Parameters for the Reaction



T (°C)	k <sub>obs</sub> (x 10 <sup>5</sup> s <sup>-1</sup> )
55.0	10
63.5	35
68.5	64
73.5	128

$\Delta H^\ddagger = 30.1 \pm 0.6 \text{ kcal/mol}^{-1}$ ,  $\Delta S^\ddagger = +15 \pm 2 \text{ eu}$ .  
 $\Delta G^\ddagger_{328} = 25.2 \pm 1 \text{ kcal/mol}^{-1}$ ;  $\rho = -0.9995$

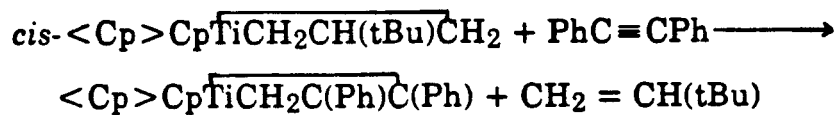
Table 3.8 Activation Parameters for the Reaction:



T (°C)	k <sub>obs</sub> (x 10 <sup>5</sup> s <sup>-1</sup> )
55.0	4.5
63.5	15
68.5	30
73.5	55

$\Delta H^\ddagger = 30.1 \pm 0.4 \text{ kcal/mol}^{-1}$ ,  $\Delta S^\ddagger = +13 \pm 1 \text{ eu}$ ;  
 $\Delta G^\ddagger_{328} = 25.8 \pm 21 \text{ kcal/mol}^{-1}$ ;  $\rho = -0.9990$ .

Table 3.9 Activation Parameters for the Reaction:



T (°C)	k <sub>obs</sub> (x 10 <sup>5</sup> s <sup>-1</sup> )
55.0	4.3
63.5	12
68.5	24
73.5	46

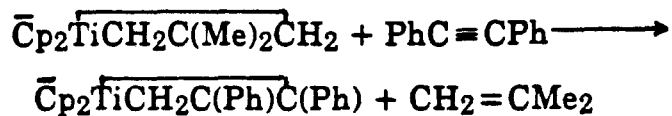
$\Delta H^\ddagger = 28.3 \pm 0.9 \text{ kcal/mol}^{-1}$ ,  $\Delta S^\ddagger = 8 \pm 3 \text{ eu}$ ;  
 $\Delta G^\ddagger_{328} = 25.7 \pm 2 \text{ kcal/mol}^{-1}$ ;  $\rho = -0.9990$ .



Table 3.10 Comparison of  $\Delta G^\ddagger_{328}$  Values Obtained from  $k_{\text{obs}}$  value vs.  
Values Obtained from Activation Parameters

$\bar{\text{Cp}}$	Metallacycle	$\Delta G^\ddagger_{328}$ (Act. Parameters)	$\Delta G^\ddagger_{328}$ (from $k_{\text{obs}}$ data)
Cp <sub>2</sub>	17	24.0 <sup>a</sup>	24.0
CpCp'	<i>trans</i> - and <i>cis</i> -12	---	24.4
Cp <sub>2</sub> '	11	25.2	25.3
<Cp>Cp	<i>trans</i> -13	25.8	25.8
<Cp>Cp	<i>cis</i> -13	25.7	25.8

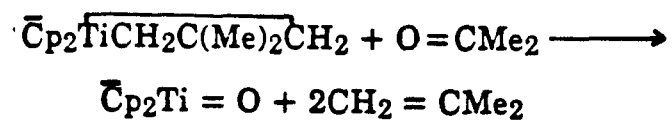
a) From Ref. 10.

Table 3.11 Kinetics Data for the Reaction:<sup>a</sup>

$\overline{\text{Cp}}$	Metallacycle	$k_{\text{obs}} (\times 10^4 \text{ s}^{-1})$	rel. rates
$\text{Cp}_2$	18	18.7	8.9
$\text{Cp}_2'$	10	2.1	1

a) Ref. 9b.

Table 3.12 Kinetics Data for the Reaction:



$\overline{\text{Cp}}$	Metallacycle	$k_{\text{obs}} (\times 10^4 \text{ s}^{-1})$	rel. rates
$\text{Cp}_2$	18	34	7.1
$\text{Cp}_2'$	10	4.8	1

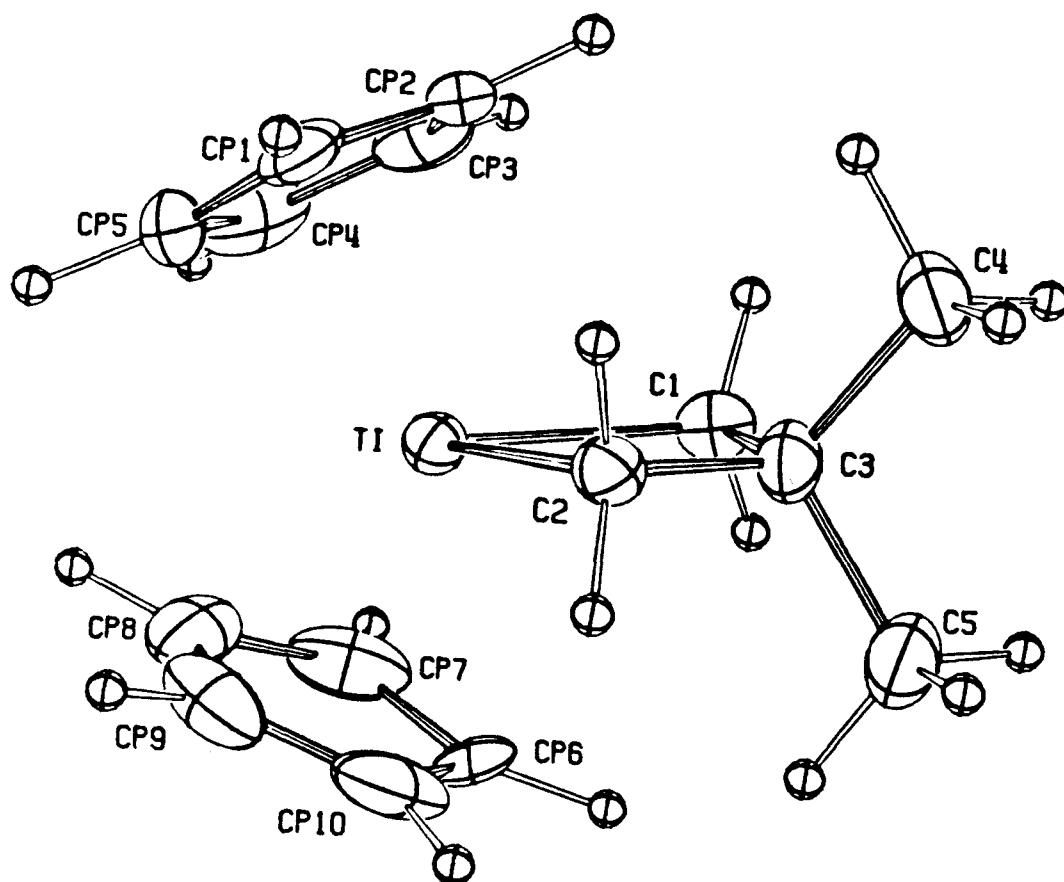
[Ti]<sub>TOT</sub> = 0.18 M; [O=CMe<sub>2</sub>]<sub>0</sub> = 1.1 M

### III. 3 Discussion

Substitution of the cyclopentadienyl rings can affect the reactivity of bis(cyclopentadienyl)titanacyclobutanes through steric and electronic effects. Several titanacyclobutanes have been structurally characterized. The structure of 18 is shown in Figure 3.6. The substituents on the  $\beta$ -carbon of the metallacyclic ring interact with the cyclopentadienyl rings. In mono- $\beta$ -substituted metallacycles, the steric interaction is relieved by a rocking of the  $\beta$ -carbon fragment and not by ring puckering, as revealed by the structures of 17 and  $\text{Cp}_2\text{TiCH}_2\text{CHPhCH}_2$ .<sup>5b</sup> Straus has found that increasing steric bulk at the  $\beta$ -position increasingly destabilizes the metallacycles.<sup>8</sup> Thus, one would expect that increasing the steric bulk of the cyclopentadienyl groups by substitution should destabilize the metallacycles.

We see from the 1:1 ratio of *trans*-12 to *cis*-12 that adding one methyl group to the ring does not have much steric effect. With three methyl groups on a ring steric effects appear; *trans*-13 is *ca.* 0.5 kcal/mol<sup>-1</sup> more stable than *cis*-13.

Ring-substitution can affect these complexes electronically. Gassman<sup>18</sup> has shown from ESCA data that substitution of two Cp\* ligands for the two Cp ligands in titanocene dichloride produces an effect on the titanium core orbitals equivalent to a one-electron reduction at titanium. Thus, electron donating substituents on the rings increase the electron density at the metal center.



We have observed from the absorption spectra of various titanocene dichlorides that ring substitution affects the energy difference between the ground and first excited states of these complexes. It seems that electron donating groups on the rings tend to make this energy difference smaller; there are exceptions to this generalization cf. the absorption spectrum of  $\langle \text{Cp} \rangle \text{CpTiCl}_2$ .

The C-H coupling constants of methyl groups depend on the amount of s-character at carbon in the C-H bonds.<sup>19</sup> To a first approximation the amount of s-character depends on the effective electronegativity of the group to which the methyl group is bonded; the larger the electronegativity of this group the lower the s-character of its bond with the methyl carbon. This leaves more s-character in the C-H bonds and hence, increasing the electronegativity of the group attached to the carbons should increase the C-H coupling constant observed for a methyl group. Conversely, decreasing the electronegativity of the group attached to carbon should lower the C-H coupling constant. Increasing the electron density at the atom to which the methyl group is bonded effectively lowers the electronegativity and should lower the C-H coupling constant. Such an effect was observed by Yoder<sup>20</sup> in his study of the variation of C-H coupling constants of methyl groups in several types of compounds as a function of substitutions on aromatic rings. His results from substituted toluenes are shown in Table 3.13. He found a linear correlation between  $J_{\text{CH}}$  and the Hammett  $\sigma$  values of the substituents. Electron-withdrawing substituents increased  $J_{\text{CH}}$  and electron-donating substituents decreased  $J_{\text{CH}}$ . Yoder found similar correlations for substituted t-butyl benzenes and anisoles.

We found similar effects in ring-substituted titanocene methyl chlorides (Table 3.3). Increasing the electron-density at Ti by adding methyl groups to the cyclopentadienyl rings causes a lowering of the  $J_{CH}$  of the methyl group bonded directly to the metal center. Conversely, substitution of electron-withdrawing chlorides on the rings causes an increase in  $J_{CH}$ .

Since Zr is more electropositive than Ti, the Zr compounds shown in Table 3.3 all exhibit lower  $J_{CH}$  values than their analogous Ti compounds; however, the same trend is observed. Increasing the electron density at Zr lowers the  $J_{CH}$  of the methyl group bonded to the metal.

NMR chemical shift values are not always an indication of electron density at the atom being observed. A striking example of this is found in the  $^{49,47}\text{Ti}$  NMR data for a number of ring-substituted titanocene dichlorides (Table 3.2). Replacing two chlorides in  $\text{TiCl}_4$  with more electron donating cyclopentadienyl rings does shift the Ti resonances upfield as expected, but the titanocene dichloride complex that should be the most electron-rich at titanium,  $\text{Cp}^*_2\text{TiCl}_2$ , exhibits the lowest field  $^{49,47}\text{Ti}$  resonance. Also note that the  $\text{TiBr}_4$  resonances are downfield relative to those of  $\text{TiCl}_4$ . Gassman<sup>21</sup> has found an inverse relationship between core electron binding energy and  $^{49,47}\text{Ti}$  chemical shift for  $\text{Cp}_2\text{TiX}_2$ ,  $\text{Cp}^*\text{CpTiX}_2$ , and  $\text{Cp}^*_2\text{TiX}_2$  ( $X = \text{F}, \text{Cl}, \text{Br}$ ) compounds. Spinney<sup>22</sup> has attributed the counter intuitive chemical shift values found in titanium NMR to large paramagnetic shielding terms.

Chemical shifts in NMR spectroscopy<sup>23</sup> arise from differences between the actual field at a nucleus,  $H_N$ , and applied field,  $H_O$ , due to shielding by the electrons of the molecule being observed.  $H_N$  is given by

Table 3.13 Variation of C-H Coupling Constant of the Methyl Group of Substituted Toulenes,  $\text{CH}_3\text{C}_6\text{H}_5\text{X}$  as a Function of the Hammett  $\sigma$  of the Substituents

X	$J_{\text{CH}}$ (Hz)	$\sigma$
m- $\text{NO}_2$	127.3	0.710
m-F	126.9	0.337
m-Cl	126.4	0.373
p-Cl	126.3	0.227
m-OMe	125.9	0.115
H	125.8	0.0
m-Me	125.6	-0.069
p-Me	125.5	-0.170

$$J_{\text{CH}} = \rho\sigma + C; \rho = 1.72 \text{ Hz}/\sigma.$$

$$H_{\text{N}} = H_{\text{O}} (1 - \sigma), \quad (3.8)$$

where  $\sigma$  is the isotropic shielding constant (appropriate for molecules in solution) which can be different at each atom of a molecule. Chemical shift shielding is in reality a tensor quantity and  $\sigma$  is given by:

$$\sigma = 1/3 (\sigma_{\text{xx}} + \sigma_{\text{yy}} + \sigma_{\text{zz}}), \quad (3.9)$$

when  $\sigma_{\alpha\alpha}$  ( $\alpha = x, y, z$ ) are the diagonal elements of the tensor. The shielding terms can be thought of as composed of two terms, an isotropic term, called the diamagnetic shielding term,  $\sigma_d$ , and an anisotropic term, called the paramagnetic shielding term,  $\sigma_p$ , where:

$$\sigma_{\alpha\alpha} = \sigma_d - \sigma_p. \quad (3.10)$$

These terms can be estimated by treating the magnetic field as a perturbation to the electronic ground state of the molecule.. The chemical shift shielding tensor elements are given by:

$$\sigma_{\alpha\alpha} = \frac{e^2}{2mc^2} \langle 0 | \frac{x^2 + y^2}{r^3} | 0 \rangle - \left( \frac{e\hbar}{2mc} \right)^2 \sum_n \left\{ \frac{\langle 0 | L_\alpha | n \rangle \langle n | 2L_\alpha / r^3 | 0 \rangle}{E_n - E_0} + \frac{\langle 0 | 2L_\alpha / r^3 | n \rangle \langle n | L_\alpha | 0 \rangle}{E_n - E_0} \right\},$$

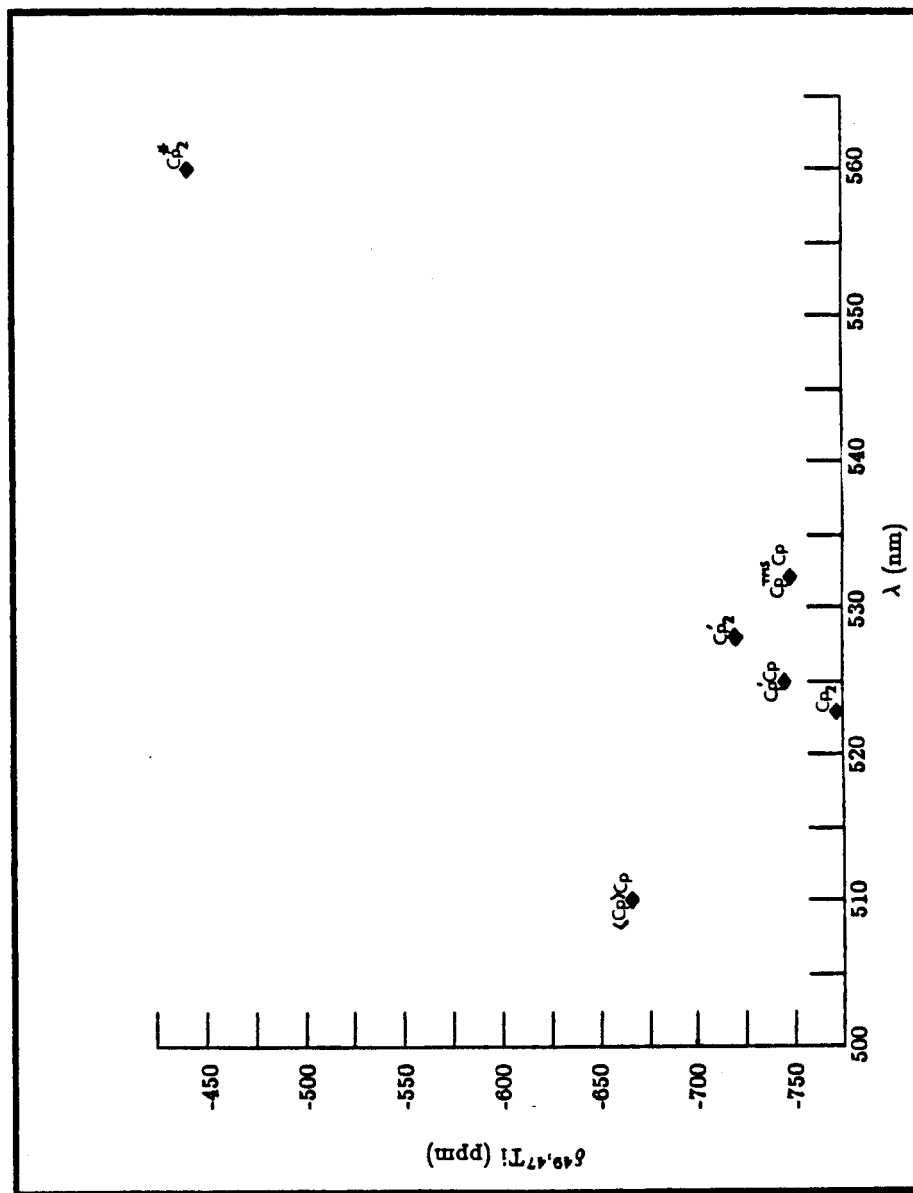
where  $\alpha = x, y, z$ ;  $\langle 0 |$  = ground electronic state;  $\langle n |$  =  $n^{\text{th}}$  excited state,  $L_\alpha$  = angular momentum operator centered on the observed nucleus;  $E_0$  = energy of the ground state; and  $E_n$  = energy of the  $n^{\text{th}}$  excited state. The first term on the right-hand side of 3.11 is  $\sigma_d$  and allows spherically symmetric electron circulations about the observed nucleus. The summation term in 3.11 is  $\sigma_p$  and is the result of field-induced mixing of the ground and excited electronic states. This term allows non-spherically symmetric electron circulations about the observed nucleus.



Increasing the electron density at a nucleus increases the  $\sigma_d$  term leading to an upfield shift of an NMR resonance ( $\sigma_d$  acts to decrease the field at a nucleus so that a stronger applied field is necessary to reach resonance). In molecules with high lying excited states, e.g. saturated hydrocarbons,  $\sigma_p$  is negligible; the  $E_n - E_0$  factors in 3.11 are large. The  $\sigma_d$  term dominates, and the chemical shifts are as we would predict from our chemical intuition about electron density (*cf* the  $^{13}\text{C}$  chemical shifts of methyl halides:<sup>24</sup>  $\text{CH}_3\text{Cl}$ ,  $\delta$  25.1;  $\text{CH}_3\text{Br}$ ,  $\delta$  10.2;  $\text{CH}_3\text{I}$ ,  $\delta$  -20.5).

In molecules with low lying excited states, such as the titanium complexes we have studied, the  $\sigma_p$  term, which acts to deshield the nucleus, can become dominant in determining the observed chemical shifts. The largest-contribution to  $\sigma_p$  should arise from the first excited state;  $E_n - E_0$  is the smallest for this state. Thus, for systems in which  $\sigma_p$  is playing the major role in determining the observed chemical shifts, there should be a correlation between the lowest energy transition observed in the absorption spectrum and the observed chemical shift ( $\delta$  should be related to  $(E_1 - E_0)^{-1}$  or to  $\lambda_{\text{max}}$ ,  $(E_1 - E_0)^{-1} = \lambda_{\text{max}}c/h$ ). Such correlations were found for  $\text{TiX}_4$  and  $\text{Cp}_2\text{TiX}_2$  ( $\text{X} = \text{Cl}, \text{Br}, \text{I}$ ).<sup>12</sup> We have plotted the observed  $\delta_{49,47}\text{Ti}$  values vs. the wave length of the observed lowest energy transition in the absorption spectrum of a number of ring-substituted titanocene dichlorides (Figure 3.7). We do not expect linear correlations since both  $\sigma_d$  and  $\sigma_p$  will change with substitutions on the rings. In general it does seem that the lower the energy of the first optical transition the farther downfield the observed  $^{49,47}\text{Ti}$  resonance. The chemical shift of  $\langle \text{Cp} \rangle \text{CpTiCl}_2$  may seem anomalously low; however, since  $\sigma_p$  depends on the sum of contributions from all excited states and

**Figure 3.7. Plot of  $\delta_{49,47}\text{Ti}$  vs.  $\lambda_{\text{max}}$  (lowest energy transition) of a Number of Ring-Substituted Titanocene Dichlorides.**

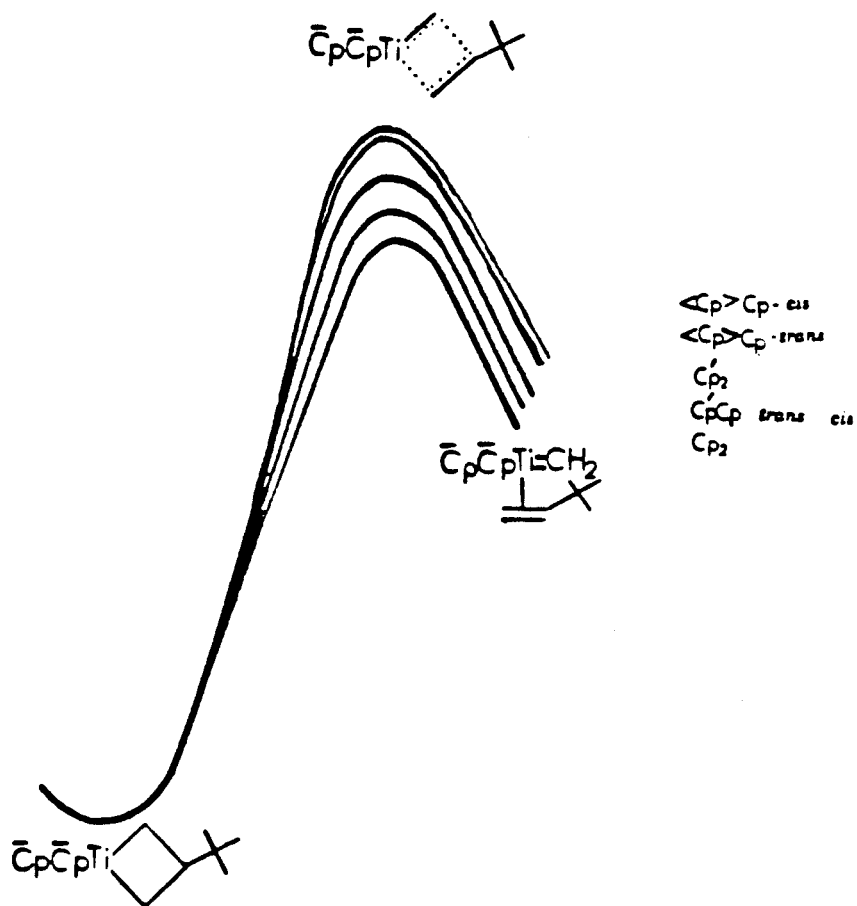


$\langle \text{Cp} \rangle \text{CpTiCl}_2$  has more than one low lying excited state (vide supra), its chemical shift may not be unreasonably low.

Since our kinetics were done under saturation conditions, they essentially give us only information about the relative energies of the titanacyclobutanes and the first transition state of the mechanism shown in Scheme 1, *i.e.*,  $k_{\text{obs}} = k_1$ . We can see how the relative energy difference varies as a function of ring-substitution. The data we have does not let us determine the relative stabilities of metallacycles having different substituents on the cyclopentadienyl rings. Thus, we cannot separate ground state from transition state effects. In our discussion we make the assumption that differential ground state effects are not important in determining the rate differences observed; *i.e.*, we place all metallacycles at the zero of a relative energy scale (Figure 3.8). Then we can discuss the observed rates on the basis of the relative energies of the transition states. Using this assumption we are able to rationalize the observed changes in rate constant as a function of methyl group substitution on the cyclopentadienyl rings. Anslyn has some results that indicate this assumption is not always valid (vide infra).

We see from all our kinetic results that increasing methyl substitution of the rings decreases  $k_{\text{obs}}$ . Steric effects seem to be playing a very small part in determining the observed rate; *trans*-12 and *cis*-12 react at the same rate, and *trans*-13 and *cis*-13 react essentially at the same rate. For a number of reasons we rule out isomer equilibration as the cause for the equal values of  $k_{\text{obs}}$  for reactions of the *trans* and *cis* isomers of the mixed-ring metallacycles. First, the reactions are carried out under saturation conditions, *i.e.*,  $k_2[\text{T}] \gg k_1$  in Scheme 1. Closure of carbene-olefin back to metallacycle, which would be required for isomer equilibration, should not

Figure 3.8. Comparison of Relative Transition State Energies for the Opening of Metallacycles to Carbene-Olefin Complexes Assuming Negligible Differential Ground State Effects.



competitive with the trapping reaction. Second, the observed forward and reverse rate constants for the equilibration of *trans*-13 and *cis*-13 were smaller than  $k_{\text{obs}}$  values obtained in trapping experiments. Third, the  $k_{\text{obs}}$  values for the reaction of *trans*-13 and *cis*-13 with diphenylacetylene were the same whether the material was 3.5:1 *trans/cis* to start or 2.2:1 *trans/cis* to start. Lastly, while labeled added olefin is incorporated into a *cis/trans* mixture of 13 in the absence of added trapping reagent, no labeled olefin is incorporated into starting material or product when a concentration of diphenylacetylene equivalent to that used in the kinetic studies is present.

Electronic effects then seem to play the major role in determining the relative reactivities of the metallacycles studied. The cleavage of a metallacyclobutane to a carbene-olefin complex is formally a reductive process.<sup>1</sup> In a carbene-olefin complex the CH<sub>2</sub> group can be considered either a dianionic donor or a neutral donor. Thus, in these titanium systems we should assign the oxidation state of titanium in metallacycles as Ti<sup>IV</sup> while in carbene-olefin complexes the titanium can have some Ti<sup>II</sup> character (equation 3.12).



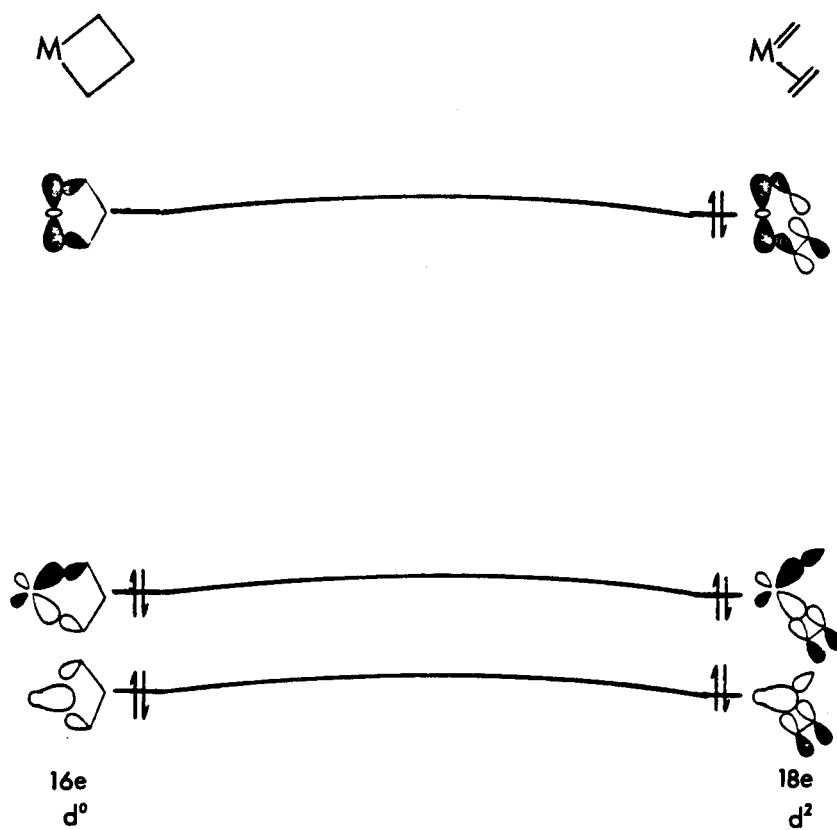
A look at the MO description of the two species in equation 3.12 also leads to the conclusion that formation of the carbene-olefin complex from metallacycle involves reduction at titanium. Hoffmann<sup>6</sup> has studied these systems using the extended Hückel method. While quantitatively incorrect, his calculations lead to a qualitative understanding of this system. He calls the titanacyclobutanes  $d^0$  complexes and carbene-olefin complexes  $d^2$ . We can

see his reasoning from the orbital correlation diagram shown in Figure 3.9. The metallacycles are 16e<sup>-</sup> species, one d orbital, the 1a<sub>1</sub> orbital in the bent metallaocene system,<sup>25</sup> does not interact strongly with the three carbon fragment and remains empty. In the carbene-olefin complex, which is an 18e<sup>-</sup> species, this orbital interacts with the  $\pi^*$  orbital of the olefin and the  $\pi$  symmetry orbital of the carbene. The combination of these orbitals having net positive overlap must be occupied and hence there is d<sup>2</sup> character at the metal.

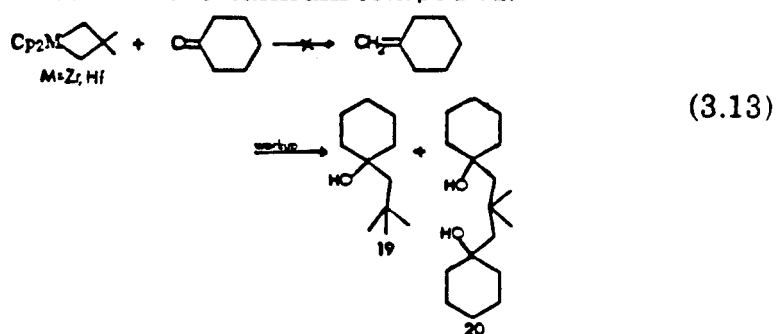
By the Hammond<sup>26</sup> postulate the transition state for the endothermic formation of carbene-olefin from metallacycle should most closely resemble the carbene-olefin species. Thus, effects that change the stability of carbene-olefin relative to metallacycle should cause similar changes to the stability of the transition state relative to metallacycle. Since the formation of carbene-olefin from metallacycle involves formal reduction at titanium, increasing the electron density at titanium by increasing the electron-donating ability of the ancillary ligands should destabilize the carbene olefin relative to the metallacycle. Thus, we predicted that increasing methyl substitution of the cyclopentadienyl rings, making them better donors, of the biscyclopentadienyl titanacyclobutane system should slow cleavage of metallacycle to carbene-olefin. This predicted result is what we observed. Similar effects of ring substitution were observed in the formation of the Tebbe reagent from mixed-ring titanocene dichlorides.<sup>10</sup> In that system increasing methyl substitution of the cyclopentadienyl rings lowered the kinetic acidity of the  $\alpha$ -hydrogens of a  $L_nTi-Me$  intermediate.

Using our idea that the formation of carbene-olefin from metallacycles is a reduction process, we may rationalize the difference in

Figure 3.9. Orbital Correlation Diagram for the Titanocene Metallacycle/Carbene-Olefin System.



reactivity between the titanium and zirconium biscyclopentadienyl-metallacyclobutanes. The titanium metallacycles react with organic carbonyls in a Wittig manner (Figure 3.3). Their zirconium and hafnium analogs do not react through metal-carbene intermediates, but instead the carbonyl inserts into the metal carbon bonds of the metallacycle (equation 3.13).<sup>15</sup> Both 19 and 20 are formed by the reaction of the zirconium compound, only 19 is formed by the reaction of the hafnium compound.



Reduction of zirconium and hafnium complexes is much more difficult than the reduction of their titanium analogs. For instance  $\text{Cp}_2\text{ZrCl}_2$  is harder to reduce than  $\text{Cp}_2\text{TiCl}_2$  by ca. 0.8 V; their reduction potentials are -1.7 V and -0.86 V, respectively.<sup>27</sup> The reduction potential of  $\text{Cp}_2\text{HfCl}_2$  has not been reported; however in the complexes  $\text{Cp}_2\text{M}(\text{o}-(\text{CH}(\text{SiMe}_3)_2\text{C}_6\text{H}_4))$  the measured reduction potentials are: -1.46 V ( $\text{M} = \text{Ti}$ ), -2.02 V ( $\text{M} = \text{Zr}$ ), and -2.46 V ( $\text{M} = \text{Hf}$ ).<sup>28</sup> Thus, hafnium complexes are even harder to reduce than analogous zirconium complexes. Since reduction of zirconium and hafnium complexes is much more difficult than the reduction of titanium complexes, pathways that maintain the high formal oxidation state at the metal, eg the insertion reaction of carbonyls, dominate the reaction chemistry of zirconium and hafnium metallacyclobutanes. In the reactivity of titanacyclobutanes, which should more readily undergo reduction processes, carbene-olefin pathways dominate.



The results by Anslyn<sup>9b</sup> that indicate that the neglect of differential ground state effects is not always valid involve the reactivity of  $\text{CpCl}_2\overline{\text{TiCH}_2\text{CH}(\text{tBu})\text{CH}_2}$ , **21**. The chloro substitution on the cyclopentadienyl rings should decrease their electron-donating ability, which seems confirmed by the fact that the  $J_{\text{CH}}$  coupling constant of the methyl bonded to titanium in  $\text{CpCl}_2\text{TiMeCl}$  is larger than the corresponding constant in  $\text{Cp}_2\text{TiMeCl}$  (Table 3.3). From our argument (*vide supra*) we would predict that **21** should react faster with diphenylacetylene than would the plain-ring analog, **17**. Anslyn has found, however, the  $k_{\text{obs}}$  for the reaction of **21** with diphenylacetylene is smaller than  $k_{\text{obs}}$  for the same reaction of **17**. One possible explanation for this effect is that while the transition state for the slow step in the reaction of **21** is stabilized by the chloro substitution, relative to the plain-ring transition state, the metallacyclic ground state is stabilized to a greater extent. The chloro substituted cyclopentadienyl rings may be removing s-character from the titanium leaving more d-character to form stronger metal carbon bonds in the metallacycle.<sup>29</sup> Some empirical evidence for stronger metal carbon bonds in the metallacycle may come from the fact that the preparation of the  $\text{CpCl}$  analog of the Tebbe reagent is made difficult because of the formation of a large amount of  $\text{CpCl}_2\text{TiMe}_2$  in the reaction of  $\text{CpCl}_2\text{TiCl}_2$  with  $\text{AlMe}_3$ . The other substituted titanocene dichlorides studied do not readily form  $\text{Cp}_2\text{TiMe}_2$ . Thus, dialkyls including metallacyclobutanes, in the  $\text{CpCl}_2\text{Ti}$  system may enjoy special stabilization.

### III.4 Conclusions

Substitution on the cyclopentadienyl rings of bis(cyclopentadienyl) titanium compounds can exert steric and electronic effects. In the reactions of ring-substituted titanacyclobutanes with trapping reagents the steric effects play only a small role in determining the relative rates observed; electron effects seem to dominate. The electronic effects can be discussed from the view that increasing the electron-donating ability of the substituted-rings causes a destabilization of the transition state between metallacycle and carbene-olefin. This destabilization arises from the "reductive" nature of the conversion of metallacycle to carbene-olefin. Some results also indicate that ground state effects cannot always be ignored.

### III.5 Experimental Section

All manipulations of air and/or moisture sensitive compounds were carried out using standard Schlenk line, vacuum line, and dry box techniques. Argon used in Schlenk work was purified by passage through columns of BASF-RS-11 (Chemalog) and Linde 4Å molecular sieves.

Routine  $^1\text{H}$  and  $^{13}\text{C}$  spectra were recorded on JEOL FX-90Q or JEOL GX-400 spectrometers. Kinetics by  $^1\text{H}$  NMR spectroscopy were obtained in automated mode on the JEOL FX-90Q. Temperatures were determined from measurement of  $\Delta\nu_{\text{MeOH}}$  and were constant to within  $\pm 0.1^\circ\text{C}$ . Difference NOE spectra were measured on either a Bruker WM-500 or the JEOL GX-400. The ring-substituted titanocene methyl chloride Ti-Me C-H coupling constants were measured either from non-decoupled  $^{13}\text{C}$  INEPT spectra or from observation of the  $^{13}\text{C}$  satellites of the Ti-Me resonance in  $^1\text{H}$  spectra.

The  $^{49,47}\text{Ti}$  NMR spectra were recorded on the JEOL GX-400 at 22.52 MHz. The  $90^\circ$  pulse length, 40  $\mu\text{sec}$ , was determined from a sample of neat  $\text{TiCl}_4$  sealed in a 5 mm tube held concentrically in a 10 mm NMR tube filled with 2 ml of  $\text{CDCl}_3$  as a lock solvent.  $^{49,47}\text{Ti}$  spectra of the ring-substituted titanium compounds were obtained from saturated solutions of the titanium compounds in 2 ml of  $\text{CDCl}_3$  held in 10 mm NMR tubes. Deuterium locking was used. The FID data were collected using  $90^\circ$  pulses and an acquisition time of 0.272 sec. The pulse delay between the end of acquisition and the beginning of the next pulse was 1 sec. The spectral window was 30 KHz wide and 16 k data points were collected yielding a digital resolution of 3.7 Hz. An exponential line broadening factor of 10 Hz was applied to the raw FID which was then Fourier transformed to yield the spectrum. Both  $^{49}\text{Ti}$  and  $^{47}\text{Ti}$

resonances appear in a single spectrum separated by 268.1 ppm with the  $^{49}\text{Ti}$  resonance downfield relative to the  $^{47}\text{Ti}$  resonance. Chemical shifts were referenced relative to external neat  $\text{TiCl}_4$  using the convention that positive  $\delta$  values are downfield. The reported linewidths include the 10 Hz of line-broadening. No proton decoupling was used as its use produced no effect on the line-shape of the resonances.

The uv/vis absorption spectra of the ring-substituted titanocene dichlorides were obtained on an HP 8451A diode array spectrophotometer. Solutions ( $3.3 \times 10^{-3}$  M) of the titanocene dichlorides in spectra grade chloroform were prepared in air. The solutions were transferred to 1 cm pathlength cuvettes and the absorption spectra were recorded in air. The  $\lambda_{\text{max}}$  of the lowest energy transition was located at the point where the first derivative of the spectrum was zero.

Analyses were performed by Mr. L. Henling at the Caltech Analytical Facility.

The solvents used were treated as follows. Pentane was freed of olefinic impurities by stirring over conc.  $\text{H}_2\text{SO}_4$ . It was washed with water, pre-dried over anhydrous  $\text{MgSO}_4$ , and dried with  $\text{CaH}_2$ . It was degassed and stirred over sodium benzophenone ketyl solubilized by the addition of a small amount of tetraglyme. Toluene, diethylether, tetrahydrofuran, benzene, benzene- $\text{d}_6$  and toluene- $\text{d}_8$  were degassed and stirred over sodium benzophenone ketyl. All solvents were vacuum transferred into dry storage flasks equipped with Teflon closures and stored under Ar.

Trimethylphosphine (Strem) was distilled from Na, degassed and stored under Ar in a tube equipped with a Teflon closure. Diphenylacetylene (Aldrich) was recrystallized from hot toluene. Trimethylaluminum, 2 M in

toluene (Aldrich), was transferred into a storage flask equipped with a Teflon closure and stored under Ar. Titanocene dichloride,  $\text{Cp}_2\text{TiCl}_2$  (Boulder), was purified by Soxhlet extraction with  $\text{CH}_2\text{Cl}_2$ .  $\text{CpTiCl}_3$  (Aldrich) was used as received.

The ring-substituted titanocene dichlorides  $\text{Cp}'_2\text{TiCl}_2$ ,  $\text{Cp}'\text{CpTiCl}_2$  and  $\langle\text{Cp}\rangle\text{CpTiCl}_2$  were prepared by a literature method<sup>10</sup> with the modification for the preparation of  $\text{Cp}'\text{CpTiCl}_2$  and  $\langle\text{Cp}\rangle\text{CpTiCl}_2$  that solvent chilled to  $0^\circ\text{C}$  was added *via* cannulus to a mixture of solid  $\text{CpTiCl}_3$  and solid ring-substituted lithium cyclopentadienide. The reaction mixture was allowed to warm slowly to room temperature and stirred at this temperature for 30 min. Work-up of these reactions was identical to the literature procedure.<sup>10</sup>

$\text{Cp}^*\text{TiCl}_3$  and  $\text{Cp}^*_2\text{TiCl}_2$  were prepared by a literature method<sup>30</sup> with the modification that  $\text{LiCp}^*$  was used in place of  $\text{NaCp}^*$ .

$\text{Cp}^*\text{CpTiCl}_2$  was prepared by a literature method<sup>10</sup> with the modification that solvent chilled to  $0^\circ\text{C}$  was added *via* cannulus to a mixture of solid  $\text{Cp}^*\text{TiCl}_3$  and solid  $\text{LiCp}$ . The reaction mixture was allowed to warm slowly to room temperature and stirred at this temperature for 30 min. Work-up then followed the literature procedure.

All titanocene dichlorides could be recrystallized from either hot toluene or hot chloroform. All were obtained in pure form except  $\text{Cp}'\text{CpTiCl}_2$  which typically contained 5-10%  $\text{Cp}_2\text{TiCl}_2$  ( $^1\text{H}$  NMR).

The Tebbe reagent,<sup>31</sup>  $\text{Cp}_2\text{Ti}(\overline{\text{CH}_2\text{Al}(\text{Me})_2})\text{Cl}$ , and the metallacycles 17,<sup>31</sup> and 18<sup>8</sup> were prepared by literature method.<sup>10</sup>

$\text{Cp}^{\text{Cl}}_2\text{TiCl}_2$  and  $\text{Cp}^{\text{Cl}}\text{CpTiCl}_2$  were prepared by E.V. Anslyn<sup>9b</sup> and  $\text{CpTMS}\text{CpTiCl}_2$  was prepared by K.C. Ott.<sup>10</sup>

### Preparation of Cp'CpTi(Me)Cl (5)

This procedure is analogous to the method<sup>32</sup> used to prepare Cp<sub>2</sub>TiMeCl. AlMe<sub>3</sub> (7 ml of 2 M AlMe<sub>3</sub> in toluene, 14 mmol) was added via syringe to an Ar-flushed flask containing a solution of Cp'CpTiCl<sub>2</sub> (3.27 g, 12.4 mmol) in 30 ml CH<sub>2</sub>Cl<sub>2</sub> at 0°C. The reaction mixture immediately becomes a very dark brown-red. The reaction mixture was stirred for 2.5 h at 0°C. 15 ml of diethyl ether were then added at 0°C; the solution immediately changes color from dark brown-red to orange. The solution is warmed to room temperature and all volatiles are removed *in vacuo*. The resulting oily residue is dissolved in 6 ml CH<sub>2</sub>Cl<sub>2</sub> and 10 ml of diethyl ether is carefully layered on top of the solution. The mixture is slowly cooled to -50°C and orange-red crystals form. The mother liquor is decanted off and the crystals are washed with two 5 ml aliquots of diethyl ether and dried *in vacuo*. (Yield 1.51g 50%). Material typically contains 5-10% Cp<sub>2</sub>TiMeCl impurity. <sup>1</sup>H NMR (C<sub>6</sub>D<sub>6</sub>): δ 5.81 (s, 5H, Cp), 5.93 (m, 1H, C<sub>5</sub>H<sub>4</sub>Me), 5.54 (m, 1H, C<sub>5</sub>H<sub>4</sub>Me), 5.38 (m, 1H, C<sub>5</sub>H<sub>4</sub>Me), 5.23 (m, 1H, C<sub>5</sub>H<sub>4</sub>Me), 2.15 (s, 3H, C<sub>5</sub>H<sub>4</sub>Me), 0.79 (s, 3H, Ti-Me). <sup>13</sup>C {<sup>1</sup>H} NMR (C<sub>6</sub>D<sub>6</sub>): δ 123.5, 120.6, 116.3, 113.3, 110.4 (C<sub>5</sub>H<sub>4</sub>Me), 115.3 (Cp), 48.1 (Ti-Me), 16.6 (C<sub>5</sub>H<sub>4</sub>Me).

### Preparation of Cp'<sub>2</sub>TiMeCl (6)

This compound was prepared as for 5. Yield was 73% of orange-red crystals. <sup>1</sup>H NMR (C<sub>6</sub>D<sub>6</sub>): δ 5.92 (m, 2H, C<sub>5</sub>H<sub>4</sub>Me), 5.54 (m, 2H, C<sub>5</sub>H<sub>4</sub>Me), 5.42 (m, 2H, C<sub>5</sub>H<sub>4</sub>Me), 5.27 (m, 2H, C<sub>5</sub>H<sub>4</sub>Me), 2.14 (s, 6H, C<sub>5</sub>H<sub>4</sub>Me), 0.74 (s, 3H, Ti-Me). <sup>13</sup>C {<sup>1</sup>H} NMR (C<sub>6</sub>D<sub>6</sub>): δ 120.1, 115.8, 113.2, 110.5 (C<sub>5</sub>H<sub>4</sub>Me), 46.4 (Ti-Me), 16.1 (C<sub>5</sub>H<sub>4</sub>Me).

### Preparation of $\langle \text{Cp} \rangle \text{CpTiMeCl}$ (7)

This compound was prepared as for 5. Yield was 41% of orange-red crystals.  $^1\text{H}$  NMR ( $\text{C}_6\text{D}_6$ ):  $\delta$  5.84 (s, 5H, Cp), 5.62, (s, 1H,  $\text{C}_5\text{H}_2\text{Me}_3$ ), 5.06 (s, 1H,  $\text{C}_5\text{H}_2\text{Me}_3$ ), 1.99 (s, 3H,  $\text{C}_5\text{H}_2\text{Me}_3$ ), 1.72 (s, 3H,  $\text{C}_5\text{H}_2\text{Me}_3$ ), 1.51 (s, 3H,  $\text{CC}_5\text{H}_2\text{Me}_3$ ), 0.73 (s, 3H, Ti-Me).  $^{13}\text{C}$   $\{^1\text{H}\}$  NMR ( $\text{C}_6\text{D}_6$ ):  $\delta$  121.8, 121.2, 115.1 ( $\text{C}_5\text{H}_2\text{Me}_3$ ), 115.7 (Cp), 47.7 (Ti-Me), 16.0, 14.3, 14.1 ( $\text{C}_5\text{H}_2\text{Me}_3$ ).

### Preparation of $\text{Cp}^*\text{CpTiMeCl}$ (8)

This compound was prepared as for 5. Yield was 57% of orange-red crystals.  $^1\text{H}$  NMR ( $\text{C}_6\text{D}_6$ ):  $\delta$  5.78 (s, 5H, Cp), 1.65 (s, 15H,  $\text{C}_5\text{Me}_5$ ), 0.51 (s, 3H, Ti-Me).  $^{13}\text{C}$   $\{^1\text{H}\}$  NMR ( $\text{C}_6\text{D}_6$ ):  $\delta$  123.7 ( $\text{C}_5\text{Me}_5$ ), 116.1 (Cp), 51.0 (Ti-Me), 12.6 ( $\text{C}_5\text{Me}_5$ ).

### Preparation of $\text{Cp}^*_2\text{TiMeCl}$ (9)

This compound was prepared as for 5 with the modification that initial  $\text{CH}_2\text{Cl}_2$  solution was stirred for 7 h at  $0^\circ\text{C}$  before the diethyl ether was added. Yield was 67% of orange-red crystals.  $^1\text{H}$  NMR ( $\text{C}_6\text{D}_6$ ):  $\delta$  1.77 (s, 30H,  $\text{C}_5\text{Me}_5$ ), 0.22 (s, 3H, Ti-Me).  $^{13}\text{C}$   $\{^1\text{H}\}$  NMR ( $\text{C}_6\text{D}_6$ ):  $\delta$  123.1 ( $\text{C}_5\text{Me}_5$ ), 54.4 (Ti-Me), 13.0 ( $\text{C}_5\text{Me}_5$ ). Calculated for  $\text{C}_{21}\text{H}_{33}\text{ClTi}$ : C, 68.38, H, 9.02. Found: C, 67.38, H, 8.58.

### Preparation of $\text{Cp}'_2\text{TiCH}_2\text{Al}(\text{Me})_2\text{Cl}$

$\text{AlMe}_3$  (3 ml of 2M  $\text{AlMe}_3$  in toluene) was added *via* syringe to a solution of  $\text{Cp}'_2\text{TiMeCl}$  (1.5g, 5.8 mmol) in 7 ml toluene at room temperature. The resulting deep brown-red solution was heated to  $50^\circ\text{C}$  for 28 h. The volatiles were then removed at room temperature.  $^1\text{H}$  NMR of the resulting residue showed  $\text{Cp}'_2\text{TiMeCl}$  was still present. The residue was dissolved in 5 ml toluene and 0.6 ml of 2M  $\text{AlMe}_3$  in toluene was added. The reaction mixture was stirred at room temperature for *ca* 56 hrs. The volatiles were

removed *in vacuo* leaving a red oily residue. The residue was dissolved in 1 ml toluene and 5 ml of pentane was layered on top. The mixture was slowly cooled to  $-20^{\circ}\text{C}$  to obtain the product as a red powder. (Yield 725 mg, 39%)  $^1\text{H}$  NMR ( $\text{C}_6\text{D}_6$ ):  $\delta$  7.94 (s, 2H,  $\mu\text{-CH}_2$ ), 5.91, 5.52, 5.27 (all m, 8H tot,  $\text{C}_5\text{H}_4\text{Me}$ ), 1.74 (s, 6H,  $\text{C}_5\text{H}_4\text{Me}$ ), -0.27 (s, 6H, Al-Me).

#### Preparation of $\langle\text{Cp}\rangle\text{CpTiCH}_2\text{Al}(\text{Me})_2\text{Cl}$

This compound was prepared as for  $\text{Cp}'_2\text{TiCH}_2\text{Al}(\text{Me})_2\text{Cl}$ . Yield was 22% of red powder. Spectral data were identical to the published data.<sup>10</sup>

#### Preparation of $\text{Cp}^*\text{CpTiCH}_2\text{Al}(\text{Me})_2\text{Cl}$

$\text{AlMe}_3$  (5.5 ml of 2 M  $\text{AlMe}_3$  in toluene, 11 mmol) was added to an Ar-flushed flask containing  $\text{Cp}^*\text{CpTiCl}_2$  (1.73g, 5.4 mmol). The resulting deep brown-red solution was heated to  $40^{\circ}\text{C}$  and stirred for *ca* 60 h. The volatiles were removed to yield a red oil which consisted of  $\text{Cp}^*\text{CpTiMeCl}$  (80%) and product (20%). Several such cycles were repeated until no  $\text{Cp}^*\text{CpTiMeCl}$  was observed. The resulting tacky solid was extracted with pentane (60 ml) and resulting solution was concentrated to 30 ml. The solution was slowly cooled to  $-50^{\circ}\text{C}$  and 810 mg of product *ca* 85% pure by  $^1\text{H}$  NMR was isolated as a red powder. The spectral data were identical to published data.<sup>10</sup>

#### Preparation of $\text{Cp}'_2\text{TiCH}_2\text{C}(\text{Me})_2\text{CH}_2$ (10)

This compound was prepared as for 18.<sup>8</sup> Isobutylene *ca* 5 ml was condensed at  $-70^{\circ}\text{C}$  into a flask containing  $\text{Cp}'_2\text{TiCH}_2\text{Al}(\text{Me})_2\text{Cl}$  (2.99g, 9.6 mmol) and N,N-dimethyl aminopyridine (DMAP) (1.17g, 9.6 mmol). The resulting paste was dissolved in 15 nml of  $\text{CH}_2\text{Cl}_2$ . The resulting red solution was warmed to  $-20^{\circ}\text{C}$  and added dropwise *via* cannulus to 100 ml of rapidly stirred pentane cooled to  $-40^{\circ}\text{C}$ . An orange solid precipitates out and the mixture is filtered (Schlenk filtration) to yield a red filtrate. The volatiles



were removed *in vacuo* at low temperature ( $\leq -10^{\circ}\text{C}$ ) and a red residue was left. This residue was dissolved in a minimum of diethyl ether at  $0^{\circ}\text{C}$  and the resulting red solution was slowly cooled to  $-50^{\circ}\text{C}$  yielding **10** as a red powder. (Yield 0.67g, 25%.) The product is temperature sensitive and must be stored cold ( $-40^{\circ}\text{C}$ ) under inert atmosphere.  $^1\text{H}$  NMR ( $\text{C}_6\text{D}_6$ ):  $\delta$  5.59 (m, 4H,  $\text{C}_5\text{H}_4\text{Me}$ ), 5.27 (m, 4H,  $\text{C}_5\text{H}_4\text{Me}$ ), 2.36 (s, 4H,  $\text{TiCH}_2\text{C}(\text{Me})_2\text{CH}_2$ ), 1.79 (s, 6H,  $\text{C}_5\text{H}_4\text{Me}$ ), 1.14 (s, 6H,  $\text{TiCH}_2\text{C}(\text{Me})_2\text{CH}_2$ ).  $^{13}\text{C}$   $\{^1\text{H}\}$  ( $\text{C}_6\text{D}_6$ ):  $\delta$  120.7, 112.7, 110.3 ( $\text{C}_5\text{H}_4\text{Me}$ ), 8.31 ( $\text{TiCH}_2\text{C}(\text{Me})_2\text{CH}_2$ ), 38.0 ( $\text{TiCH}_2\text{C}(\text{Me})_2\text{CH}_2$ ), 15.5 ( $\text{C}_5\text{H}_4\text{Me}$ ), 8.8 ( $\text{TiCH}_2\text{C}(\text{Me})_2\text{CH}_2$ ).

Preparation of *cis* and *trans*  $\text{Cp}'\text{CpTiCH}_2\text{CH}(\text{tBu})\text{CH}_2$  (**12**)

These compounds are prepared by a modification of the procedures used for **17**.<sup>31</sup> Neohexene (0.51 ml, 8.4 mmol) was added *via* syringe to a red solution of  $\text{Cp}'\text{CpTiCH}_2\text{Al}(\text{Me})_2\text{Cl}$  (0.5g, 1.7 mmol) in 2 ml toluene cooled to  $0^{\circ}\text{C}$ . DMAP (0.21g, 1.7 mmol) was added to the solution which was stirred for 5 min at  $0^{\circ}\text{C}$ . DMAP (0.21g, 1.7 mmol) was added to the solution which was stirred for 5 min at  $0^{\circ}\text{C}$  and then cooled to  $-35^{\circ}\text{C}$ . Pentane (20 ml) was slowly added *via* syringe to the solution which was rapidly stirred at  $-35^{\circ}\text{C}$ . An orange precipitate forms and the reaction mixture is filtered. The volatiles are removed from the filtrate *in vacuo* leaving a red powder. This powder was dissolved in 0.5 ml toluene at room temperature and the resulting red solution was cooled to  $-50^{\circ}\text{C}$ . A 1:1 mixture of *cis* and *trans* **12** is isolated as a red powder. (Yield 0.33g, 67%.) This material contains *ca* 20% **17**.  $^1\text{H}$  NMR data are shown Table 3.14.  $^{13}\text{C}$   $\{^1\text{H}\}$  NMR ( $\text{C}_6\text{D}_6$ ):  $\delta$  123.1, 119.5, 112.5, 111.4, 110.3, 109.7 ( $\text{C}_5\text{H}_4\text{Me}$ ); 110.7, 110.4 (Cp); 67.7, 67.4 ( $\alpha\text{C}$ ); 34.4, 34.3 ( $-\text{CMe}_3$ ); 29.53, 29.5 ( $-\text{CMe}_3$ ); 21.5, 20.2 ( $\beta\text{C}$ ); 16.5, 15.9 ( $\text{C}_5\text{H}_4\text{Me}$ ). The signals could not be assigned to the individual isomers. Attempts to separate the isomers failed.

Preparation of  $\text{Cp}'_2\text{TiCH}_2\text{CH}(\text{tBu})\text{CH}_2$  (11)

This compound was prepared as for 12. The yield was 46%. NMR data are included in Table 3.14.

Preparation of *cis* and *trans*  $\langle \text{Cp} \rangle \text{CpTiCH}_2\text{CH}(\text{tBu})\text{CH}_2$ , (13)

The method of preparation of 12 was used. Recrystallization from toluene gave a 25% yield of a 3.5:1 mixture of *trans*-13 and *cis*-13. Calculated for  $\text{C}_{20}\text{H}_{30}\text{Ti}$ : C, 75.46; H, 9.50. Found: C, 75.29; H, 8.79. NMR data are included in Table 3.14. Attempts to separate the isomers failed. Recrystallization from diethyl ether yielded a 2.2:1 mixture of *trans*-13 and *cis*-13.

Preparation of  $\text{Cp}'\text{CpTiCH}_2\text{C}(\text{Ph})\text{C}(\text{Ph})$ , (19)

A solution of diphenylacetylene (120 mg, 0.69 mmol) in 3 ml THF at 0°C was added to Ar-flushed flask containing  $\text{Cp}'\text{CpTiCH}_2\text{Al}(\text{Me})_2\text{Cl}$  (205mg, 0.69 mmol). The resulting red solution was stirred at 0°C for 1/2 h gradually becoming deep purple in color. The reaction mixture was warmed to room temperature and stirred for an additional 15 min. The volatiles were removed *in vacuo* leaving a dark purple residue which was left under dynamic vacuum overnight. The residue was dissolved in 1 ml toluene and 1 ml pentane and cooled to -50°C. Dark purple crystals of product were collected. (Yield 127 mg, 48%.) An analytical sample was obtained by recrystallization from diethyl ether; this sample contained 11%  $\text{Cp}_2\text{TiCH}_2\text{C}(\text{Ph})\text{C}(\text{Ph})$  by  $^1\text{H}$  NMR. Calculated for 89%  $\text{C}_{26}\text{H}_{24}\text{Ti}$  and 11%  $\text{C}_{25}\text{H}_{22}\text{Ti}$ : C, 81.22; H, 6.26. Found: C, 80.93; H, 6.23. NMR data are included in Table 3.14.

Preparation of  $\text{Cp}'_2\text{TiCH}_2\text{C}(\text{Ph})\text{C}(\text{Ph})$ , (20)

This compound was prepared as for 19. The yield of dark purple crystalline material was 47%. An analytical sample was obtained from

recrystallization from diethyl ether. Calculated for  $C_{27}H_{26}Ti$ : C, 81.40; H, 6.58. Found: C, 81.42; H, 6.50. NMR data are included in Table 3.14.

Preparation of  $\langle Cp \rangle CpTiCH_2C(Ph)C(Ph)$ , (21)

This compound was prepared as for 19. It could only be obtained as an impure oil. The NMR data are shown in Table 3.14.

Equilibration Studies of *cis* and *trans*-12

In the drybox a 1:1 mixture of *cis* and *trans*-12 (14 mg) was weighed into an NMR tube and dissolved in 400  $\mu$ l of  $C_6D_6$ . The tube was capped with a rubber septum and removed from the drybox. The tube was heated in an oil bath to 55°C. It was periodically removed and cooled to room temperature to be examined by  $^1H$  NMR spectroscopy. Over days there is no change in the *cis/trans* ratio, but the metallacycles gradually decompose. The experiment was repeated with the inclusion of 2 equivalents of neohexene; the *cis/trans* ratio stayed at 1:1 in this experiment also.

Equilibration of *cis* and *trans*-13

In the drybox a 3.5:1 *trans*-13/*cis*-13 mixture (14 mg) was loaded into an NMR tube and dissolved in 400  $\mu$ l of  $C_6D_6$  (0.11 M solution). The tube was capped with a rubber septum and removed from the drybox. The tube was heated to 55°C in an oil bath. The tube was periodically removed from the bath and the sample quickly frozen with  $LN_2$ . The sample was warmed to room temperature, a temperature where equilibration is slow (*vide infra*), and immediately examined by  $^1H$  NMR spectroscopy. The ratio *trans*-13/*cis*-13 eventually stabilizes at 2.0:1. The procedure was repeated at oil bath temperatures of 65, 75, and 83°C. At these temperatures the ratio *trans*-13/*cis*-13 also stabilizes at 2.0:1. Decomposition of metallacycles is  $\leq 5\%$  of the course of experiment at temperatures  $\leq 75^\circ C$ , at 83°C decomposition is

more pronounced *ca* 20% over 5 h; however, the ratio of *trans*-13/*cis*-13 stays constant after reaching 2.0:1 even during decomposition. At 83°C it appears that one decomposition pathway is the formation of the dimer [ $\text{Cp} > \text{CpTi}(\text{CH}_2)_2$ ]<sub>2</sub> as the solution turns purple and peaks appear at  $\delta$  6.01 (Cp), 7.59 and 7.58 (possibly  $\mu\text{-CH}_2$  signals).  $\text{CH}_4$  ( $\delta$  0.15) was also produced.

The entire procedure was repeated with the inclusion of 12  $\mu\text{l}$  (2 equivalents) of neohexene. The ratio *trans*-13/*cis*-13 was the same as before. Qualitatively, the addition of olefin did not greatly affect the rate of isomerization.

#### Kinetics of Equilibration of *trans*-13 and *cis*-13

In the drybox a NMR tube was loaded with a 3.5:1 mixture of *trans*-13 and *cis*-13 (14 mg, 0.044 mmol). The solid was dissolved in 400  $\mu\text{l}$  of  $\text{C}_6\text{D}_6$  and the tube was capped with a rubber septum. The sample was placed in the probe of the JEOL FX-90Q maintained at 63.5°C and spectra were recorded at regular intervals. The relative concentrations of *trans*-13 and *cis*-13 were determined from the integrals of their respective Cp resonances. The resonance due to residual protons of the solvent was used as an internal standard, and it was observed that *ca* 8% decomposition of the metallacycles occurs over the experimental period. The combined constant  $k_1 + k_{-1}$ , Table 3.4, was obtained from least squares analysis of a plot<sup>33</sup> of  $\ln (X_e - X/X_e)$  vs.  $t$  where  $X_e = (R_0 - R_e)/(R_e + 1)R_0 A_0$  and  $X = (R_0 - R_t)/(R_t + 1)R_0 A_0$  where  $R_0$  = initial ratio of *trans*/*cis* 13,  $R_e$  = the equilibrium ratio,  $R_t$  = the ratio at time  $t$ , and  $A_0$  = initial concentration of *trans*-13.  $A_0$  does not have to be known explicitly. The individual rate constants  $k_1$  and  $k_{-1}$  could then be determined using the fact that  $K = k_1/k_{-1}$ . The procedure was repeated at several temperatures and the rate constants determined. The errors in these

constants, as estimated from their standard deviations determined in the least squares analysis are on the order of  $\pm 5\%$ . Activation parameters were obtained from least squares analysis of  $\ln(k/T)$  vs.  $1/T$  plots.<sup>34</sup>

#### Reaction of $\text{Cp}'_2\text{TiCH}_2\text{CMe}_2\text{CH}_2$ (10) with Pivaldehyde

In the drybox 10 (10 mg, 0.036 mmol) was loaded into a NMR tube and dissolved in 400  $\mu\text{l}$  of  $\text{C}_6\text{D}_6$ . The tube was capped with a rubber septum and removed from the drybox. Pivaldehyde (4  $\mu\text{l}$ , 0.036 mmol) was added *via* syringe and the reaction was monitored by  $^1\text{H}$  NMR spectroscopy. Within 20 min at room temperature the pivaldehyde is completely converted to neohexene. Broad resonances  $\delta$  6.8-5.2 indicate titanium oxo polymer is formed. No intermediates were observed.

#### Reaction of *trans* and *cis* 13 with $\text{PMe}_3$

In the drybox a mixture of 3.5:1 *trans*-13/*cis*-13 (15 mg, 0.047 mmol) was loaded into a NMR tube and dissolved in 400  $\mu\text{l}$  of toluene- $d_8$ . The tube was capped with a rubber septum and removed from the drybox. The tube was cooled to  $-25^\circ\text{C}$  and  $\text{PMe}_3$  (25  $\mu\text{l}$ ) was added *via* syringe. The tube was placed in the probe of the JEOL GX-400 maintained at  $-25^\circ\text{C}$ . No reaction was observed  $^1\text{H}$  NMR spectroscopy at this temperature. No reaction occurs until the probe is heated to  $65^\circ\text{C}$ . The probe was then heated to  $80^\circ\text{C}$ . New signals grow in and are assigned to the species  $\langle\text{Cp}\rangle\text{CpTi}(\text{CH}_2)\text{PMe}_3$ :  $\delta$  11.80, 1.54 (2d,  $J_{\text{H-H}} = 6$  Hz,  $\text{Ti}(\text{CH}_2)$ ; 5.35 (s, Cp), 2.20 (br s,  $\text{C}_5\text{H}_2\text{PMe}_3$ ). Other signals could not be observed. Equilibrium is established within 30 min. The ratio (*trans*-13 and *cis*-13)/ $\langle\text{Cp}\rangle\text{CpTi}(\text{CH}_2)\text{PMe}_3$  as determined from the relative integrals of their respective Cp resonances was 2.2:1 (*trans*-13/*cis*-13 ratio was 2:1) at  $83^\circ\text{C}$ . Apparently at  $83^\circ\text{C}$  the phosphine ligand is exchanging rapidly on the NMR time-scale, as upon cooling the sample to room temperature the

downfield doublets become doublets of doublets and sharp signals for the  $\langle \text{Cp} \rangle$  ligand appear. The room temperature  $^1\text{H}$  NMR data are:  $\delta$  11.82, 11.55 (2dd,  $J_{\text{HH}} = 6$  Hz,  $J_{\text{PH}} = 8$  Hz,  $\text{TiCH}_2$ ); 5.38 (s, Cp); 4.99, 4.65 (2s,  $\text{C}_5\text{H}_2\text{Me}_3$ ); 2.20, 1.83, 1.79 (3s,  $\text{C}_5\text{H}_2\text{Me}_3$ ). After 12 h at room temperature the ratio (*trans*-13 and *cis*-13)/ $\langle \text{Cp} \rangle \text{CpTi}(\text{CH}_2)\text{PMe}_3$  had risen to 6.3:1 while the *trans*-13/*cis*-13 ratio stayed at 2.0:1.

Measurement of the Kinetics of Reaction  $\bar{\text{Cp}}\bar{\text{Cp}}\text{TiCH}_2\text{CH}(\text{tBu})\text{CH}_2$  with Diphenylacetylene.<sup>35</sup>

A NMR tube was loaded with diphenylacetylene (0.33 mmol) and taken into the drybox. Metallacycle (0.044 mmol) was added to the tube which was capped with a rubber septum,  $\text{C}_6\text{D}_6$  (400  $\mu\text{l}$ ) was added to the tube which was agitated briefly to dissolve all materials. The sample was placed in the probe of the JEOL FX-90Q, maintained at  $55^\circ\text{C}$ , and spectra were obtained at regular intervals. For the mixed-ring systems the mole fraction of each isomer of metallacyclobutane<sup>36</sup> was determined from the integral of its  $\text{C}_5\text{H}_5$  signal and the total integral of all  $\text{C}_5\text{H}_5$  signals. For  $\text{Cp}'_2\text{TiCH}_2\text{CH}(\text{tBu})\text{CH}_2$  (11) the upfield  $\text{C}_5\text{H}_4\text{Me}$  signal of 11 and the  $\alpha\text{H}$  signal of the product, 20, were used to determine the mole-fraction of 11. Using the phenyl region as an internal standard, minimal decomposition of materials occurred during kinetic runs. First-order plots of  $\ln X$ , where  $X$  is the mole-fraction of metallacyclobutane, vs  $t$  were linear to three half-lives.  $k_{\text{obs}}$  values were derived from least-squares analysis of these plots. The error in the  $k_{\text{obs}}$  values as estimated from their standard deviations found in the least-square analysis was on the order of  $\pm 5\%$ . At the concentration of titanium species used (0.11 M), it had been determined from experiments with various concentrations of diphenylacetylene that initial concentrations  $\geq 0.55$  M of diphenylacetylene

were sufficient to reach saturation. For 11, and 13 this procedure was repeated at several temperatures. Activation parameters were obtained from least-squares analysis of  $\ln(k/T)$  vs  $1/T$  plots.

#### Reaction of 13 with Labeled Olefin

In the drybox a NMR tube was loaded with a 3.5:1 mixture of *trans/cis*-13 (14 mg, 0.044 mmol). The metallacycle was dissolved in 400  $\mu$ l of toluene. The tube was capped with a rubber septum and removed from the drybox. A solution of 25 mole% *cis*-1,2-dideuterio-3,3-dimethyl butene in toluene (40  $\mu$ l, 0.986 mmol olefin) was added *via* syringe.  $C_6D_6$  (1 mg) was added as an internal deuterium standard. The mixture was heated to 68°C in the probe of the FX-90Q for 75 min after which time *ca* 20% of the labeled olefin had been incorporated into metallacycle as determined by integration of the vinyl deuterium signals of free olefin and the  $\beta$ -D signal of metallacycle in the  $^2H$  NMR spectrum (non-decoupled spectrum).

#### Reaction of 13 with Labeled Olefin in the Presence of Diphenylacetylene

In the drybox a NMR tube was loaded with a 3.5:1 mixture of *trans/cis*-13 (14 mg, 0.044 mmol) and diphenylacetylene (61 mg, 0.34 mmol). The solids were dissolved in 400  $\mu$ l of  $C_6D_6$ . The tube was capped with a rubber septum and removed from the drybox. A solution of 25 mole% *cis*-1,2-dsideuterio-3,3-dimethyl butene in toluene (200  $\mu$ l, 0.44 mmol of olefin) was added *via* syringe. The sample was heated to 72°C for 75 min. The tube was placed in an Ar-flushed Schlenk tube and the septum was pierced with a needle. The Schlenk tube was then evacuated and the volatiles in the NMR tube were removed. The residue in the NMR tube was redissolved in 400  $\mu$ l of  $C_6H_6$  with 2  $\mu$ l of toluene- $d_8$  added as a deuterium internal standard. The  $^1H$  spectrum of the solution (run lockless on the GX-400) showed *ca* 60% conversion of the

metallacyclobutanes **13** to the metallacyclobutane product, **21**. The  $^2\text{H}$  NMR spectrum showed no deuterium incorporation into either the starting material or the product.

Measurement of the Kinetics of Reaction of  $\bar{\text{C}}\text{p}\bar{\text{C}}\text{p}\overline{\text{TiCH}_2\text{CH}(\text{tBu})\text{CH}_2}$  Metallacycles with Acetone<sup>37</sup>

In the drybox (0.064 mmol) of the desired metallacycle was loaded into a NMR tube. The metallacycle was dissolved in 400  $\mu\text{l}$  of  $\text{C}_6\text{D}_6$  and the tube was capped with a rubber septum. Acetone (15  $\mu\text{l}$ , 0.19 mmol) was added to the tube *via* syringe. The tube was heated to  $55^\circ\text{C}$  in an oil bath. It was periodically removed and the sample rapidly frozen with  $\text{LN}_2$ ; the sample was then warmed to room temperature, a temperature where the reaction is not rapid, and examined by  $^1\text{H}$  NMR spectroscopy. The sample was then returned to the oil bath. The ratio of the initial concentration of metallacycle,  $M_0$ , to the concentration of metallacycle at time  $t$ ,  $M_t$ , was measured from the integral of the  $\text{C}_5\text{H}_5$  signal ( $\text{C}_5\text{H}_4$  Me signal for **11**) using the signal due to residual protons of the solvent as an internal standard. The rate constants were determined from the relationship<sup>38</sup>  $k = 1/t \ln(M_0/M_t)$  as an average of several measurements at different times. The estimated error of these values as estimated from the range of the values averaged is on the order of  $\pm 10\%$ .

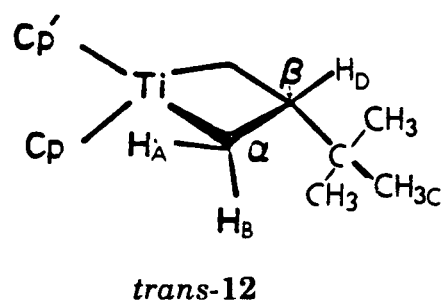
Measurement of the Kinetics of Reaction of  $\text{Cp}_2\overline{\text{TiCH}_2\text{CMe}_2\text{CH}_2}$  (**18**) and  $\text{Cp}'_2\overline{\text{TiCH}_2\text{CMe}_2\text{CH}_2}$  (**10**) with Acetone<sup>37</sup>

In the drybox of **18** (9 mg, 0.036 mmol) and **10** (10 mg, 0.036 mmol) was loaded into a NMR tube and dissolved in 400  $\mu\text{l}$  of toluene- $d_8$ . The tube was capped with a rubber septum and removed from the drybox. The tube was placed in the probe of the FX-90Q maintained at  $10^\circ\text{C}$ . Acetone (20  $\mu\text{l}$ , 0.44 mmol) was added *via* syringe and NMR spectrum were obtained at regular



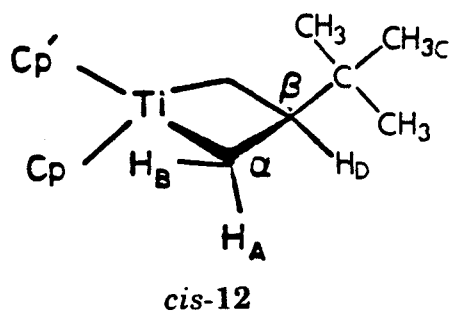
intervals. The ratio of 10 to 18 rapidly grows larger than its initial value of 1:1 as 18 is consumed more rapidly than 10. The concentrations of the two metallacycles as a function of time were determined from the integrals of their  $\alpha$ H signals as well as their  $\beta$ -Me group signals. First order plots for each metallacycle were linear. The rate constants were determined from a least-squares analysis of these plots. The errors of these constants as estimated from their standard deviations found in the least-squares analysis was on the order of  $\pm 10\%$ .

Table 3.14 NMR Data

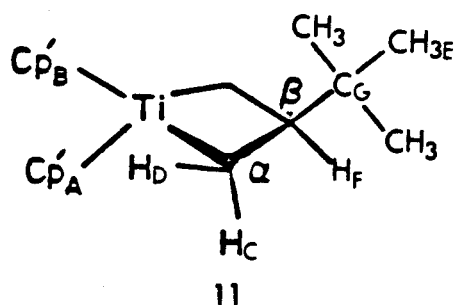


$^1\text{H}$  NMR ( $\text{C}_6\text{D}_6$ )<sup>a</sup>:  $\delta$  5.63 (s, Cp); 5.42, 5.18 (2m,  $\text{C}_5\text{H}_4\text{Me}$ ); 2.10 (t,  $J = 10\text{Hz}$ ,  $\text{H}_\text{A}$ ); 1.94 (t,  $J = 10\text{ Hz}$ ,  $\text{H}_\text{B}$ ); 1.72 (s,  $\text{C}_5\text{H}_4\text{Me}$ ); 0.96 (s,  $\text{H}_\text{C}$ ), 0.06 (qn,  $J = 10\text{ Hz}$ ,  $\text{H}_\text{D}$ ).

Table 3.14 (continued)

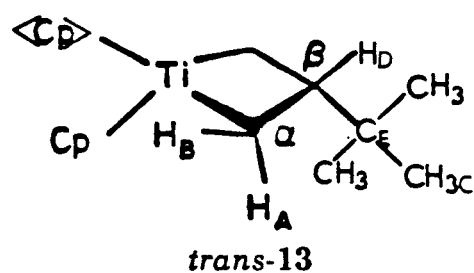


<sup>1</sup>H NMR (C<sub>6</sub>D<sub>6</sub>)<sup>a</sup>: δ 5.59, 5.30 (2m, C<sub>5</sub>H<sub>4</sub>Me); 5.46 (s, Cp); 2.18 (t, J = 10Hz, H<sub>A</sub>); 1.83 (t, J = 10 Hz, H<sub>B</sub>); 1.85 (s, C<sub>5</sub>H<sub>4</sub>Me); 0.97 (s, H<sub>C</sub>), 0.10 (qn, J = 10 Hz, H<sub>D</sub>).



**$^{13}\text{C}\{^1\text{H}\}(\text{C}_6\text{D}_6)^b$ :  $\delta$  123.5 (s), 119.4 (s), 112.8 (d), 111.6 (d), 110.3 (d), 109.8 (d) ( $\text{C}_5\text{H}_4\text{Me}$ ,  $\text{Cp}'_A$  and  $\text{Cp}'_B$ ); 67.2 (t,  $\alpha\text{C}$ ); 34.4 (s,  $\text{C}_G$ ), 29.5 (q,  $\text{C}_E$ ), 22.8 (d,  $\beta\text{C}$ ); 16.3 (q), 15.8 (q), ( $\text{C}_5\text{H}_4\text{Me}$ ,  $\text{Cp}'_A$  and  $\text{Cp}'_B$ ).**

Table 3.14 (continued)

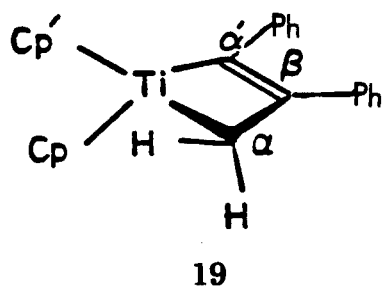


$^1\text{H}$  NMR ( $\text{C}_6\text{D}_6$ )<sup>a</sup>:  $\delta$  5.68 (s, Cp); 4.89 (s,  $\text{C}_5\text{H}_2\text{Me}_3$ ); 1.95 (t,  $J = 10\text{Hz}$ ,  $\text{H}_\text{B}$ ); 1.65, 1.61 (2s ratio 2:1,  $\text{C}_5\text{H}_2\text{Me}_3$ ); 0.99 (s,  $\text{H}_\text{C}$ ); -0.19 (qn,  $J = 10\text{ Hz}$ ,  $\text{H}_\text{D}$ ).  $\text{H}_\text{A}$  is obscured by  $\langle\text{Cp}\rangle$ -Me resonances.

$^{13}\text{C}\{^1\text{H}\}$  ( $\text{C}_6\text{D}_6$ )<sup>c</sup>:  $\delta$  119.8, 117.6, 111.0 ( $\text{C}_5\text{H}_2\text{Me}_3$ ); 110.8 (Cp) 67.9 ( $\alpha\text{C}$ ); 34.4 ( $\text{C}_\text{E}$ ); 29.5 ( $\text{C}_\text{C}$ ); 20.9 ( $\beta\text{C}$ ); 16.0, 13.7 ( $\text{C}_5\text{H}_2\text{Me}_3$ ).

Table 3.14 (continued)

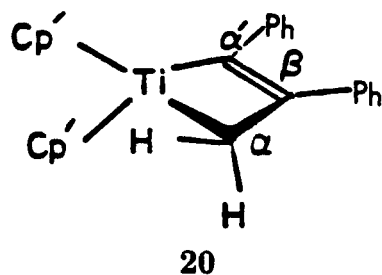
Table 3.14 (continued)



$^1\text{H NMR (C}_6\text{D}_6\text{)}^a$ :  $\delta$  7.67-7.24 (m, Ph); 5.72 (s, Cp); 5.56, 5.23 (2m,  $\text{C}_5\text{H}_4\text{Me}$ ); 3.29, 3.21 (2d,  $J = 17.6$  Hz ( $\alpha\text{H}$ )); 1.79 (s, 2.09 (t,  $J = 10$  Hz,  $\text{H}_A$ )).

$^{13}\text{C}\{^1\text{H}\}(\text{C}_6\text{D}_6)$ :  $\delta$  209.1 ( $\alpha'\text{C}$ ); 147.4, 131.9, 129.6, 128.6, 128.5, 126.2, 126.1, 124.5 (Ph); 125.6, 115.3, 113.7, 110.2, 107.8 ( $\text{C}_5\text{H}_2\text{Me}_3$ ); 111.8 (Cp); 103.5 ( $\beta\text{C}$ ); 72.3 ( $\alpha\text{C}$ ); 15.7 ( $\text{C}_5\text{H}_5\text{Me}$ ).

Table 3.14 (continued)

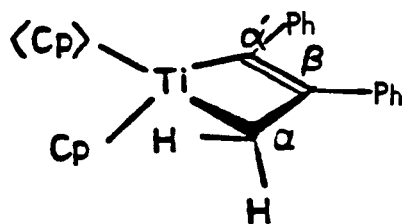


$^1\text{H}$  NMR ( $\text{C}_6\text{D}_6$ )<sup>a</sup>:  $\delta$  7.49-6.75 (m, Ph); 5.71, 5.52, 5.27 (3m ratio 2:1:1,  $\text{C}_5\text{H}_4\text{Me}$ ); 3.12 (s,  $\alpha\text{H}$ ); 1.80 (s,  $\text{C}_5\text{H}_4\text{Me}$ ).

$^{13}\text{C}$  { $^1\text{H}$ } ( $\text{C}_6\text{D}_6$ )<sup>b</sup>:  $\delta$  207.9 (s,  $\alpha'\text{C}$ ); 147.2 (s), 138.7 (s), 129.6 (d), 128.4 (d), 126.3 (d), 126.2 (d) (Ph); 125.2 (s), 114.8 (d), 112.8 (d), 110.2 (d), 107.4 (d) ( $\text{C}_5\text{H}_4\text{Me}$ ); 105.6 (s,  $\beta\text{C}$ ); 71.1 (t,  $\alpha\text{C}$ ), 15.8 (q,  $\text{C}_5\text{H}_4\text{Me}$ ).



Table 3.14 (continued)



21

$^1\text{H NMR}$  ( $\text{C}_6\text{D}_6$ )<sup>a</sup>:  $\delta$  7.7-6.7 (m, Ph); 5.78 (s, Cp); 5.53, 5.03 (2d,  $J = 2.4$  Hz,  $\text{C}_5\text{H}_2\text{Me}_3$ ); 3.21, 2.86 (2d,  $J = 11.7$  Hz,  $\alpha\text{H}$ ); 1.68, 1.67, 1.62 (3s,  $\text{C}_5\text{H}_2\text{Me}_3$ )

$^{13}\text{C}\{^1\text{H}\}$  ( $\text{C}_6\text{D}_6$ ):  $\delta$  208.1 ( $\alpha'\text{C}$ ); 147.2, 139.2, 131.9, 129.7, 126.5, 126.1, 124.4, 123.7 (Ph); 122.4, 119.5, 115.7, 115.2, 112.2 ( $\text{C}_5\text{H}_2\text{Me}_3$ ); 111.9 (Cp); 106.0 ( $\beta\text{C}$ ); 71.0 ( $\alpha\text{C}$ ); 16.1, 14.1, 13.7 ( $\text{C}_5\text{H}_2\text{Me}_3$ ).

- a)  $^1\text{H NMR}$  resonances assigned by difference NOE spectroscopy.
- b) Multiplicities are from a separate off-resonance decoupling experiment.
- c) Assigned on the basis of relative intensities.

### III.6 References

1. For recent reviews of olefin metathesis; see a) Grubbs, R.H. *Prog. Inorg. Chem.* **1978**, *24*, 1; b) Grubbs, R.H. in "Comprehensive Organometallic Chemistry," Vol. 8 Wilkinson, G., Ed.; Pergamon Press:1982, p. 499..
2. a) Kress, J.; Wesolak, M.; Osborn, J.A., *J. Chem. Soc. Chem. Commun.* **1982**, 514, b) Kress, J.; Osborn, J.A. *J. Am. Chem. Soc.* **1983**, *105*, 6346.
3. Schrock, R.R., private communication.
4. a) Tebbe, F.N.; Parshall, G.W.; Reddy, G.S.; *J. Am. Chem. Soc.* **1978**, *100*, 3611; b) Tebbe, F.N.; Parshall, G.W.; Overall, D.W. *J. Am. Chem. Soc.* **1979**, *101*, 5074; c) Klabunde, U.; Tebbe, F.N.; Parshall, G.W.; Harlow, R.L. *J. Mol. Catal.* **1980**, *8*, 37.
5. a) Howard, T.R.; Lee, J.B.; Grubbs, R.H. *J. Am. Chem. Soc.* **1980**, *102*, 6876; b) Lee, J.B.; Gajda, G.J.; Schaefer, W.P.; Howard, T.R.; Irkariya, T.; Straus, D.A.; Grubbs, R.H. *J. Am. Chem. Soc.* **1981**, *103*, 7358; c) Straus, D.A., Ph.D. Thesis, California Institute of Technology, 1982; d) Ott, K.C., Ph.D. Thesis ,California Institute of Technology, 1983.
6. Eisentein, O.; Hoffmann, R.; Rossi, A.R. *J. Am. Chem. Soc.* **1981**, *103*, 5582.
7. a) Rappé, A.K.; Upton, T.H., *Organometallics* **1984**, *3*, 1440; b) Upton, T.H.; Rappé, A.K. *J. Am. Chem. Soc.* **1985**, *107*, 1206.
8. Straus, D.A.; Grubbs, R.H. *Organometallics* **1982**, *1*, 1658.

9. a) Brown-Wensley, K.A. Ph.D. Thesis, California Institute of Technology, 1981; b) Anslyn, E.V. unpublished results; c) Lee, J.B.; Ott, K.C.; Grubbs, R.H. *J. Am. Chem. Soc.* **1982**, *104*, 7491.
10. Ott, K.C.; Grubbs, R.H. *Organometallics* **1984**, *3*, 223.
11. Chien, J.C.W. *J. Phys. Chem.* **1963**, *67*, 2477.
12. Hao, N.; Sayer, B.G.; Dénès, G.; Bickley, D.G.; Detellier, C.; McGlinchey, M.J. *J. Magn. Res.* **1982**, *50*, 50.
13. Straus, D.A.; Grubbs, R.H. unpublished results.
14. Proton resonances in  $^1\text{H}$  NMR could be assigned on the basis of results from difference NOE NMR experiments.
15. Seetz, J.W.F.C.; Schat, G.; Akkerman, O.S., Bickelhaupt, F. *Angew Chem. Int. Ed. Engl.* **1983**, *22*, 248.
16. The low field  $^{13}\text{C}$  resonance of  $\text{sp}^2$  hybridized carbons bound to early transition metals is typical.<sup>17</sup>
17. a) Meinhart, J.D.; Grubbs, R.H. *J. Am. Chem. Soc.* in press; b) Erker, G.; Kropp, K.; Atwood, J.C.; Hunter, W.E. *Organometallics* **1983**, *2*, 1555.
18. Gassman, P.G.; Macomber, D.W.; Hershberger, J.W. *Organometallics* **1983**, *2*, 1470.
19. Levy, G.C.; Nelson, G.L. "Carbon-13 Nuclear Magnetic Resonance for Organic Chemists" Wiley, New York:1972, pp. 25-28.
20. Yoder, C.H.; Tuck, R.H.; Hess, R.G. *J. Am. Chem. Soc.* **1969**, *91*, 539.
21. Gassman, P.G.; Campbell, W.H.; Macomber, D.W. *Organometallics* **1984**, *3*, 385.

22. Kidd, R.G.; Matthew, R.W.; Spinney, H.G. *J. Am. Chem. Soc.* **1973**, *94*, 6686.
23. The following discussion is a summary of the discussion found in Drago, R.S. "Physical Methods in Chemistry" W.B. Saunders Co., Philadelphia:1977, pp 198, 283-294.
24. Strothers, J.B. "Carbon-13 NMR Spectroscopy" Academic Press, New York:1972, p. 128.
25. Lauher, J.W.; Hoffman, R. *J. Am. Chem. Soc.* **1976**, *98*, 1729.
26. Hammond, G.S. *J. Am. Chem. Soc.* **1955**, *77*, 334.
27. a) El Murr, N.; Chaloyard, A. *J. Organomet. Chem.* **1982**, *231*, 1.; b) El Murr, N.; Chaloyard, A.; Tironflat, J. *J. Chem. Soc. Chem. Commun.* **1980**, 446; c) Connelly, N.G.; Geiger, W.E. *Adv. Organomet. Chem.* **1984**, *23*, 1.
28. Lappert, M.F.; Raston, C.L. *J. Chem. Soc. Chem. Commun.* **1980**, 1284.
29. For a discussion of bonding in these systems see Rappé, A.K.; Goddard, W.A. *J. Am. Chem. Soc.* **1982**, *104*, 297.
30. Bercaw, J.W.; Marvich, R.H.; Bell, L.G.; Brintzinger, H.H. *J. Am. Chem. Soc.* **1972**, *94*, 1219. Only one equivalent of LiCp\* per TiCl<sub>3</sub>·3THF was used in the preparation of Cp\*TiCl<sub>3</sub>. The initial formed Cp\*TiCl<sub>2</sub> is converted to Cp\*TiCl<sub>3</sub> with anhydrous HCl.
31. Lee, J.B.; Ott, K.C.; Grubbs, R.H. *J. Am. Chem. Soc.* **1982**, *104*, 7491.
32. "Chem. Abstracts" *54*, 18546f, 1960.
33. Capallos, C.; Bielski, B.H.J. "Kinetic Systems" Wiley, New York:1972, p. 34.

34. Since the initial ratio of *trans*-12 to *cis*-13 is very close to its equilibrium value the accuracy of the rate constants is questionable. The data is presented to indicate the order of magnitude of the rate of equilibration. In light of the kinetic results for the trapping reactions of 13, the measured activation parameters do not seem unreasonable.
35. The reaction of these metallacyclobutanes with diphenylacetylene cleanly produces their corresponding metallocyclobutenes having spectral properties identical to independently synthesized samples prepared from the ring-substituted Tebbe analogs. No intermediates were observed during the course of the reactions.
36. Since the *trans* and *cis* isomers of the mixed ring complexes 12 and 13 could not be separated, kinetics data were obtained from samples containing both isomers. For 13 samples with starting ratio of *trans/cis* of 3.5:1 and of 2.2:1 were used and gave identical results.
37. These metallacycles react with acetone in a Wittig manner producing isobutylene via methylene transfer. No intermediates are observed with <sup>1</sup>H NMR spectroscopy. Titanocene oxo polymer is the other product of the reaction; broad peaks appear in the region  $\delta$  6.8-5.2 (Cp ring protons) and also 2.5-2.0 (Cp ring methyl groups).
38. Moore, J.W.; Pearson, R.G. "Kinetics and Mechanism" Wiley, New York:1981, p. 69.